Doctoral theses at NTNU, 2023:229

Saad Hamayoon

Advanced Control Methods for Modular Multilevel Converters

Doctoral thesis

NTNU
Norwegian University of Science and Technology
Thesis for the Degree of Philosophiae Doctor
Faculty of Information Technology and Electrical Engineering
Department of Engineering Cybernetics

NTNU
Norwegian University of Science and Technology

Saad Hamayoon

Advanced Control Methods for Modular Multilevel Converters

Thesis for the Degree of Philosophiae Doctor

Trondheim, July 2023

Norwegian University of Science and Technology
Faculty of Information Technology and Electrical Engineering
Department of Engineering Cybernetics

NTNU
Norwegian University of
Science and Technology

NTNU
Norwegian University of Science and Technology

Thesis for the Degree of Philosophiae Doctor

Faculty of Information Technology and Electrical Engineering
Department of Engineering Cybernetics

© Saad Hamayoon

ISBN 978-82-326-7158-8 (printed ver.)
ISBN 978-82-326-7157-1 (electronic ver.)
ISSN 1503-8181 (printed ver.)
ISSN 2703-8084 (online ver.)

ITK report number 2023-17-W

Doctoral theses at NTNU, 2023:229

Printed by NTNU Grafisk senter

Summary

Climate change has forced the global energy sector to transition from energy production based on fossil fuels such as oil, natural gas, and coal towards renewable energy sources i.e., solar energy, wind energy, biomass, etc. Countries across the world have set targets to reduce greenhouse gas (GHG) emissions significantly by 2050. For example, the EU is committed to reducing GHG emissions by 85-90% by 2050. Renewable energy would serve as a key driver in achieving these ambitious targets.

To meet these ambitious goals, many projects have been launched in recent years, for example, Supergrid with the aim to interconnect various European countries. However, this is not a simple task. Cross-border electricity flow would require high voltage direct current (HVDC) technology, which can carry more electricity efficiently over long distances. Many HVDC projects interconnecting different countries have been recently launched. For instance, a 190 km HVDC interconnection (Piedmont-Savoy HVDC Line) links the French and Italian electricity networks. Similarly, other projects such as NorthSea DC grid, Medtech, Desertec, etc have been undertaken.

Modular multilevel converters (MMCs) have emerged as one of the most promising technologies for HVDC applications owing to their remarkable features such as their modular nature, reduced or no filter requirements, and redundancy. However, the control of MMC is a difficult problem as in addition to the control of output current, the internal dynamics of the MMC need to be well controlled. Moreover, the bilinear model of the MMC introduces non-linearity through the product of the states and inputs.

At the start of this thesis work (early 2020), many control methods had already been investigated for MMC. These included conventional cascade control methods which due to their linear nature result in sluggish dynamic performance as compared to advanced control methods such as model predictive control. Moreover, due to the presence of multiple control loops, their design becomes complex. Then many non-linear methods such as backstepping, sliding mode control, feedback linearization, and model predictive control had also been tried.

Among the existing methods, model predictive control is an effective method to deal with the multi-input multi-output (MIMO) nature, nonlinearity of MMC and can easily handle the constraints. For power converters generally, finite control set model predictive control (FCS-MPC) is used. The existing methods based on FCS-MPC for MMC were not able to achieve high performance with low computational complexity simultaneously. The methods with low computational complexity resulted in sluggish dynamic response whereas the methods which offered high dynamic performance had high computational complexity making the real-time application of FCS-MPC difficult. As a result, an extended prediction horizon which generally improves the performance of the system as it can prepare early for the effects in the future could not be used with existing methods.

Moreover, at the start of this work, there was no published work based on MPC that considered all the practical delays i.e., forward (control) and backward (feedback) for MMCs. Only a forward delay of one sampling instant is considered mostly in the existing literature.

The steady-state performance of FCS-MPC for MMC is also an issue that has been investigated. In the existing literature, this is handled by modulated MPC. These modulated MPC techniques are either based on continuous control set MPC (CCS-MPC) or indirect FCS-MPC methods where duty cycles are calculated for each SM by considering the two or three voltage levels that give the minimum cost. However, CCS-MPC methods have very high computational complexity due to non-convexity (introduced by the nonlinear model) and having very small sampling times. On the other hand, the methods that are based on indirect FCS-MPC strategies do not have very good control of the circulating current.

In addition, when this work was started, all the methods based on MPC for MMC required an outer loop to regulate the summation voltages. The methods that proposed an equivalent of the outer loop within MPC suffered from continuous ripples in the circulating current. The methods without the outer loop or its equivalent within MPC resulted in a slow deviation of summation voltages away from reference.

Another issue that has been investigated for FCS-MPC for MMC is the variable and high switching frequency. The existing methods modify the sorting algorithm to lower the switching frequency, however, the variable switching frequency is not addressed by modification of the sorting algorithm. Methods that result in fixed switching frequency are based on modulated MPC with carrier phase-shifted PWM. However, as the number of SMs increases, the number of carriers also increases which makes it implementation complicated for applications with hundreds of SMs.

Finally, the existing methods for fault detection, localization, and tolerance for open circuit switch failure in MMCs are mainly based on conventional cascade control. Very few works based on MPC have addressed this issue. These works based on MPC either have very high computational complexity or their operating range is limited.

The main contributions of this work can be summarized as:

- Various methods with high performance and low computational complexity based on FCS-MPC are proposed
- Method to make the computational complexity of MPC for MMCs independent of the number of SMs is proposed.
- Methods to improve the steady-state performance of FCS-MPC are developed.
- A novel cost function is proposed to remove an outer loop or any kind of additional control over circulating current reference for summation voltage regulation.
- A novel circulating current reference is proposed to remove the need for an outer loop to regulate the summation voltages.

- Experimental verification of proposed methods by considering all the practical delays i.e., forward and backward is done
- A method for fault detection, localization, and tolerance using Indirect FCS-MPC for open circuit switch fault in MMCs is developed
- A modified sorting algorithm is also proposed that results in low and almost fixed switching frequency on an average of a few cycles. This ensures that the losses between the SMs are balanced.
- The transition from simulations to experimental verification led to some problems. As a solution to these problems, a very simple method for grid voltage estimation was developed. In addition, a virtual ac-side voltage approach is also developed in this thesis.

Preface

This thesis is submitted as a partial fulfilment of the requirements for the Degree of Philosophiae Doctor (Ph.D.) at the Norwegian University of Science and Technology (NTNU). This research work has been carried out at the Department of Engineering Cybernetics, Faculty of Information Technology and Electrical Engineering from March 2020 to June 2023, with Professor Morten Hovd and Dr. Jon Are Suul as main supervisor and co-supervisor, respectively.

Acknowledgements

First and foremost I offer gratitude to the God Almighty who bestowed me with all the wisdom, strength, and ability to carry out this work.

Then I would like to express my deepest gratitude to my supervisor, Professor Morten Hovd for all his cooperation, guidance, encouragement, and confidence he showed in me. I would also like to thank my co-supervisor Dr. Jon Are Suul for his valuable feedback and guidance throughout the course of my Ph.D. and for arranging for experimental verification of the proposed methods at the National Smart Grid Laboratory. I would also like to thank Dr. Giuseppe Guidi who took out time and helped me with laboratory tests at the National Smart Grid Laboratory.

Finally, my deepest gratitude goes to my beloved parents for their prayers, endless love, and encouragement, and to my wife for her love, patience, and support. Thanks must also be given to my grandmother and my wife's parent for their prayers. I am also grateful to my brothers for their support and encouragement.

Contents

List of Figures

List of Tables

Chapter 1

Introduction

This chapter gives a brief overview of the thesis. The main objectives and contributions are highlighted.

Climate change has forced the global energy sector to transition from energy production based on fossil fuels such as oil, natural gas, and coal towards renewable energy sources i.e., solar energy, wind energy, biomass, etc. Countries across the world have set targets to reduce greenhouse gas (GHG) emissions significantly by 2050. For example, the EU is committed to reducing GHG emissions by 85-90% by 2050. Renewable energy would serve as a key driver in achieving these ambitious targets.

To meet these ambitious goals, many projects have been launched in recent years, for example, Supergrid with the aim to interconnect various European countries. However, this is not a simple task. Cross-border electricity flow would require high voltage direct current (HVDC) technology, which can carry more electric power efficiently over long distances. Many HVDC projects interconnecting different countries have been recently launched. For instance, a 190 km HVDC interconnection (Piedmont-Savoy HVDC Line) links the French and Italian electricity networks. Similarly, other projects such as NorthSea DC grid, Medtech, Desertec, etc have been undertaken.

Modular multilevel converters (MMCs) have emerged as one of the most promising technology for HVDC applications owing to their remarkable features such as modular nature, reduced or no filter requirements, and redundancy. However, the control of MMCs is a difficult problem as in addition to the control of output current, the internal dynamics of the MMC need to be well controlled. Moreover, the bilinear model of MMC introduces non-linearity through the product of the states and inputs.

Among the existing techniques in literature, model predictive control (MPC) is an effective technique to control multiple objectives, the non-linear nature, and the constraints of MMC. However, the existing techniques based on MPC fail to give high performance and low computational complexity at the same time. This thesis's main goal was to develop a control method based on MPC for MMC whose application is possible in real-time and offers high performance and reduced complexity at the same time.

1.1 Objectives

The main objectives of the thesis can be summarized as:

- To develop control strategies based on MPC for MMC that achieve high performance with low computational complexity.
- To address shortcomings of existing MPC techniques for MMC
- To validate the developed methods by experiment
- To address any issues encountered while trying to achieve the above objectives

1.2 Outline and Main Contributions of the Thesis

The chapters and main contributions in each chapter are summarized as follows:

- **Chapter 2**: A brief introduction to modular multilevel converters, modeling and basic operation of MMC, existing control methods, their shortcomings, and the need for model predictive control is presented.

- **Chapter 3**: The existing MPC-based methods for MMC and their shortcomings are highlighted.

- **Chapter 4**: A modified reduced indirect FCS-MPC (MRI-FCS-MPC) method is presented in this chapter. The technique is developed from reduced indirect FCS-MPC which limits the change in inserted submodules (SMs) to one with respect to the previous sampling instant. This results in very low computational complexity but at the cost of sluggish dynamic response. In order to improve the dynamic performance of the MMC, the proposed method allows the number of inserted SMs to change by more than one only in the initial time step within the prediction horizon. This increases the computational complexity slightly but improves the dynamic response significantly. The proposed method gives a nearly similar dynamic performance as full indirect FCS-MPC (which has very high computational complexity). In addition, a novel cost function is proposed which removes the need for an outer loop or its equivalent within MPC to regulate summation voltages.

- **Chapter 5**: Two methods to reduce the computational complexity of indirect FCS-MPC while achieving high dynamic performance are proposed. Both methods consist of two steps. In the first method bisection algorithm is applied as the first step whereas backstepping is applied as the first step of modulation control in the second method. The second step is almost common to both methods where reduced indirect FCS-MPC is applied to the rounded-off solution from the first step. In the bisection-based method, the maximum change allowed from the rounded-off result is fixed to two whereas for backstepping this change is fixed to one.

- **Chapter 6**: In this chapter, modulated MPC based on an enumera-

tion of active sets is proposed. The enumeration of active sets makes the problem independent from the number of SMs and the modulator improves the steady-state response of the system. The total number of active sets per phase model of MMC is just nine. The equations are formulated for these nine active sets offline and then based on the measurement data the equation which satisfies the Karush–Kuhn–Tucker (KKT) conditions is used for the implementation of the modulation stage.

- **Chapter 7**: In this chapter, an equivalent of the outer loop used for regulation of summation voltages within the MPC framework is presented. Then based on a quadratic cost function the stability analysis is conducted. It is shown that without the outer loop or its equivalent in design, the system is marginally stable with MPC.

- **Chapter 8**: In this chapter, non-linear model predictive control (NMPC) without an explicit modulator is presented for MMCs. To avoid the modulator, two strategies are presented to handle the continuous solution of NMPC. In the first strategy, the number of SMs to be inserted for each arm is obtained by rounding the continuous solution for the insertion index from the NMPC to the nearest integer value. In the second strategy, the optimal solution obtained from the NMPC is further evaluated by rounding it up and down for both arms. This leads to evaluating the cost function (same as NMPC stage cost) for four discrete cases, independently from the number of SMs per arm. This evaluation is conducted only for the initial time step within the prediction horizon. Then the solution that minimizes the cost function is applied to the MMC.

- **Chapter 9**: In this chapter, the setup and modifications in the proposed methods for real-time implementation are presented. A problem associated with ac-side voltage is identified and as a solution to this, a very easy method to estimate the grid voltage is presented. The experimental results for each of the proposed methods are also presented and compared with conventional cascade control.

- **Chapter 10**: A modified sorting algorithm is presented to address the issue of the variable and high switching frequency.

- **Chapter 11**: A simple method is presented to improve the steady-state response of indirect finite control set model predictive control (I-FCS-MPC) techniques. The method is based on the assumption that the solution obtained from I-FCS-MPC is at a maximum of ± 0.5 away from the actual continuous solution. Based on this observation, a few more options within the range ± 0.5 are evaluated on the solution from I-FCS-MPC. Then the option among these that gives the minimum cost is used for the modulation stage.

- **Chapter 12**: In this chapter, I-FCS-MPC is used for detecting, localizing, and handling the open-circuit failures in the transistors without the use of arm voltage sensors. The fault is detected by the main controller whereas the localization is performed in the local controller which is used for the sorting algorithm. The main controller utilizes the discrete mathematical model to estimate the arm voltages using state measurements from present and previous sampling instants. Then this estimated arm voltage is compared with the arm voltage command by the main controller in the previous sampling instant to detect the fault. The fault signal is sent to the local controller where the counter is increased for the potentially faulty SMs. The fault is then localized to the specific SM whose count first goes above the threshold value. Finally, this SM is bypassed using a bypass switch and a redundant SM is inserted in its place. The proposed fault detection and localization method do not require any additional sensors.

- **Chapter 13**: In this chapter, conclusions and potential future research directions are highlighted.

1.2.1 List of Publications

Journal Papers

[$J1$] S. Hamayoon, J. A. Suul, M. Hovd and G. Guidi, "Reduced Complex-

ity Indirect Finite Control Set Model Predictive Control with High Dynamic Performance for Modular Multilevel Converters" in IEEE Journal of Emerging and Selected Topics in Power Electronics (Under Preparation)

[$J2$] S. Hamayoon, J. A. Suul, M. Hovd and G. Guidi, "Bisection and Backstepping based Indirect Finite Control Set Model Predictive Control for Modular Multilevel Converters" in IEEE Transactions on Industrial Electronics (Under Preparation)

[$J3$] S. Hamayoon, M. Hovd and J. A. Suul, "Non-linear Model Predictive Control for Modular Multilevel Converter" in IEEE Transactions on Industry Applications (Under Review)

[$J4$] S. Hamayoon, J. A. Suul, M. Hovd and G. Guidi, "Active Set Method based Modulated Model Predictive Control of Modular Multilevel Converters" in IEEE Journal of Emerging and Selected Topics in Power Electronics (Under Preparation)

[$J5$] S. Hamayoon, J. A. Suul, M. Hovd and G. Guidi, "Circulating Current Reference Based on Average and Instantaneous Information of Summation Voltages for Modular Multilevel Converter using Model Predictive Control" in IEEE Journal of Emerging and Selected Topics in Power Electronics (Under Preparation)

Conference Papers

[$C1$] S. Hamayoon, M. Hovd and J. A. Suul, "Fault Detection, Localization and Clearance for MMC based on Indirect Finite Control Set Model Predictive Control," 2023 IEEE 32nd International Symposium on Industrial Electronics (ISIE), Helsinki-Espoo, Finland, 2023

[$C2$] S. Hamayoon, M. Hovd and J. A. Suul, "Enhancement of Steady State Response of Indirect Finite Control Set Model Predictive Control," 2023 IEEE 32nd International Symposium on Industrial Electronics (ISIE),

Helsinki-Espoo, Finland, 2023

[$C3$] S. Hamayoon, M. Hovd and J. A. Suul, "Non-Linear Model Predictive Control for Modular Multilevel Converters," 2022 International Power Electronics Conference (IPEC-Himeji 2022- ECCE Asia), 2022, pp. 562-568

[$C4$] S. Hamayoon, M. Hovd and J. A. Suul, "Bisection Algorithm based Indirect Finite Control Set Model Predictive Control for Modular Multilevel Converters," 2021 IEEE 22nd Workshop on Control and Modelling of Power Electronics (COMPEL), 2021, pp. 1-6

[$C5$] S. Hamayoon, M. Hovd and J. A. Suul, "Combination of Backstepping and Reduced Indirect FCS-MPC for Modular Multilevel Converters," IECON 2021 – 47th Annual Conference of the IEEE Industrial Electronics Society, 2021, pp. 1-6

[$C6$] S. Hamayoon, M. Hovd, J. A. Suul and M. Vatani, "Modified Reduced Indirect Finite Control Set Model Predictive Control of Modular Multilevel Converters," 2020 IEEE 21st Workshop on Control and Modeling for Power Electronics (COMPEL), 2020, pp. 1-6

Chapter 2

The Modular Multilevel Converter

This chapter first presents the mathematical model development of the modular multilevel converters (MMCs) and then concludes by highlighting state-of-the-art control methods for MMC, their shortcomings, and the need for model predictive control.

2.1 Model and Basic Operation of the MMC

The same model development is followed in this thesis as in [11]. The three-phase MMC system shown in Fig. 2.1 is one of the typical topologies of MMCs used in HVDC applications. The MMC consists of three identical phase legs. Each phase-leg of the MMC consists of two arms *i.e.*, an upper arm (denoted by subscript 'u') and a lower arm (denoted by subscript 'l') connected to the positive and negative dc terminal respectively. Each arm can be represented by N half-bridge submodules (SM), an inductor, and a resistor. The arm inductor is used to limit the harmonics and fault currents and the arm resistance is used for modeling the losses of the MMC. Depending on the switching states of S_1 and S_2, each SM can provide two voltage levels *i.e.*, 0 or $v_{\mathrm{Cmi,j}}$ where m=u,l; i=1,2,...,N, j=a,b,c. That is,

when S_1 is on and S_2 is off then the SM is inserted resulting in $v_{\mathrm{Cmi,j}}$ and if S_2 is on and S_1 is off then the SM is bypassed resulting in 0 V.

The per-phase mathematical model of the MMC shown in Fig. 2.1 with respect to fictitious midpoint 'O' can be expressed as:

$$\frac{V_{dc}}{2} - v_{u,j} - Ri_{u,j} - L\frac{di_{v,j}}{dt} + R_c i_{v,j} + L_c\frac{di_{v,j}}{dt} - v_f = 0 \tag{2.1}$$

$$\frac{V_{dc}}{2} - v_{l,j} - Ri_{l,j} - L\frac{di_{l,j}}{dt} - R_c i_{v,j} - L_c\frac{di_{v,j}}{dt} + v_f = 0 \tag{2.2}$$

where $v_{u,j}$ and $v_{l,j}$ represent the upper and lower arm voltages of phase j, $i_{u,j}$ and $i_{l,j}$ represent the upper and lower arm currents of phase j, $i_{v,j}$ is the ac-side current, V_{dc} is the dc-side voltage, v_f is the grid side voltage, R is the arm resistance, L is the arm inductance, R_c and L_c are the grid side converter resistance and inductance, respectively.

The ac-side current, arm currents and circulating currents are given by:

$$i_{v,j} = i_{l,j} - i_{u,j} \tag{2.3}$$

$$i_{u,j} = -\frac{i_{v,j}}{2} + i_{cir,j} \tag{2.4}$$

$$i_{l,j} = \frac{i_{v,j}}{2} + i_{cir,j} \tag{2.5}$$

$$i_{cir,j} = \frac{i_{u,j} + i_{l,j}}{2} \tag{2.6}$$

where $i_{cir,j}$ is the circulating current and flows through the three-phases of the MMC.

By subtracting (2.1) and (2.2) and using (2.3) the dynamic equation for ac-side current is obtained as:

$$\frac{di_{v,j}}{dt} = \frac{-(R+2R_c)}{L+2L_c} i_{v,j} + \frac{v_{u,j} - v_{l,j}}{L+2L_c} + \frac{2v_{f,j}}{L+2L_c} \tag{2.7}$$

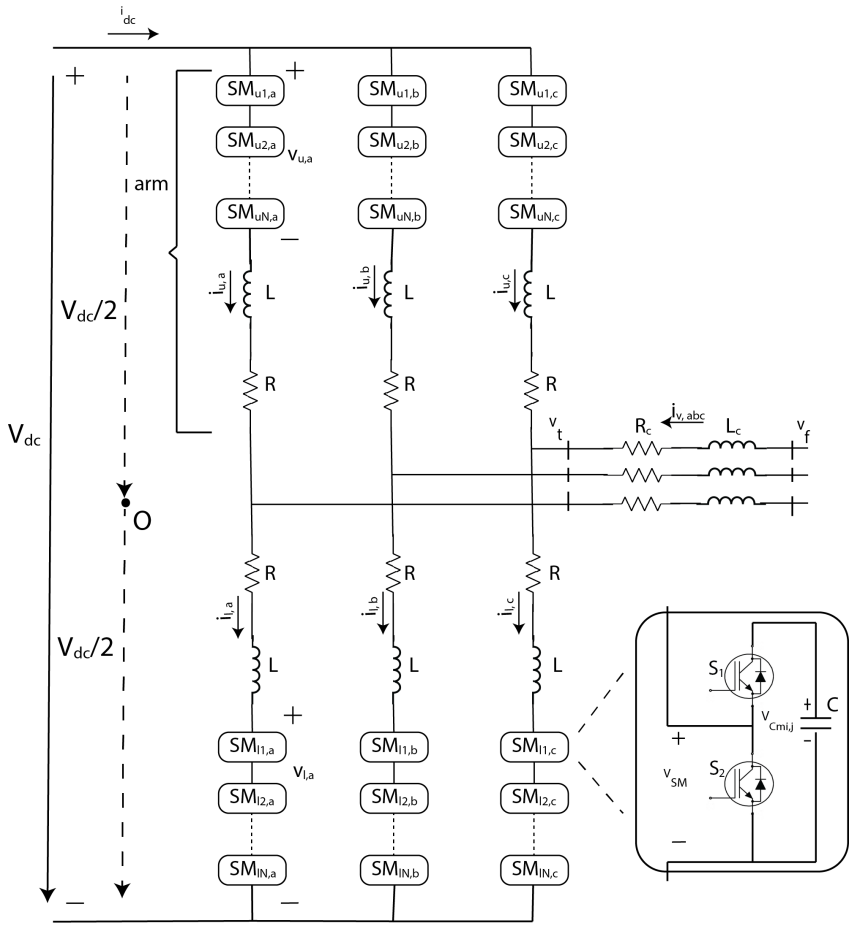

Figure 2.1: Circuit Diagram of an MMC

Similarly, by adding (2.1) and (2.2) and using (2.4) and (2.5), the dynamic equation for the circulating current is obtained as:

$$\frac{di_{cir,j}}{dt} = \frac{-R}{L} i_{cir,j} - \frac{1}{2L}(v_{u,j} + v_{l,j}) + \frac{1}{2L} V_{dc} \tag{2.8}$$

The arm voltages $v_{u,j}$ and $v_{l,j}$ depend on the number of SMs inserted in that arm. Assuming that the SM capacitor voltages are well balanced at their reference values, the arm voltages can be expressed as:

$$v_{u,j} \approx \frac{n_{u,j}}{N} v_{u,j}^{\Sigma} \tag{2.9}$$

$$v_{l,j} \approx \frac{n_{l,j}}{N} v_{l,j}^{\Sigma} \tag{2.10}$$

where $n_{u,j}$ and $n_{l,j}$ are the number of SMs to be inserted in upper and lower arm respectively and $v_{u,j}^{\Sigma}$ and $v_{l,j}^{\Sigma}$ are the summation of all capacitor voltages in the upper and lower arm respectively.
The dynamics of the total arm capacitor voltages can be expressed as:

$$\frac{dv_{m,j}^{\Sigma}}{dt} = \frac{i_{m,j}}{C_{m,j}^{e}} = \frac{n_{m,j} i_{m,j}}{C} \tag{2.11}$$

where $C_{m,j}^{e}$ is the equivalent arm capacitance of inserted SMs in arm m. Now equations (2.4) and (2.5) can be substituted into (2.11) to give the following dynamic equations for total arm capacitor voltages of both arms:

$$\frac{dv_{u,j}^{\Sigma}}{dt} = -\frac{n_{u,j} i_{v,j}}{2C} + \frac{n_{u,j} i_{cir,j}}{C} \tag{2.12a}$$

$$\frac{dv_{l,j}^{\Sigma}}{dt} = \frac{n_{l,j} i_{v,j}}{2C} + \frac{n_{l,j} i_{cir,j}}{C} \tag{2.12b}$$

Using the definition of $v_{u,j}$ and $v_{l,j}$ from (2.9) and (2.10) into (2.7) and (2.8) the dynamic equations for ac-side current and circulating current are

modified as:

$$\frac{di_{v,j}}{dt} = \frac{-(R+2R_c)}{L+2L_c} i_{v,j} + \frac{n_{u,j}v^{\Sigma}_{u,j} - n_{l,j}v^{\Sigma}_{l,j}}{N(L+2L_c)} + \frac{2v_{f,j}}{L+2L_c} \tag{2.13a}$$

$$\frac{di_{cir,j}}{dt} = \frac{-R}{L} i_{cir,j} - \frac{(n_{u,j}v^{\Sigma}_{u,j} + n_{l,j}v^{\Sigma}_{l,j})}{2NL} + \frac{V_{dc}}{2L} \tag{2.13b}$$

Using (2.12) and (2.13) the state space equation of the MMC is shown by (2.14) where $x = [i_{v,j}, i_{cir,j}, v^{\Sigma}_{u,j}, v^{\Sigma}_{l,j}]^T$ is the state vector and $u = [u_1 u_2]^T = [n_{u,j} n_{l,j}]^T$ is the input vector.

$$\begin{aligned}\dot{x}(t) = &\begin{bmatrix} \frac{-(R+2R_c)}{L+2L_c} & 0 & 0 & 0 \\ 0 & \frac{-R}{L} & 0 & 0 \\ 0 & 0 & 0 & 0 \\ 0 & 0 & 0 & 0 \end{bmatrix} x(t) + \begin{bmatrix} 0 & 0 & \frac{1}{(L+2L_c)N} & 0 \\ 0 & 0 & \frac{-1}{2NL} & 0 \\ \frac{-1}{2C} & \frac{1}{C} & 0 & 0 \\ 0 & 0 & 0 & 0 \end{bmatrix} x(t)u_1 \\ &+ \begin{bmatrix} 0 & 0 & 0 & \frac{-1}{(L+2L_c)N} \\ 0 & 0 & 0 & \frac{-1}{2NL} \\ 0 & 0 & 0 & 0 \\ \frac{1}{2C} & \frac{1}{C} & 0 & 0 \end{bmatrix} x(t)u_2 + \begin{bmatrix} \frac{2v_f(t)}{(L+2L_c)} \\ \frac{V_{dc}(t)}{2L} \\ 0 \\ 0 \end{bmatrix}\end{aligned} \tag{2.14}$$

Based on (2.14), and a sampling time of T_s the discrete time model of

the system is given by forward Euler approximation:

$$x(k+1) = \underbrace{\begin{bmatrix} 1-\frac{T_s(R+2R_c)}{L+2L_c} & 0 & 0 & 0 \\ 0 & 1-\frac{T_sR}{L} & 0 & 0 \\ 0 & 0 & 1 & 0 \\ 0 & 0 & 0 & 1 \end{bmatrix}}_{A} x(k) + \underbrace{\begin{bmatrix} 0 & 0 & \frac{T_s}{(L+2L_c)N} & 0 \\ 0 & 0 & \frac{-T_s}{2NL} & 0 \\ \frac{-T_s}{2C} & \frac{T_s}{C} & 0 & 0 \\ 0 & 0 & 0 & 0 \end{bmatrix}}_{B_1} x(k)u_1(k)$$
$$+ \underbrace{\begin{bmatrix} 0 & 0 & 0 & \frac{-T_s}{(L+2L_c)N} \\ 0 & 0 & 0 & \frac{-T_s}{2NL} \\ 0 & 0 & 0 & 0 \\ \frac{T_s}{2C} & \frac{T_s}{C} & 0 & 0 \end{bmatrix}}_{B_2} x(k)u_2(k) + \underbrace{\begin{bmatrix} \frac{2T_sv_f(k)}{(L+2L_c)} \\ \frac{T_sV_{dc}(k)}{2L} \\ 0 \\ 0 \end{bmatrix}}_{d} \tag{2.15}$$

Equation (2.14) & (2.15) show that the MMC is a bilinear system with multiple inputs and outputs. This introduces non-linearity through the product of the states and inputs.

2.2 Existing Methods, their Shortcomings and Need of Model Predictive Control

Despite the many advantages offered by MMC, the control of MMCs is difficult as compared to other VSCs. This is mainly because of the requirement to control the internal dynamics of MMC *i.e.*, circulating currents, and SM capacitor voltages [12], in addition to control of output currents/voltages. Moreover, MMCs have a bilinear model which introduces the non-linearity through the product of the states and inputs. Different control methods and modulation techniques have been investigated in literature for MMCs [13–15].

The conventional cascade control methods [16–18] are based on multiple loops *i.e.* inner and outer loops using proportional-integral (PI) regulators. In addition, these methods include the design of an appropriate modulation scheme and voltage balancing algorithm. Therefore, the performance

of these methods highly depends on the design and tuning of PI regulators, choice of the modulation scheme, and voltage balancing technique. The presence of multiple loops and tuning of PI or proportional resonant (PR) controllers make the conventional cascade control design complex. Moreover, MMC has a non-linear model, and these methods due to their linear nature result in sluggish dynamic response.

Some of the notable control techniques using cascade structure for MMC have been presented in [10, 16, 17, 19–64]. In the following, these techniques have been divided into two categories based on circulating current control and modulation techniques along with voltage balancing.

2.2.1 Circulating Current Control

A circulating current suppression controller (CCSC) is proposed in [19] based on the double line-frequency, negative sequence rotational dq-coordinate. The proposed method decouples the control of the output side and the circulating current. In [23], two methods for circulating current control based on instantaneous values of output current and modulation signal are proposed. It is shown that the method based on an energy point of view results in fewer ripples in the capacitor voltages. Circulating current control in the $\alpha\beta$ reference frame using a non-ideal Proportional Resonant (PR) regulator is presented in [24] both for balanced and unbalanced conditions. It is shown that under unbalanced grid conditions, the circulating current is asymmetric and needs to be decomposed into positive, negative, and zero sequence components. A repetitive controller paralleled with PI control for circulating current harmonic elimination is proposed in [27]. The circulating current control in [29] is in the stationary frame and based on parallel PR regulators with the resonant frequencies of $2\omega_0, 4\omega_0, 6\omega_0, \ldots$ where ω_0 is the fundamental frequency. However, not all the even order harmonics are required as the implementation of the PR regulators would then become difficult. An energy-based controller is proposed in [30]. It is shown that energy sum and energy difference oscillate at twice the fundamental frequency and at the fundamental frequency respectively. Therefore, to decouple the energy sum and difference control, a decoupled double synchronous refer-

ence frame for MMC is used. The desired circulating current references for energy sum and difference control are then sent to the circulating current controller. A controller in a stationary frame using a proportional-integral-resonant (PIR) regulator is proposed for circulating current control under unbalanced conditions in [31]. A PI control in cascade with repetitive control is proposed in [33] to simplify the design of repetitive control and avoid limitations on PI design as compared to [27] while claiming to give a similar dynamic performance. An optimization algorithm is applied to determine the optimal set of circulating currents to reduce SM capacitor voltage ripples by evaluating all the possibilities within a bounded range in [36]. PI controllers in double fundamental frequency, negative sequence rotational frame are proposed for circulating current control in [39,52]. In [43], the desired second-order harmonic in circulating current is numerically estimated with the aim to shape the ripple in capacitor voltage to avoid high capacitor voltages. In [45], the controller coefficients are determined using the loop shaping technique from an experimentally identified non-parametric model of circulating currents. This method gives better suppression of circulating currents as it is based on an accurate model. The desired second-order harmonic in circulating current control is determined to minimize the capacitor voltage fluctuations by minimizing an objective function in [46]. Circulating current suppression based on improved PR controllers under unbalanced grid conditions is presented in [49]. In [51], a circulating control method based on frequency adaptive dual spatial repetitive controller (SRC) is used to inject a second harmonic component in the circulating current to suppress the capacitor voltage ripple. Reference [54] proposes optimization based on the Lagrange multipliers method to generate references for circulating current in the stationary reference frame. A novel method to control circulating current using selective harmonic elimination (SHE) is presented in [55]. The circulating current suppression without the need for a separate circulating current controller is proposed in [57]. Reference [58] proposes an even harmonic repetitive control for circulating current suppression. A loss optimization technique to inject optimal second harmonic circulating current in arm current is proposed in [59]. Reference [62] shows that circulating current control suppression by control of the internally stored energy

can improve the small signal stability of the MMC. Circulating current injection reference generation using instantaneous information from MMC is proposed in [64].

2.2.2 Modulation and Voltage Balancing

Reference [19] proposes a modified voltage balancing algorithm to reduce the switching frequency by sorting only bypassed SMs if more SMs need to be inserted and sorting only inserted SMs if some SMs need to be removed. In [20], only one SM in both the upper and lower arm operates in PWM mode and a conventional sorting algorithm is used for the remaining SMs. Reference [21], improves the operating range of the converter by introducing arm balance control. In [22], the computational requirement of the processor is reduced by reducing the burden of different stages of voltage balancing *i.e.* from sorting to the selection of SMs. A novel selective virtual loop mapping method based on phase disposition PWM is proposed in [25] to ensure dynamic capacitor voltage balance. The proposed method avoids sorting and just needs to identify the SMs with maximum and minimum voltage. In [26], a phase-shifted carrier-based PWM technique is proposed to balance the capacitor voltages without the need to measure arm current. A novel modulation method based on predetermined pulse patterns to allow MMC operation at the fundamental switching frequency is proposed in [28]. A modified nearest level modulation technique is proposed in [32] to increase the number of levels to $2N+1$ where N is the total number of SMs per arm. The modulation is modified by using a different rounding function. In [34], three different strategies for voltage balancing are proposed. In the first strategy, the execution period for the sorting part is increased which results in avoiding unnecessary switching transitions within each control period. The second strategy proposes to sort the capacitors based on their absolute difference from nominal value and only uses the conventional sorting algorithm if the absolute difference is more than a threshold. If this error is less than a threshold then SMs with the least errors are switched on or off. In the third strategy, the sorting is done only when the ac-side voltage is $V_{dc}/2$ or $-V_{dc}/2$ in order to achieve fundamental frequency balancing.

An improved phase disposition PWM and voltage balancing control is proposed in [35]. The improved modulation uses only a single reference and single carrier, thus reducing the hardware requirements. In addition, the method only modifies the pulse width of the maximum and minimum SM capacitor voltage according to the direction of the arm current rather than the full sorting algorithm. A predictive sorting algorithm is proposed in [37] where the SMs are switched on and off in a manner that they are balanced when the stored energy in the arm reaches its maximum or minimum value. However, the pulse pattern needs to be known in advance for this method's application. An improved voltage balancing control based on maximum and minimum SM capacitor voltages is proposed in [38]. A novel voltage balancing strategy is presented and evaluated for staircase and phase disposition PWM in [40]. The reduction in switching frequency is achieved by modifying capacitor voltage measurements before sending them to the sorting algorithm. The Tortoise and the Hare sorting algorithm in [41] is another approach based on the minimum and maximum SM capacitor voltage. However, these min/max approaches limit the change in the number of inserted SMs to one or two which may have consequences on dynamic performance. An improved nearest level modulation for a low number of SMs is proposed in [42]. The number of levels is increased to $2N + 1$ by adding a small offset alternating at twice the fundamental frequency to reference signals. A hybrid particle swarm optimization (PSO) using staircase modulation for the elimination of harmonics in the MMC is proposed in [44]. First, the classical PSO algorithm is used to obtain the optimized iterative initial values of switching angles, and then the Newton method is applied to get the exact solutions of the switching angles. A dual space vector modulation is used to eliminate the need for an external controller for arm voltage balancing in [47]. In addition, voltage balancing is based on the direction of the load current instead of the arm current which results in the reduction of current sensors. In [48], a novel modulation method and simplified voltage balancing algorithm based on a relative comparison method instead of sorting is presented. A currentless sorting algorithm based on the derivative of the total capacitor voltage of an arm, instead of arm current is presented in [50]. A modified rotative phase disposition

PWM is presented in [53] to deal with uneven power distribution. A novel method for individual voltage balancing of capacitors is proposed which does not require a sorting algorithm and knowledge of arm current in [56]. A modified carrier phase shifted PWM technique along with a fundamental frequency sorting algorithm is proposed in [60]. Reference [61], proposes an adaptive voltage balancing method that makes a compromise between the balancing effect and switching losses through closed-loop control of the alternating number of SMs. A modified phase disposition (PD) PWM that uses a single PD modulator for the entire phase leg is proposed in [63].

2.2.3 Need of Model Predictive Control

As highlighted earlier, most of the conventional cascade control techniques are linear in nature. However, the MMC has a non-linear model. Moreover, the classical control methods with proportional-integral or proportional-resonant controllers suffer from sluggish dynamic performance. The cascade structure in addition makes the control problem complex and also requires the tuning of PI controllers.

Therefore, in past few years, many non-linear control methods such as feedback linearization [65, 66], sliding mode control [67, 68], backstepping [69–71], passivity-based control [72, 73] and model predictive control [74] have been considered. The techniques based on feedback linearization often cancel out useful non-linearities [75] and sliding mode control suffers from the chattering problem. The backstepping controllers in [70, 71] are not in abc reference frame and therefore, do not directly allow the control of each phase independently. The design process in [69] is complicated and results in a coupled effect between circulating current and output current [76]. Moreover, circulating currents are not fully diminished.

Among these methods, model predictive control is an effective method to deal with the non-linearity, constraints, and the MIMO nature of MMCs, and is very easy to understand. A simple cost function can be designed to meet the objectives of MMC operation directly in the abc reference frame thus providing more direct and independent control of each phase. However, the existing methods based on MPC cannot give high dynamic performance

and low computational complexity simultaneously along with some other deficiencies. A detailed literature review of the existing methods based on MPC and their shortcomings will be provided in the following chapters.

Bibliography

[1] D'Andrade, B., *The Power Grid: Smart, Secure, Green and Reliable.* Academic Press, 2017

[2] Teodorescu, R., M. Liserre, and P. Rodriguez, *Grid converters for photovoltaic and wind power systems.* Vol. 29. John Wiley & Sons, 2011

[3] Anaya-Lara, O., et al., *Offshore Wind Energy Technology.* Wiley Online Library. 2018

[4] S. Kouro et al., "Recent Advances and Industrial Applications of Multilevel Converters," in *IEEE Transactions on Industrial Electronics,* vol. 57, no. 8, pp. 2553-2580, Aug. 2010,

[5] J. Rodriguez et al., "Multilevel Converters: An Enabling Technology for High-Power Applications," in *Proceedings of the IEEE,* vol. 97, no. 11, pp. 1786-1817, Nov. 2009

[6] A. Lesnicar and R. Marquardt, "An innovative modular multilevel converter topology suitable for a wide power range," in *Proc. IEEE PowerTec Conf.*, Bologna, Italy, Jun. 2003, vol. 3, pp. 272–277.

[7] K. Sharifabadi, L. Harnefors, H.-P. Nee, S. Norrga, and R. Teodorescu, *Design, Control and Application of Modular Multilevel Converters for HVDC Transmission Systems.* United States: Wiley-IEEE press, 2016.

[8] D. Sixing, A. Dekka, B. Wu and N. Zargari, *Modular Multilevel Converters: Analysis Control and Applications,* Hoboken, NJ, USA:Wiley, Feb. 2018.

[9] A. Nami, J. Liang, F. Dijkhuizen and G. D. Demetriades, "Modular Multilevel Converters for HVDC Applications: Review on Converter Cells and Functionalities," in *IEEE Transactions on Power Electronics,* vol. 30, no. 1, pp. 18-36, Jan. 2015

[10] M. Saeedifard and R. Iravani, "Dynamic Performance of a Modular Multilevel Back-to-Back HVDC System," *IEEE Transactions on Power Delivery,* vol. 25, no. 4, pp. 2903-2912, Oct. 2010

[11] M. Vatani, B. Bahrani, M. Saeedifard and M. Hovd, "Indirect Finite Control Set Model Predictive Control of Modular Multilevel Converters," in *IEEE Transactions on Smart Grid,* vol. 6, no. 3, pp. 1520-1529, May 2015

[12] L. Harnefors, A. Antonopoulos, S. Norrga, L. Angquist and H. Nee, "Dynamic Analysis of Modular Multilevel Converters," in *IEEE Transactions on Industrial Electronics,* vol. 60, no. 7, pp. 2526-2537, July 2013

[13] A. Dekka, B. Wu, R. L. Fuentes, M. Perez and N. R. Zargari, "Evolution of Topologies, Modeling, Control Schemes, and Applications of Modular Multilevel Converters," *IEEE Journal of Emerging and Selected Topics in Power Electronics,* vol. 5, no. 4, pp. 1631-1656, Dec 2017

[14] A. Antonio-Ferreira, C. Collados-Rodriguez and O. Gomis-Bellmunt, "Modulation techniques applied to medium voltage modular multilevel converters for renewable energy integration: A review", *Electric Power Systems Research,* vol. 155, no. 7, pp. 21-39, Feb 2018

[15] S. Debnath, J. Qin, B. Bahrani, M. Saeedifard and P. Barbosa, "Operation, Control, and Applications of the Modular Multilevel Converter:

A Review," *IEEE Transactions on Power Electronics*, vol. 30, no. 1, pp. 37-53, Jan. 2015

[16] M. Hagiwara and H. Akagi, "Control and Experiment of Pulsewidth-Modulated Modular Multilevel Converters," in *IEEE Transactions on Power Electronics,* vol. 24, no. 7, pp. 1737-1746, July 2009

[17] L. Angquist, A. Antonopoulos, D. Siemaszko, K. Ilves, M. Vasiladiotis and H. Nee, "Open-Loop Control of Modular Multilevel Converters Using Estimation of Stored Energy," in *IEEE Transactions on Industry Applications,* vol. 47, no. 6, pp. 2516-2524, Nov.-Dec. 2011

[18] S. Wang, G. P. Adam, A. M. Massoud, D. Holliday and B. W. Williams, "Analysis and Assessment of Modular Multilevel Converter Internal Control Schemes," in *IEEE Journal of Emerging and Selected Topics in Power Electronics,* vol. 8, no. 1, pp. 697-719, March 2020,

[19] Q. Tu, Z. Xu and L. Xu, "Reduced Switching-Frequency Modulation and Circulating Current Suppression for Modular Multilevel Converters," in *IEEE Transactions on Power Delivery,* vol. 26, no. 3, pp. 2009-2017, July 2011

[20] S. Rohner, S. Bernet, M. Hiller and R. Sommer, "Modulation, Losses, and Semiconductor Requirements of Modular Multilevel Converters," in *IEEE Transactions on Industrial Electronics,* vol. 57, no. 8, pp. 2633-2642, Aug. 2010

[21] M. Hagiwara, R. Maeda and H. Akagi, "Control and Analysis of the Modular Multilevel Cascade Converter Based on Double-Star Chopper-Cells (MMCC-DSCC)," in *IEEE Transactions on Power Electronics,* vol. 26, no. 6, pp. 1649-1658, June 2011

[22] P. M. Meshram and V. B. Borghate, "A Simplified Nearest Level Control (NLC) Voltage Balancing Method for Modular Multilevel Converter (MMC)," in *IEEE Transactions on Power Electronics,* vol. 30, no. 1, pp. 450-462, Jan. 2015

[23] J. Pou, S. Ceballos, G. Konstantinou, V. G. Agelidis, R. Picas and J. Zaragoza, "Circulating Current Injection Methods Based on Instantaneous Information for the Modular Multilevel Converter," in *IEEE Transactions on Industrial Electronics,* vol. 62, no. 2, pp. 777-788, Feb. 2015,

[24] S. Li, X. Wang, Z. Yao, T. Li and Z. Peng, "Circulating Current Suppressing Strategy for MMC-HVDC Based on Nonideal Proportional Resonant Controllers Under Unbalanced Grid Conditions," in *IEEE Transactions on Power Electronics,* vol. 30, no. 1, pp. 387-397, Jan. 2015,

[25] J. Mei, B. Xiao, K. Shen, L. M. Tolbert and J. Y. Zheng, "Modular Multilevel Inverter with New Modulation Method and Its Application to Photovoltaic Grid-Connected Generator," in *IEEE Transactions on Power Electronics,* vol. 28, no. 11, pp. 5063-5073, Nov. 2013

[26] F. Deng and Z. Chen, "A Control Method for Voltage Balancing in Modular Multilevel Converters," in *IEEE Transactions on Power Electronics,* vol. 29, no. 1, pp. 66-76, Jan. 2014

[27] M. Zhang, L. Huang, W. Yao and Z. Lu, "Circulating Harmonic Current Elimination of a CPS-PWM-Based Modular Multilevel Converter With a Plug-In Repetitive Controller," in *IEEE Transactions on Power Electronics,* vol. 29, no. 4, pp. 2083-2097, April 2014

[28] K. Ilves, A. Antonopoulos, S. Norrga and H. Nee, "A New Modulation Method for the Modular Multilevel Converter Allowing Fundamental Switching Frequency," in *IEEE Transactions on Power Electronics,* vol. 27, no. 8, pp. 3482-3494, Aug. 2012

[29] Z. Li, P. Wang, Z. Chu, H. Zhu, Y. Luo and Y. Li, "An Inner Current Suppressing Method for Modular Multilevel Converters," in *IEEE Transactions on Power Electronics,* vol. 28, no. 11, pp. 4873-4879, Nov. 2013

[30] G. Bergna et al., "An Energy-Based Controller for HVDC Modular Multilevel Converter in Decoupled Double Synchronous Reference Frame for Voltage Oscillation Reduction," in *IEEE Transactions on Industrial Electronics,* vol. 60, no. 6, pp. 2360-2371, June 2013,

[31] J. -W. Moon, C. -S. Kim, J. -W. Park, D. -W. Kang and J. -M. Kim, "Circulating Current Control in MMC Under the Unbalanced Voltage," in *IEEE Transactions on Power Delivery,* vol. 28, no. 3, pp. 1952-1959, July 2013

[32] P. Hu and D. Jiang, "A Level-Increased Nearest Level Modulation Method for Modular Multilevel Converters," in *IEEE Transactions on Power Electronics,* vol. 30, no. 4, pp. 1836-1842, April 2015

[33] L. He, K. Zhang, J. Xiong and S. Fan, "A Repetitive Control Scheme for Harmonic Suppression of Circulating Current in Modular Multilevel Converters," in *IEEE Transactions on Power Electronics,* vol. 30, no. 1, pp. 471-481, Jan. 2015

[34] J. Qin and M. Saeedifard, "Reduced Switching-Frequency Voltage-Balancing Strategies for Modular Multilevel HVDC Converters," in *IEEE Transactions on Power Delivery,* vol. 28, no. 4, pp. 2403-2410, Oct. 2013

[35] S. Fan, K. Zhang, J. Xiong and Y. Xue, "An Improved Control System for Modular Multilevel Converters with New Modulation Strategy and Voltage Balancing Control," in *IEEE Transactions on Power Electronics,* vol. 30, no. 1, pp. 358-371, Jan. 2015

[36] R. Picas, J. Pou, S. Ceballos, J. Zaragoza, G. Konstantinou and V. G. Agelidis, "Optimal injection of harmonics in circulating currents of modular multilevel converters for capacitor voltage ripple minimization," *2013 IEEE ECCE Asia Downunder,* 2013, pp. 318-324

[37] K. Ilves, L. Harnefors, S. Norrga and H. Nee, "Predictive Sorting Algorithm for Modular Multilevel Converters Minimizing the Spread in

the Submodule Capacitor Voltages," in *IEEE Transactions on Power Electronics,* vol. 30, no. 1, pp. 440-449, Jan. 2015

[38] H. Saad, X. Guillaud, J. Mahseredjian, S. Dennetière and S. Nguefeu, "MMC Capacitor Voltage Decoupling and Balancing Controls," in *IEEE Transactions on Power Delivery,* vol. 30, no. 2, pp. 704-712, April 2015

[39] Q. Tu, Z. Xu and J. Zhang, "Circulating current suppressing controller in modular multilevel converter," *IECON 2010 - 36th Annual Conference on IEEE Industrial Electronics Society,* 2010, pp. 3198-3202

[40] R. Darus, J. Pou, G. Konstantinou, S. Ceballos, R. Picas and V. G. Agelidis, "A Modified Voltage Balancing Algorithm for the Modular Multilevel Converter: Evaluation for Staircase and Phase-Disposition PWM," in *IEEE Transactions on Power Electronics,* vol. 30, no. 8, pp. 4119-4127, Aug. 2015

[41] D. Siemaszko, "Fast Sorting Method for Balancing Capacitor Voltages in Modular Multilevel Converters," in *IEEE Transactions on Power Electronics,* vol. 30, no. 1, pp. 463-470, Jan. 2015

[42] L. Lin, Y. Lin, Z. He, Y. Chen, J. Hu and W. Li, "Improved Nearest-Level Modulation for a Modular Multilevel Converter With a Lower Submodule Number," in *IEEE Transactions on Power Electronics,* vol. 31, no. 8, pp. 5369-5377, Aug. 2016

[43] K. Ilves, A. Antonopoulos, L. Harnefors, S. Norrga, L. Ängquist and H. Nee, "Capacitor voltage ripple shaping in modular multilevel converters allowing for operating region extension," *IECON 2011 - 37th Annual Conference of the IEEE Industrial Electronics Society,* 2011, pp. 4403-4408

[44] K. Shen et al., "Elimination of Harmonics in a Modular Multilevel Converter Using Particle Swarm Optimization-Based Staircase Modulation Strategy," in *IEEE Transactions on Industrial Electronics,* vol. 61, no. 10, pp. 5311-5322, Oct. 2014

[45] B. Bahrani, S. Debnath and M. Saeedifard, "Circulating Current Suppression of the Modular Multilevel Converter in a Double-Frequency Rotating Reference Frame," in *IEEE Transactions on Power Electronics,* vol. 31, no. 1, pp. 783-792, Jan. 2016

[46] R. Picas, J. Pou, S. Ceballos, V. G. Agelidis and M. Saeedifard, "Minimization of the capacitor voltage fluctuations of a modular multilevel converter by circulating current control," *IECON 2012 - 38th Annual Conference on IEEE Industrial Electronics Society,* 2012, pp. 4985-4991

[47] A. Dekka, B. Wu, N. R. Zargari and R. L. Fuentes, "A Space-Vector PWM-Based Voltage-Balancing Approach With Reduced Current Sensors for Modular Multilevel Converter," in *IEEE Transactions on Industrial Electronics,* vol. 63, no. 5, pp. 2734-2745, May 2016

[48] A. Dekka, B. Wu and N. R. Zargari, "A Novel Modulation Scheme and Voltage Balancing Algorithm for Modular Multilevel Converter," in *IEEE Transactions on Industry Applications,* vol. 52, no. 1, pp. 432-443, Jan.-Feb. 2016

[49] J. Wang, J. Liang, C. Wang and X. Dong, "Circulating Current Suppression for MMC-HVDC under Unbalanced Grid Conditions," in *IEEE Transactions on Industry Applications,* vol. 53, no. 4, pp. 3250-3259, July-Aug. 2017

[50] P. Hu, R. Teodorescu, S. Wang, S. Li and J. M. Guerrero, "A Currentless Sorting and Selection-Based Capacitor-Voltage-Balancing Method for Modular Multilevel Converters," in *IEEE Transactions on Power Electronics,* vol. 34, no. 2, pp. 1022-1025, Feb. 2019

[51] S. Kolluri, N. B. Y. Gorla and S. K. Panda, "Capacitor Voltage Ripple Suppression in a Modular Multilevel Converter Using Frequency-Adaptive Spatial Repetitive-Based Circulating Current Controller," in *IEEE Transactions on Power Electronics,* vol. 35, no. 9, pp. 9839-9849

[52] Y. Xu, Z. Xu, Z. Zhang and H. Xiao, "A Novel Circulating Current Controller for MMC Capacitor Voltage Fluctuation Suppression," in *IEEE Access,* vol. 7, pp. 120141-120151, 2019

[53] D. Ronanki and S. S. Williamson, "Modified Phase-disposition PWM Technique for Modular Multilevel Converters," *2018 IEEE Transportation Electrification Conference and Expo (ITEC),* 2018, pp. 26-31

[54] G. Bergna-Diaz, J. A. Suul, E. Berne, J. Vannier and M. Molinas, "Optimal Shaping of the MMC Circulating Currents for Preventing AC-Side Power Oscillations From Propagating Into HVdc Grids," in *IEEE Journal of Emerging and Selected Topics in Power Electronics,* vol. 7, no. 2, pp. 1015-1030, June 2019

[55] A. Perez-Basante et al., "Circulating Current Control for Modular Multilevel Converters With (N+1) Selective Harmonic Elimination—PWM," in *IEEE Transactions on Power Electronics,* vol. 35, no. 8, pp. 8712-8725, Aug. 2020

[56] F. Deng, C. Liu, Q. Wang, R. Zhu, X. Cai and Z. Chen, "A Currentless Submodule Individual Voltage Balancing Control for Modular Multilevel Converters," in *IEEE Transactions on Industrial Electronics,* vol. 67, no. 11, pp. 9370-9382, Nov. 2020

[57] D. Samajdar, T. Bhattacharya and S. Dey, "A Reduced Switching Frequency Sorting Algorithm for Modular Multilevel Converter With Circulating Current Suppression Feature," in *IEEE Transactions on Power Electronics,* vol. 34, no. 11, pp. 10480-10491, Nov. 2019

[58] S. Yang, P. Wang, Y. Tang, M. Zagrodnik, X. Hu and K. J. Tseng, "Circulating Current Suppression in Modular Multilevel Converters With Even-Harmonic Repetitive Control," in *IEEE Transactions on Industry Applications,* vol. 54, no. 1, pp. 298-309, Jan.-Feb. 2018

[59] L. Yang, Y. Li, Z. Li, P. Wang, S. Xu and R. Gou, "Loss Optimization of MMC by Second-Order Harmonic Circulating Current Injection," in

IEEE Transactions on Power Electronics, vol. 33, no. 7, pp. 5739-5753, July 2018

[60] K. Wang, Y. Deng, H. Peng, G. Chen, G. Li and X. He, "An Improved CPS-PWM Scheme-Based Voltage Balancing Strategy for MMC With Fundamental Frequency Sorting Algorithm," in *IEEE Transactions on Industrial Electronics,* vol. 66, no. 3, pp. 2387-2397, March 2019

[61] Y. Luo, Z. Li, L. Xu, X. Xiong, Y. Li and C. Zhao, "An Adaptive Voltage-Balancing Method for High-Power Modular Multilevel Converters," in *IEEE Transactions on Power Electronics,* vol. 33, no. 4, pp. 2901-2912, April 2018

[62] J. Freytes et al., "Improving Small-Signal Stability of an MMC With CCSC by Control of the Internally Stored Energy," in *IEEE Transactions on Power Delivery,* vol. 33, no. 1, pp. 429-439, Feb. 2018

[63] B. P. McGrath, C. A. Teixeira and D. G. Holmes, "Optimized Phase Disposition (PD) Modulation of a Modular Multilevel Converter," in *IEEE Transactions on Industry Applications,* vol. 53, no. 5, pp. 4624-4633, Sept.-Oct. 2017

[64] J. Wang, X. Han, H. Ma and Z. Bai, "Analysis and Injection Control of Circulating Current for Modular Multilevel Converters," in *IEEE Transactions on Industrial Electronics,* vol. 66, no. 3, pp. 2280-2290, March 2019

[65] S. Yang, P. Wang and Y. Tang, "Feedback Linearization-Based Current Control Strategy for Modular Multilevel Converters," *IEEE Transactions on Power Electronics*, vol. 33, no. 1, pp. 161-174, Jan. 2018

[66] Z. Li, Q. Hao, F. Gao, L. Wu and M. Guan, "Nonlinear Decoupling Control of Two-Terminal MMC-HVDC Based on Feedback Linearization," *IEEE Transactions on Power Delivery,* vol. 34, no. 1, pp. 376-386, Feb. 2019

[67] Q. Yang, M. Saeedifard and M. A. Perez, "Sliding Mode Control of the Modular Multilevel Converter," in *IEEE Transactions on Industrial Electronics*, vol. 66, no. 2, pp. 887-897, Feb. 2019

[68] X. Yang, Z. Li, T. Q. Zheng, X. You and P. Kobrle, "Virtual Impedance Sliding Mode Control-Based MMC Circulating Current Suppressing Strategy," in *IEEE Access,* vol. 7, pp. 26229-26240, 2019

[69] M. Ahmadijokani, M. Mehrasa, M. Sleiman, M. Sharifzadeh, A. Sheikholeslami and K. Al-Haddad, "A Back-Stepping Control Method for Modular Multilevel Converters," *IEEE Transactions on Industrial Electronics*, vol. 68, no. 1, pp. 443-453, Jan. 2021

[70] X. Zhang, J. Huang, X. Zhang and X. Tong, "Backstepping based nonlinear control strategy for MMC topology," *IECON 2017 - 43rd Annual Conference of the IEEE Industrial Electronics Society*, 2017, pp. 5707-5712

[71] M. Ishfaq et al., "Output Current Control of Modular MultiLevel Converter Using BackStepping Controller," *2019 15th International Conference on Emerging Technologies (ICET)*, 2019, pp. 1-5

[72] R. Cisneros, R. Ortega, M. Pirro, G. Ippoliti, G. Bergna and M. M. Cabrera, "Global tracking passivity-based PI control for power converters: An application to the boost and modular multilevel converters," *2014 IEEE 23rd International Symposium on Industrial Electronics (ISIE),* 2014, pp. 1359-1365

[73] G. Bergna-Diaz, D. Zonetti, S. Sanchez, R. Ortega and E. Tedeschi, "PI Passivity-Based Control and Performance Analysis of MMC Multiterminal HVDC Systems," in *IEEE Journal of Emerging and Selected Topics in Power Electronics,* vol. 7, no. 4, pp. 2453-2466, Dec. 2019

[74] A. Dekka, B. Wu, V. Yaramasu, R. L. Fuentes and N. R. Zargari, "Model Predictive Control of High-Power Modular Multilevel Converters—An Overview," in *IEEE Journal of Emerging and Selected Topics in Power Electronics,* vol. 7, no. 1, pp. 168-183, March 2019

[75] M. Krstic, I. Kanellakopoulos and P. V. Kokotovic, *Nonlinear and Adaptive Control Design,* New York:Wiley, 1995.

[76] Y. Jin et al., "A Dual-Layer Back-Stepping Control Method for Lyapunov Stability in Modular Multilevel Converter Based STATCOM," in *IEEE Transactions on Industrial Electronics,* vol. 69, no. 3, pp. 2166-2179, March 2022

Chapter 3

Model Predictive Control for Modular Multilevel Converter

This chapter provides a brief overview of the existing model predictive control methods for modular multilevel converters and highlights the shortcomings that are addressed in this thesis.

3.1 Introduction

As indicated in the previous chapter, model predictive control is an effective technique for the control of MMC. In recent years, many techniques based on model predictive control have been presented. These techniques can be divided into the following categories:

- Finite Control Set MPC (FCS-MPC)
  - Switching state based MPC (SS-MPC)
  - Voltage level based MPC (VL-MPC)
- Continuous Control Set MPC (CCS-MPC)

As indicated from the names FCS-MPC evaluates a finite set to determine the optimal control whereas the control problem is treated as continuous in CCS-MPC. The FCS-MPC can be divided into SS-MPC and VL-MPC. The SS-MPC evaluates all the possible switching combinations for a predefined cost function and selects the one that minimizes this cost function. This method does not require a modulation stage. However, as the number of switching combinations increase, the computational complexity increases significantly. For HVDC applications, MMCs typically have SMs in the range from 200 SMs/arm to 400 SMs/arm. Therefore, the total number of switching states is very high which makes the computational complexity so high that real time application of SS-MPC becomes almost impossible.

In order to reduce the computational complexity, optimization based on voltage levels is proposed instead of switching combinations in VL-MPC. This significantly reduces the computational complexity with respect to SS-MPC.

Some of the main contributions of SS-MPC, VL-MPC, and CCS-MPC are presented next.

3.2 State of the Art

3.2.1 SS-MPC

One of the first attempts of predictive control was for a single-phase ac-ac MMC [1]. In this work, the output, input, and circulating current references are followed and capacitor voltages are also balanced. In addition, a reduced subset of switching states was also proposed. However, only two SMs/arm were considered and still the reduced set compromised of 361 switching states. A predictive control for a back-to-back HVDC system and for three phase DC-AC MMC are presented in [2, 3]. Both of these methods are based on a per-phase approach where each phase is treated independently. A direct current predictive controller with long prediction horizon for three-level MMC is presented in [4, 5]. The proposed methods control the output currents within tight bounds while ensuring good control

of circulating current and capacitor voltages. In addition, a term is added to the cost function to reduce the switching frequency. The method developed in [6] considers tracking of both balanced and unbalanced load currents. The comparison between cascade control and switching state based MPC for MMC is presented in [7]. A weighted cost function based on a normalized cost function is proposed in [15] with the aim to suppress the circulating currents properly. The method in [19] proposes a three phase MPC with common voltage injection to eliminate the circulating current control requirement. An MPC based on switching states grouping is proposed in [20] and each group is processed in parallel. The switching state that minimizes a predefined cost function in each group is selected in the first stage and then in the second stage only one switching state from each group is evaluated to determine the optimal switching combination. Reference [21] combines the branch and bound algorithm with sorting algorithm to enable long horizon MPC for modular multilevel converters. However, the computational complexity of SS-MPC makes its real time application complicated; therefore there has not been much research effort in this direction.

3.2.2 VL-MPC

In VL-MPC based methods, optimization is performed over voltage levels instead of switching states. In addition, the SM capacitor voltage balancing task is performed by a local controller using sorting techniques. For example, an MPC with reduced computational load *i.e.* $N+1$ instead of C_{2N}^{N} based on optimized voltage level is proposed in [8] where SM capacitor voltage balance is dealt by conventional sorting algorithm outside the MPC framework. However, only evaluating $N+1$ levels results in an unsatisfactory performance of circulating current. Moon *et al.*, [9] propose three stages of MPC where each stage has a separate cost function. First $N+1$ voltage levels are evaluated for stage-I *i.e.* ac-side tracking. Then in stage-II, three more levels are evaluated for circulating current control which are based on the observation that the same voltage level added or subtracted from both the arms does not have significant effect on ac-current tracking.

Finally, two different strategies with reduced complexity are proposed for capacitor voltage balance and switching frequency reduction. The same reference also presents MPC for unbalanced grid conditions. In [10], two indirect strategies are presented with reduced computational complexity where the SM capacitor voltage balancing task is performed by conventional sorting algorithm. In the first strategy, the combined total number of SMs to be switched on in both arms of each phase are not fixed to N, resulting in a computational complexity of $(N+1)^2$ with improved circulating current tracking. In the same paper, it is proposed to limit the maximum change in number of inserted SMs w.r.t previous sampling instant to one. This reduces the computational complexity to evaluating only 9 voltage levels at the cost of sluggish dynamic performance. A nearest level predictive control is proposed by F. Zhang and G. Joos [11] where the optimal voltage levels are directly calculated from the predicted values of ac-current and circulating current and then using a round function the optimal level is converted to an integer. However, such an approach neglects the bilinearity of the MMC model and can result in a coupled effect between circulating current and output current. A space vector based based hierarchical MPC by considering a reduced set of space vectors is proposed in [12] to reduce the computational burden of conventional MPC. P. Liu *et al.*, [13] reduced the overall computational burden to $2X + M + 3$ by distributing the SMs evenly into M groups with each containing X SMs. However, no details were provided on how to group the SMs. Experimental verification of the second strategy proposed in [10] with a different cost function is presented in [14]. A dual-stage MPC based on voltage vector redundancy in the first stage and SM redundancy in the second stage is proposed in [16]. This method achieves high dynamic performance and does not require a sorting algorithm. However, as the second stage is based on switching states the computational complexity of this method increases significantly with the increase in number of SMs as compared to [10,13,14]. F. Zhang *et al.*, [17], reduce the number of voltage levels to be evaluated by using a tolerance band of capacitor voltages. A predictive control for a three-phase model of an MMC including zero sequence voltage is presented in [18] to improve the steady-state performance. However, the dynamic response is reduced

as compared to MPC based on per-phase model. A variable nearest level control (VNLC) method combined with MPC is presented by J. Yin *et al.*, [22] where the control options generated by VNLC are evaluated by MPC. Modulated MPC is proposed in [23] to improve the steady-state response of FCS-MPC methods. In this method, the two voltage levels that minimize a predefined cost function are first identified and then duty cycles are calculated for each voltage level. However, the circulating current control is not very good due to limitation of duty cycle of the selected voltage levels. Similar to the idea in [10], it is proposed by J. Huang *et al.*, [24] to limit the change in the number of inserted SMs w.r.t the previous sampling instant in order to reduce the computational burden. In addition, a new sorting approach is presented where the SMs are divided into three groups and each group is assigned a priority based on arm current. Among these only one group needs the sorting process. Reference [25–28], reduces the computational burden by a pre-selection algorithm in which the calculation of inserted SMs is again based on the inserted SMs in previous sampling instant. However, these methods suffer from reduced dynamic performance as the allowed change in inserted SMs w.r.t previous sampling instant is limited to one. An increased level MPC is presented by X. Chen *et al.*, [29] where the computational burden is reduced based on the same idea of utilizing neighboring voltage levels w.r.t previous sampling instant. References [30, 31] propose to integrate phase-shifted PWM with MPC in order to improve the steady-state response. In contrast to [23], three voltage levels are considered in [30, 31]. Multistage MPC have been proposed in [32, 33] where in the front stage two voltage levels that minimize the cost function the most are selected. Then, in the back stage both of these voltage levels are used to predict state variables for two time steps into the future. The one that minimizes the cost at two time steps into the future is selected to be applied to the MMC. J. Yin *et al.*, [34], propose to directly generate arm voltage references using the prediction model and cost function of MPC. Then using the nearest level control and a sorting method, switch settings are sent to the MMC. However, this method ignores the bilinearity of the MMC. Similar to [34], the method in [35] uses the prediction model for the MMC to determine the arm voltage references and then uses

SM unified PWM for the modulation stage. An optimized pulse pattern in combination with model predictive control is presented in [36–38]. This approach is suitable for medium voltage MMC applications. X. Chen *et al.* [39] present two increased level MPC methods with reduced computational requirements. In the first method, using the prediction model of the ac-current the arm voltage references are determined in a first step. Then these voltage references are modified by evaluating more voltage levels in the vicinity to improve circulating current control. Finally, a sorting algorithm is applied. In the second method, the computational burden is further reduced by directly calculating optimal voltage level and arm summation voltage using the prediction model for the MMC. It is shown in [40], that an outer loop is also required with MPC to determine the correct circulating current reference in order to regulate summation voltages of MMC. Based on the discrete mathematical model of the MMC, the optimal voltage levels are determined directly and then phase carrier shifted PWM is used to improve steady-state response in [41]. A deadbeat predictive controller with a separate modulator is presented by J.Wang *et al.*, [42] to improve the steady state response and fix the switching frequency of conventional MPC techniques. Another method based on modulated MPC having computational complexity independent of the number of SMs was proposed in [43]. This method, first determines two voltage levels to control the ac-current and circulating current at the same time but without evaluating all voltage levels. Then it determines the arm voltage modulation references. A modulated MPC using the prediction model of the MMC to directly determine the required output voltage level is also presented in [44]. X. Liu *et al.* [45] solve the optimization problem from a Diophantine's equation point of view and directly determines the optimal voltage level. In addition, a novel strategy for sensorless operation of MMC is also presented in the same paper. In [46], variable rounding level nearest level control is combined with MPC. In this method, a proper rounding function is used with the nearest level control, and the resulting options are evaluated by MPC. A machine learning based method to emulate the behavior of MPC is presented by S.Wang *et al.*, [47]. A predictor based neural network FCS-MPC has been presented in [48]. The developed approach does not need the information

of model parameters and therefore the performance is claimed to be independent from model mismatch. Another machine learning based emulation of FCS-MPC is presented in [49]. A sliding discrete control set modulated MPC is proposed by Y. Jin *et al.*, [50]. The proposed method improves the circulating control as compared to [23]. Sequential phase shifted MPC has been presented in [51]. A Lyapunov based finite state MPC is proposed by X. Liu *et al.*, [52] where the cost function is based on the Lyapunov function derivative. The control option that gives most negative cost is selected in order to ensure stability. Some more methods based on machine learning and MPC are presented in [53–59]. X. Gao *et al.*, [60] proposed a model predictive control for wide frequency range for medium voltage motor drive applications. An arm current based model predictive control is proposed in [61] where the optimal voltage levels are directly determined from the discrete model of the MMC. A technique to reduce the computational complexity of MPC utilizing a three phase model of the MMC is presented in [62].

3.2.3 CCS-MPC

The CCS-MPC for MMC based on quadratic programming has been presented in [63, 64] where a bilinear MMC average model is linearised around the current operation point and a linear MPC algorithm based on a quadratic program (QP) is used to determine the reference voltages. In [65, 72], a comparison is provided between linear and non-linear MPC for MMC and it is shown that linear MPC does not give satisfactory results beyond a certain prediction horizon. Another quadratic programming based linear MPC with an improved prediction model for MMC is presented in [66] which gives better performance than [63, 64]. Based on [66], a simple state feedback controller is computed by solving an unconstrained LQR problem in [67] to enable easy implementation. Quadratic problems solved by infeasible active set have been presented in [68, 69]. Based on quadratic programming an MPC approach is also presented in [70]. The active set method has also been presented for three-phase MMC model based MPC in [71].

3.2.4 Summary of Shortcomings

SS-MPC based techniques for MMC have very high computational complexity which makes their real time implementation very difficult. This high computational complexity is due to the high number of switching states and the non-linear model of the MMC. Techniques such as sphere decoding exist in literature for linear models of power converters which can be easily extended for a prediction horizon upto 100. However, as per this author's best knowledge there is no technique for SS-MPC for MMC having high number of SMs that can be implemented in real-time.

VL-MPC techniques have seen much improvement in the recent years and some of them can be implemented in real-time for MMCs having large number of SMs. The techniques which evaluate all the voltage levels such as [8–10] have high computational burden and cannot be extended even for a prediction horizon of 2 or 3. Then there are techniques [11, 34, 35] and others which directly determine the optimal voltage levels from discrete time model of MMC. These methods would result in marginal stability as the summation voltages state is cancelled out by the derived controller. Therefore, these methods would require additional control over circulating current. In addition, these methods do not have a cost function and therefore cannot deal with multiple objectives. The methods [10, 25–28] and others based on limiting the change in insertion index w.r.t previous sampling instant have very low computational burden and can be implemented in real time for short prediction horizons. However, they have sluggish dynamic performance. The dual stage MPC technique [16] has a very good dynamic response but very high computational complexity as compared to indirect FCS-MPC strategies [8–10]. Most of the modulated MPC methods discussed above also need to evaluate all the voltage levels and therefore have high computational complexity. The modulated MPC method in [43] computational burden is independent of the number of SMs, however, it is not so easy to understand. Sliding discrete control set modulated MPC [50] dynamic and steady-state performance is highly dependent on the sliding discrete control set which is used to determine the change in insertion index w.r.t previous sampling instant. If it is kept small then a reduced dynamic

performance results and if it is kept large then steady state performance degrades.

Recently, a lot of approaches based on machine learning [47,53–59] have been presented. These methods can be divided into two categories. The first one tries to emulate the behavior of the FCS-MPC offline. These methods require huge amounts of data for training purposes. Therefore, a lot of time is needed to collect and clean this data. Moreover, if the data is obtained online using some simple, modestly performing controller, then the machine learning will learn modest performance control. Furthermore, the operating range of this category would be limited as the machine learning controller would be highly dependent on the model parameters of the system and its performance would be at best equivalent to the original FCS-MPC algorithm which it is trying to emulate.

The second category identifies the model parameters online using machine learning methods and uses these identified model parameters for the FCS-MPC stage. However, the model parameters are learned for an ultra local mathematical model of MMC which is linear. Therefore, these methods cannot match the performance of the FCS-MPC based methods which are based on the bilinear model of the MMC. Due to the nature of these methods, it can be said that they are model parameters independent because they do not need information about the model parameters. These methods have better performance than the FCS-MPC methods if both methods use ultra local mathematical model of the MMC and can also deal with model parameters mismatch. However, they further increase the computational burden of indirect FCS-MPC strategies as they add an additional online stage of system identification.

CCS-MPC techniques for MMC whose real time application is possible are based on a linearized model of the MMC. However, the linearized model is not accurate and results in reduced performance as compared to non-linear model of MMC for which non-linear MPC (NMPC) is required. However, as per this author's best knowledge, no real-time validation of NMPC for MMC has been conducted til date because of its high computa-

tional complexity.

Bibliography

[1] M. A. Perez, J. Rodriguez, E. J. Fuentes and F. Kammerer, "Predictive Control of AC–AC Modular Multilevel Converters," in *IEEE Transactions on Industrial Electronics,* vol. 59, no. 7, pp. 2832-2839, July 2012

[2] J. Qin and M. Saeedifard, "Predictive Control of a Modular Multilevel Converter for a Back-to-Back HVDC System," in *IEEE Transactions on Power Delivery,* vol. 27, no. 3, pp. 1538-1547, July 2012

[3] J. Qin and M. Saeedifard, "Predictive control of a three-phase DC-AC Modular Multilevel Converter," *2012 IEEE Energy Conversion Congress and Exposition (ECCE),* 2012, pp. 3500-3505

[4] B. S. Riar, T. Geyer and U. K. Madawala, "Model Predictive Direct Current Control of Modular Multi-level Converters," *2013 IEEE International Conference on Industrial Technology (ICIT),* 2013, pp. 582-587

[5] B. S. Riar, T. Geyer and U. K. Madawala, "Model Predictive Direct Current Control of Modular Multilevel Converters: Modeling, Analysis, and Experimental Evaluation," in *IEEE Transactions on Power Electronics,* vol. 30, no. 1, pp. 431-439, Jan. 2015

[6] R. N. Fard, H. Nademi and L. Norum, "Analysis of a Modular Multilevel inverter under the predicted current control based on Finite-Control-Set strategy," *2013 3rd International Conference on Electric Power and Energy Conversion Systems,* 2013, pp. 1-6

[7] J. Böcker, B. Freudenberg, A. The and S. Dieckerhoff, "Experimental Comparison of Model Predictive Control and Cascaded Control of the Modular Multilevel Converter," in *IEEE Transactions on Power Electronics,* vol. 30, no. 1, pp. 422-430, Jan. 2015

[8] Y. Wang, W. Cong, M. Li, N. Li, M. Cao and W. Lei, "Model predictive control of modular multilevel converter with reduced computational load," *2014 IEEE Applied Power Electronics Conference and Exposition - APEC 2014,* 2014, pp. 1776-1779

[9] J. Moon, J. Gwon, J. Park, D. Kang and J. Kim, "Model Predictive Control With a Reduced Number of Considered States in a Modular Multilevel Converter for HVDC System," in *IEEE Transactions on Power Delivery,* vol. 30, no. 2, pp. 608-617, April 2015

[10] M. Vatani, B. Bahrani, M. Saeedifard and M. Hovd, "Indirect Finite Control Set Model Predictive Control of Modular Multilevel Converters," in *IEEE Transactions on Smart Grid,* vol. 6, no. 3, pp. 1520-1529, May 2015

[11] F. Zhang and G. Joos, "A predictive nearest level control of modular multilevel converter," *2015 IEEE Applied Power Electronics Conference and Exposition (APEC),* 2015, pp. 2846-2851

[12] L. Huang, X. Yang, X. Ma, B. Zhang, L. Qiao and M. Tian, "Space-vectors based hierarchical model predictive control for a modular multilevel converter," *2015 IEEE Energy Conversion Congress and Exposition (ECCE),* 2015

[13] P. Liu, Y. Wang, W. Cong and W. Lei, "Grouping-Sorting-Optimized Model Predictive Control for Modular Multilevel Converter With Reduced Computational Load," in *IEEE Transactions on Power Electronics,* vol. 31, no. 3, pp. 1896-1907, March 2016

[14] Z. Gong, P. Dai, X. Yuan, X. Wu and G. Guo, "Design and Experimental Evaluation of Fast Model Predictive Control for Modular Multilevel

Converters," in *IEEE Transactions on Industrial Electronics,* vol. 63, no. 6, pp. 3845-3856, June 2016

[15] L. Ben-Brahim, A. Gastli, M. Trabelsi, K. A. Ghazi, M. Houchati and H. Abu-Rub, "Modular Multilevel Converter Circulating Current Reduction Using Model Predictive Control," in *IEEE Transactions on Industrial Electronics,* vol. 63, no. 6, pp. 3857-3866, June 2016

[16] A. Dekka, B. Wu, V. Yaramasu and N. R. Zargari, "Dual-Stage Model Predictive Control With Improved Harmonic Performance for Modular Multilevel Converter," in *IEEE Transactions on Industrial Electronics,* vol. 63, no. 10, pp. 6010-6019, Oct. 2016

[17] F. Zhang, W. Li and G. Joós, "A Voltage-Level-Based Model Predictive Control of Modular Multilevel Converter," in *IEEE Transactions on Industrial Electronics,* vol. 63, no. 8, pp. 5301-5312, Aug. 2016

[18] A. Dekka, B. Wu and N. R. Zargari, "An improved indirect model predictive control approach for modular multilevel converter," *IECON 2016 - 42nd Annual Conference of the IEEE Industrial Electronics Society,* 2016, pp. 5959-5964

[19] A. Dekka, B. Wu, V. Yaramasu and N. R. Zargari, "Model Predictive Control With Common-Mode Voltage Injection for Modular Multilevel Converter," in *IEEE Transactions on Power Electronics,* vol. 32, no. 3, pp. 1767-1778, March 2017

[20] A. Rashwan, M. A. Sayed, Y. A. Mobarak, G. Shabib and T. Senjyu, "Predictive Controller Based on Switching State Grouping for a Modular Multilevel Converter With Reduced Computational Time," in *IEEE Transactions on Power Delivery,* vol. 32, no. 5, pp. 2189-2198, Oct. 2017

[21] Z. Zhang, M. T. Larijani, W. Tian, X. Gao, J. Rodríguez and R. Kennel, "Long-horizon predictive current control of modular-multilevel converter HVDC systems," *IECON 2017 - 43rd Annual Conference of the IEEE Industrial Electronics Society,* 2017, pp. 4524-4530

[22] J. Yin, J. I. Leon, L. G. Franquelo and S. Vazquez, "A simple model predictive control strategy aiming at enhancing the performance of modular multilevel converters," *IECON 2017 - 43rd Annual Conference of the IEEE Industrial Electronics Society,* 2017, pp. 4247-4252

[23] H. Mahmoudi, M. Aleenejad and R. Ahmadi, "Modulated Model Predictive Control of Modular Multilevel Converters in VSC-HVDC Systems," in *IEEE Transactions on Power Delivery,* vol. 33, no. 5, pp. 2115-2124, Oct. 2018

[24] J. Huang et al., "Priority Sorting Approach for Modular Multilevel Converter Based on Simplified Model Predictive Control," in *IEEE Transactions on Industrial Electronics,* vol. 65, no. 6, pp. 4819-4830, June 2018

[25] B. Gutierrez and S. Kwak, "Modular Multilevel Converters (MMCs) Controlled by Model Predictive Control With Reduced Calculation Burden," in *IEEE Transactions on Power Electronics,* vol. 33, no. 11, pp. 9176-9187, Nov. 2018

[26] M. H. Nguyen, S. Kwak and J. Baek, "Improved Model Predictive Control Method for Modular Multilevel Converter (MMC) based on Insertion Indexes," *2018 IEEE Transportation Electrification Conference and Expo (ITEC),* 2018, pp. 119-123

[27] M. H. Nguyen and S. Kwak, "Simplified Indirect Model Predictive Control Method for a Modular Multilevel Converter," in *IEEE Access,* vol. 6, pp. 62405-62418, 2018

[28] B. Gutierrez and S. Kwak, "Model predictive control method with preselected control options for reduced computational complexity in modular multilevel converters (MMCs)," *2018 20th European Conference on Power Electronics and Applications (EPE'18 ECCE Europe),* 2018, pp. P.1-P.8.

[29] X. Chen, J. Liu, S. Ouyang, S. Song, H. Wu and X. Hu, "A Increased-Levels Model Predictive Control Method for Modular Multilevel Converter With Reduced Computation Burden," *2018 IEEE Energy Conversion Congress and Exposition (ECCE),* 2018, pp. 3976-3979

[30] D. Zhou, S. Yang and Y. Tang, "Integrating Phase-Shifted Pulse-Width Modulation to Model Predictive Current Control of Modular Multilevel Converters," *2018 IEEE Energy Conversion Congress and Exposition (ECCE),* 2018, pp. 4845-4850

[31] D. Zhou, S. Yang, and Y. Tang, "Model predictive current control of modular multilevel converters with phase-shifted pulse-width modulation," in *IEEE. Trans. Ind. Electron.*, vol. 66, no. 6, pp. 4368–4378, Jun. 2019.

[32] P. Guo, Y. Li, Z. He, Y. Yue, Q. Xu and A. Luo, "Multistage Model Predictive Control for Modular Multilevel Converter," *2018 IEEE International Power Electronics and Application Conference and Exposition (PEAC),* 2018, pp. 1-5

[33] P. Guo et al., "A Novel Two-Stage Model Predictive Control for Modular Multilevel Converter With Reduced Computation," in *IEEE Transactions on Industrial Electronics,* vol. 66, no. 3, pp. 2410-2422, March 2019

[34] J. Yin, J. I. Leon, L. G. Franquelo, S. Vazquez and A. Marquez, "Generating the Arm Voltage References of Modular Multilevel Converters Employing Predictive Technique," *IECON 2018 - 44th Annual Conference of the IEEE Industrial Electronics Society,* 2018, pp. 3949-3954

[35] Z. Gong, X. Wu, P. Dai and R. Zhu, "Modulated Model Predictive Control for MMC-Based Active Front-End Rectifiers Under Unbalanced Grid Conditions," in *IEEE Transactions on Industrial Electronics,* vol. 66, no. 3, pp. 2398-2409, March 2019

[36] M. Vasiladiotis, A. Christe and T. Geyer, "Model Predictive Pulse Pattern Control for Modular Multilevel Converters," in *IEEE Transactions on Industrial Electronics,* vol. 66, no. 3, pp. 2423-2431, March 2019

[37] V. Spudić and T. Geyer, "Model Predictive Control Based on Optimized Pulse Patterns for Modular Multilevel Converter STATCOM," in *IEEE Transactions on Industry Applications,* vol. 55, no. 6, pp. 6137-6149, Nov.-Dec. 2019

[38] V. Spudić and T. Geyer, "Fast control of a modular multilevel converter STATCOM using optimized pulse patterns," *2017 IEEE Energy Conversion Congress and Exposition (ECCE),* 2017, pp. 2707-2714

[39] X. Chen, J. Liu, S. Song, S. Ouyang, H. Wu and Y. Yang, "Modified Increased-Level Model Predictive Control Methods With Reduced Computation Load for Modular Multilevel Converter," in *IEEE Transactions on Power Electronics,* vol. 34, no. 8, pp. 7310-7325, Aug. 2019

[40] W. Tian, X. Gao and R. Kennel, "Model Predictive Control of Modular Multilevel Converters with Independent Arm-Balancing Control," *2019 IEEE International Symposium on Predictive Control of Electrical Drives and Power Electronics (PRECEDE),* 2019, pp. 1-5

[41] M. H. Nguyen, S. Kwak and T. Kim, "Phase-Shifted Carrier Pulse-Width Modulation Algorithm With Improved Dynamic Performance for Modular Multilevel Converters," in *IEEE Access,* vol. 7, pp. 170949-170960, 2019

[42] J. Wang, Y. Tang, P. Lin, X. Liu and J. Pou, "Deadbeat Predictive Current Control for Modular Multilevel Converters With Enhanced Steady-State Performance and Stability," in *IEEE Transactions on Power Electronics,* vol. 35, no. 7, pp. 6878-6894, July 2020

[43] J. Wang, X. Liu, Q. Xiao, D. Zhou, H. Qiu and Y. Tang, "Modulated Model Predictive Control for Modular Multilevel Converters With Easy Implementation and Enhanced Steady-State Performance," in *IEEE*

Transactions on Power Electronics, vol. 35, no. 9, pp. 9107-9118, Sept. 2020

[44] P. M. Gajare, R. Chakraborty and A. Dey, "A Simplified Modulated Model Predictive Control for Modular Multilevel Converter," *2020 IEEE First International Conference on Smart Technologies for Power, Energy and Control (STPEC),* 2020, pp. 1-6

[45] X. Liu et al., "A Fast Finite-Level-State Model Predictive Control Strategy for Sensorless Modular Multilevel Converter," in *IEEE Journal of Emerging and Selected Topics in Power Electronics,* vol. 9, no. 3, pp. 3570-3581, June 2021

[46] J. Yin et al., "Variable Rounding Level Control Method for Modular Multilevel Converters," in *IEEE Transactions on Power Electronics,* vol. 36, no. 4, pp. 4791-4801, April 2021

[47] S. Wang, T. Dragicevic, Y. Gao and R. Teodorescu, "Neural Network Based Model Predictive Controllers for Modular Multilevel Converters," in *IEEE Transactions on Energy Conversion,* vol. 36, no. 2, pp. 1562-1571, June 2021

[48] X. Liu et al., "Predictor-Based Neural Network Finite-Set Predictive Control for Modular Multilevel Converter," in *IEEE Transactions on Industrial Electronics,* vol. 68, no. 11, pp. 11621-11627, Nov. 2021

[49] S. Wang, T. Dragicevic, G. F. Gontijo, S. K. Chaudhary and R. Teodorescu, "Machine Learning Emulation of Model Predictive Control for Modular Multilevel Converters," in *IEEE Transactions on Industrial Electronics,* vol. 68, no. 11, pp. 11628-11634, Nov. 2021

[50] Y. Jin et al., "A Novel Sliding-Discrete-Control-Set Modulated Model Predictive Control for Modular Multilevel Converter," in *IEEE Access,* vol. 9, pp. 10316-10327, 2021

[51] P. Poblete, S. Neira, R. P. Aguilera, J. Pereda and J. Pou, "Sequential Phase-Shifted Model Predictive Control for Modular Multilevel Converters," in *IEEE Transactions on Energy Conversion,* vol. 36, no. 4, pp. 2691-2702, Dec. 2021

[52] X. Liu et al., "Lyapunov-Based Fast Finite-State Model Predictive Control for Sensorless Three-Phase Four-Arm MMC," in *IEEE Journal of Emerging and Selected Topics in Power Electronics*

[53] W. Wu et al., "Model-Free Sequential Predictive Control for MMC with Variable Candidate Set," in *IEEE Journal of Emerging and Selected Topics in Power Electronics*

[54] X. Liu et al., "Event-Triggered Neural-Predictor-Based FCS-MPC for MMC," in *IEEE Transactions on Industrial Electronics,* vol. 69, no. 6, pp. 6433-6440, June 2022

[55] X. Liu et al., "Neural Predictor-Based Low Switching Frequency FCS-MPC for MMC With Online Weighting Factors Tuning," in *IEEE Transactions on Power Electronics,* vol. 37, no. 4, pp. 4065-4079, April 2022

[56] X. Liu et al., "Neural Predictor-Based Dynamic Surface Predictive Control for Power Converters," in *IEEE Transactions on Industrial Electronics*

[57] X. Liu et al., "Event-Triggered ESO-Based Robust MPC for Power Converters," in *IEEE Transactions on Industrial Electronics*

[58] X. Liu et al., "Data-Driven Neural Predictors-Based Robust MPC for Power Converters," in *IEEE Transactions on Power Electronics,* vol. 37, no. 10, pp. 11650-11661, Oct. 2022

[59] X. Liu, L. Qiu, Y. Fang, K. Wang, Y. Li and J. Rodríguez, "A Fuzzy Approximation for FCS-MPC in Power Converters," in *IEEE Transactions on Power Electronics,* vol. 37, no. 8, pp. 9153-9163, Aug. 2022

[60] X. Gao, W. Tian, Y. Pang and R. Kennel, "Model-Predictive Control for Modular Multilevel Converters Operating at Wide Frequency Range With a Novel Cost Function," in *IEEE Transactions on Industrial Electronics,* vol. 69, no. 6, pp. 5569-5580, June 2022

[61] M. Li, X. Chang, N. Dong, S. Liu, H. Yang and R. Zhao, "Arm-Current-Based Model Predictive Control for Modular Multilevel Converter Under Unbalanced Grid Conditions," in *IEEE Journal of Emerging and Selected Topics in Power Electronics,* vol. 10, no. 3, pp. 3195-3206, June 2022

[62] N. Chai, W. Tian, X. Gao, J. Rodriguez, M. L. Heldwein and R. Kennel, "Three-phase Model-based Predictive Control Methods with Reduced Calculation Burden for Modular Multilevel Converters," in *IEEE Journal of Emerging and Selected Topics in Power Electronics*

[63] G. Darivianakis, T. Geyer and W. van der Merwe, "Model predictive current control of modular multilevel converters," *2014 IEEE Energy Conversion Congress and Exposition (ECCE),* 2014, pp. 5016-5023

[64] T. Geyer, G. Darivianakis and W. van der Merwe, "Model predictive control of a STATCOM based on a modular multilevel converter in delta configuration," *2015 17th European Conference on Power Electronics and Applications (EPE'15 ECCE-Europe),* 2015, pp. 1-10

[65] S. Fuchs and J. Biela, "Impact of the Prediction Error on the Performance of Model Predictive Controllers with Long Prediction Horizons for Modular Multilevel Converters - Linear vs. Nonlinear System Models," *2018 20th European Conference on Power Electronics and Applications (EPE'18 ECCE Europe),* 2018, pp. P.1-P.9

[66] S. Fuchs, M. Jeong and J. Biela, "Long Horizon, Quadratic Programming Based Model Predictive Control (MPC) for Grid Connected Modular Multilevel Converters (MMC)," *IECON 2019 - 45th Annual Conference of the IEEE Industrial Electronics Society,* 2019, pp. 1805-1812

[67] M. Jeong, S. Fuchs and J. Biela, "High Performance LQR Control of Modular Multilevel Converters with Simple Control Structure and Implementation," *2020 22nd European Conference on Power Electronics and Applications (EPE'20 ECCE Europe),* 2020, pp. P.1-P.10

[68] W. Tian, Y. Pang, X. Gao, Q. Yang and R. Kennel, "Computationally Efficient Optimization Method for Model Predictive Pulse Pattern Control of Modular Multilevel Converters," *2020 IEEE Energy Conversion Congress and Exposition (ECCE), 2020,* pp. 5723-5730

[69] X. Gao, W. Tian, Q. Yang and R. Kennel, "Model Predictive Control for Modular Multilevel Converters based on a Box-constrained Quadratic Problem Solver," *2020 IEEE 9th International Power Electronics and Motion Control Conference (IPEMC2020-ECCE Asia), 2020,* pp. 3068-3072

[70] J. Yin, J. I. Leon, M. A. Perez, L. G. Franquelo, A. Marquez and S. Vazquez, "Model Predictive Control of Modular Multilevel Converters Using Quadratic Programming," in *IEEE Transactions on Power Electronics,* vol. 36, no. 6, pp. 7012-7025, June 2021

[71] X. Gao et al., "Modulated Model Predictive Control of Modular Multilevel Converters Operating in a Wide Frequency Range," in *IEEE Transactions on Industrial Electronics,* 2022

[72] Reyes Dreke, Victor Daniel, and Mircea Lazar. "Long-Horizon Nonlinear Model Predictive Control of Modular Multilevel Converters." in *Energies* 15.4 (2022): 1376.

Chapter 4

Modified Reduced Indirect Model Predictive Control for the Modular Multilevel Converter

This chapter first provides an introduction to indirect FCS-MPC and reduced indirect FCS-MPC strategies. Then a modified reduced indirect FCS-MPC is proposed to overcome the disadvantages of both strategies with a reduced computational burden.

The proposed approach achieves nearly similar dynamic performance as the full indirect FCS-MPC, at a much lower computational burden. The proposed method is developed from the reduced indirect FCS-MPC which is a computationally efficient control strategy for MMCs. However, the reduced indirect FCS-MPC approach compromises on the dynamic performance of the converter. In the proposed approach, the issue of slow dynamic performance is addressed by allowing the number of inserted modules to change by more than one only in the initial time step within the prediction horizon. The results of the proposed methodology are validated through simulations for 21-level MMC in MATLAB/Simulink.

4.1 Indirect FCS-MPC

Indirect FCS-MPC was originally proposed in [1] to overcome the disadvantages of direct FCS-MPC. In direct FCS-MPC all the possible switching combinations are evaluated against a predefined cost function. The switching combination that minimizes this cost function is then applied to the power converter. MMCs for high voltage applications such as HVDC transmission have very high number of SMs which results in increased number of switches and hence total number of switching combinations. Therefore, the computational complexity of direct FCS-MPC is very high and cannot be implemented in real-time for MMC applications where number of SMs are large. The computational complexity grows with C_N^{2N} *i.e.*, N combinations of $2N$ options are considered to select the best option for each phase where N are the number of SMs in each arm of each phase.

In indirect FCS-MPC it is proposed to do optimization over voltage levels instead of switching states. The number of voltage levels in each arm are $N+1$, therefore, the computational complexity of indirect FCS-MPC becomes $(N+1)^2$. This is a significantly lower computational burden as compared to direct FCS-MPC. In addition, a sorting algorithm is used to carry out the capacitors voltage balancing. The sorting algorithm can be performed by a local controller which may be implemented in a Field Programmable Gate Array (FPGA). Therefore, only summation of capacitor voltages is required by the central controller instead of all the individual capacitor voltage measurements. The central controller receives the measurements from MMC and sends the insertion indices $n_{u,j}$, $n_{l,j}$ to the local controller which performs a sorting algorithm and decides the switching combination to be sent to MMC.

4.1.1 Reference Signals

The reference value for the ac-side current can be obtained based on the power equations in the dq frame [2] which is given as follows:

$$i_d = \frac{2}{3}\frac{Pv_d + Qv_q}{v_d^2 + v_q^2} \tag{4.1a}$$

$$i_q = \frac{2}{3}\frac{Pv_q - Qv_d}{v_d^2 + v_q^2} \tag{4.1b}$$

The *abc* frame reference current can be obtained by *dq* to *abc* transformation. The reference for the ac-current is propagated to the next time instant using Lagrange extrapolation. The reference for the circulating current is constant and is set in order to minimize the ac-component in the circulating current, therefore, its reference is based on the real power transferred to the dc-side and is given by [5]:

$$I_{dc,ref} = -\frac{P}{V_{dc,ref}}, I_{cir,ref} = \frac{I_{dc,ref}}{3} \tag{4.2}$$

Finally, the reference for the summation voltages is set to $V_{dc,ref}$.

4.1.2 Cost Function

The model of the MMC was derived in chapter 2. In indirect FCS-MPC, the discretized version of MMC model in (2.15) is used to predict the states one step ahead for all possible insertion indices. The index that minimizes the cost function is then selected. The per-phase cost function for the indirect FCS-MPC was chosen as following in [1]:

$$\begin{aligned} J_j = q_1|i_{v,j,ref}(k+1) - i_{v,j}(k+1)| + q_2|i_{cir,ref}(k+1) - i_{cir,j}(k+1)| \\ + q_3|V_{dc} - v_{u,j}^{\Sigma}(k+1)| + q_4|V_{dc} - v_{l,j}^{\Sigma}(k+1)| \end{aligned} \tag{4.3}$$

where q_1 to q_4 are the weighting factors to set the relative priority of different objectives. The first term in the cost function is to minimize the ac-current error. The second term is used to minimize the ac-component of the circulating currents. The third and fourth term are to regulate the summation voltages to V_{dc}.

4.1.3 Summary

The working of indirect FCS-MPC in [1] can be summarized as:

- Predict the states for all the possible insertion indices *i.e.* $(N+1)^2$ options in total using (2.15).
- The option that minimizes the cost function (4.3) is selected
- Application of a sorting algorithm by a local controller for capacitor voltage balancing

The conventional sorting algorithm [3] is used to perform the SM capacitor voltage balancing task. When the arm current is positive then among the SMs, the least charged are inserted, and in case the arm current is negative the SMs which are most charged are inserted. In this manner voltage balancing task is performed.

The flowchart for the conventional sorting algorithm and indirect FCS-MPC implementation are shown in Fig. 4.1 and Fig. 4.2 respectively.

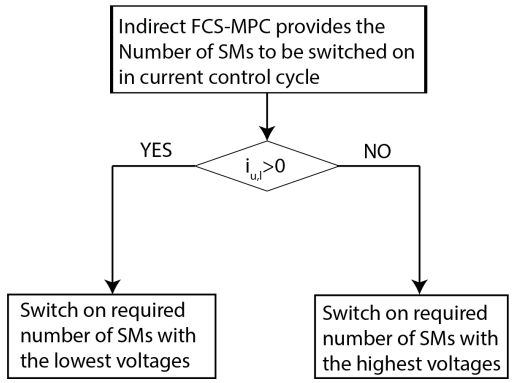

Figure 4.1: Conventional Sorting Algorithm

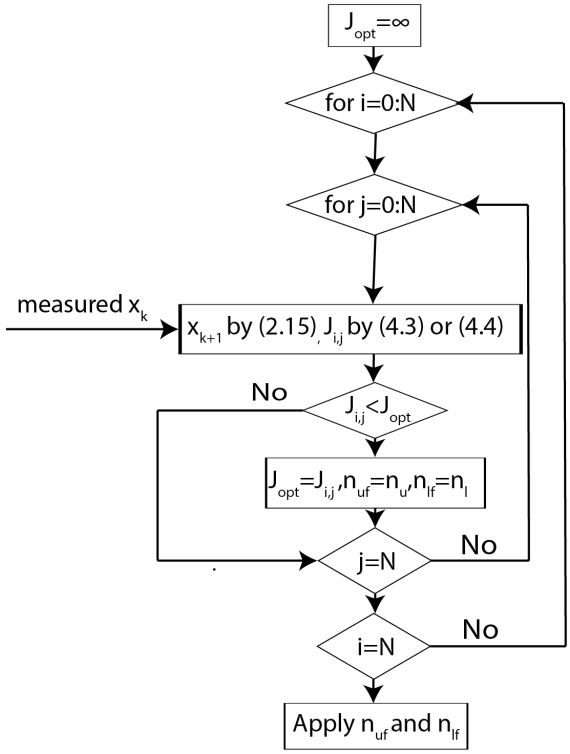

Figure 4.2: Full Indirect FCS-MPC Flowchart

4.2 Reduced Indirect FCS-MPC

Although indirect FCS-MPC significantly reduces the computational complexity as compared to direct FCS-MPC, it still has a high computational complexity when the number of SMs are large. Therefore, a reduced indirect FCS-MPC strategy has also been presented in [1].

The key idea behind reduced indirect FCS-MPC is to reduce the number of voltage levels evaluated at each time step. This is achieved by only considering the neighboring index values with respect to previous sampling

instant. This neighborhood was fixed to one in [1]. As a result, the computational complexity is drastically reduced and only 9 control options need to be evaluated at each time step within the prediction horizon. This also leads to a simplification of the sorting algorithm as now only the maximum and minimum SM voltages need to be found rather than sorting all the capacitor voltages [1].

The idea of limiting the change in insertion index to its neighborhood w.r.t previous sampling instant is reasonable for steady-state operation. However, this leads to a slow dynamic response. The flowchart of the reduced indirect FCS-MPC and modified sorting algorithm are shown in Fig. 4.3 and Fig. 4.4 respectively.

4.3 Modified Reduced Indirect FCS-MPC

The full indirect FCS-MPC developed in [1] still has a higher computational complexity *i.e.* $(N+1)^{2p}$ for a prediction horizon of p, as there are $(N+1)$ voltage levels to be selected in each arm. Whereas the reduced indirect FCS-MPC in [1], that reduced the number of possible actions for each leg to just nine per time step compromises on the dynamic response of system.

Therefore, a high performance/low complexity reduced FCS-MPC is proposed which results in nearly similar dynamic performance as given by full indirect FCS-MPC at a much lower computational burden.

An extended prediction horizon reduced FCS-MPC allows for considering different choices for changes in insertion indices at each time step in the prediction horizon. Clearly, changes of 0 and $+/-1$ should be considered at every time step, to allow for operation at or near steady state. In addition, we allow for larger changes in insertion index at the initial time step, to allow for reacting faster to large disturbances or reference changes. Therefore, in this work we consider changes in insertion index of 0, $+/-1$, and $+/-5$ at the initial time step only, and 0, $+/-1$ for all subsequent time steps. This in turn increases the number of possible actions to 25 (as there are now only five voltage levels to be selected in each arm) for the initial time step within the prediction horizon, while there are nine options for

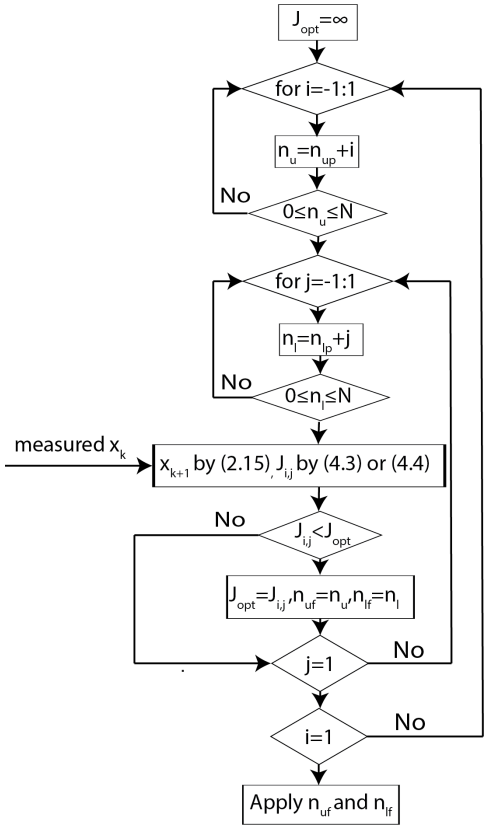

Figure 4.3: Reduced Indirect FCS-MPC Flowchart

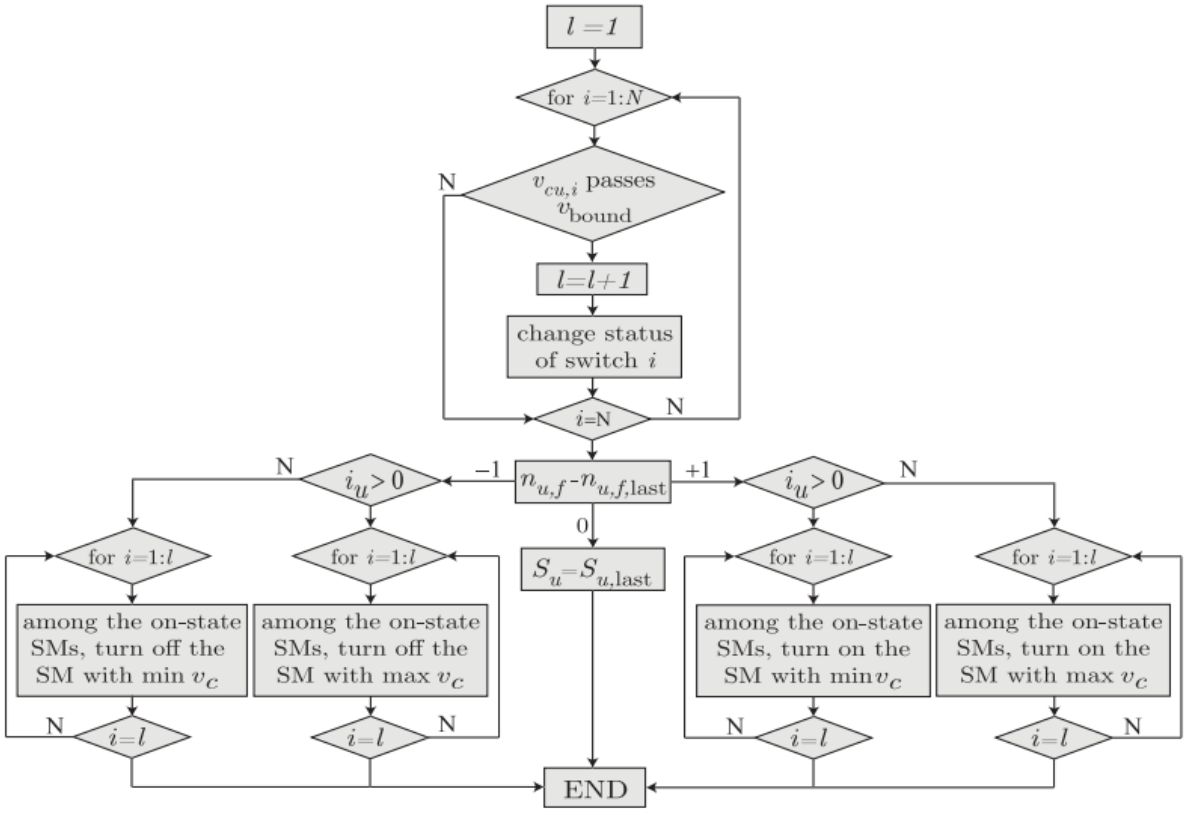

Figure 4.4: Modified Sorting Algorithm with Reduced Indirect FCS-MPC [1]

the following time steps, as in [1]. This approach has much lower computational burden as compared to full indirect FCS-MPC but nearly similar dynamic performance as will be demonstrated in simulations. It is noted that the changes other than $+/-5$ may have to be included for MMCs with larger number of SMs. The comparison of the number of control options considered by different approaches for a prediction horizon of three steps for an MMC with 20 SMs per arm is shown in Table 4.1.

Table 4.1: Number of possible control options for different FCS-MPC strategies (p=3, 20 SMs/arm)

Full Indirect FCS-MPC $(N+1)^{2p}$	**Reduced Indirect FCS-MPC** $(3)^{2p}$	**Modified Reduced Indirect FCS-MPC** $25 \cdot (3)^{2(p-1)}$
85,766,121	729	2,025

It can be noted from Table 4.1 that the proposed method has slightly more computational complexity than reduced indirect FCS-MPC but much less computational complexity as compared to full indirect FCS-MPC. This added computational complexity to reduced indirect FCS-MPC is needed to improve the dynamic response of the system.

4.3.1 Modified Cost Function

The cost function in (4.3) or similar cost functions which try to regulate instantaneous summation voltages to V_{dc} in each arm have a certain drawback. This is because the ripple in the capacitor voltages cannot be eliminated completely, and therefore the instantaneous summation voltages cannot have a constant reference. The actual goal is to regulate the average of summation voltages to V_{dc}. From the theory on MMCs [4], it is well known that there are two inputs and four outputs. Therefore, all the four objectives cannot be met at the same time. The output ac-current tracking is the most important task and no compromise can be made on its performance. Thus, it is the circulating current that should be altered in order to regulate the average of summation voltages to V_{dc} in each arm. Therefore,

the cost function (4.3) with the circulating current reference as in (4.2) cannot result in regulation of summation voltages on average to V_{dc}. It will be shown in the simulations that using such a cost function would result in a slow drift of summation voltages away from the reference. Therefore, an outer loop as in [5] on circulating current reference or the equivalent of outer loop within MPC implementation as in [6] have been proposed to be used with MPC.

During this PhD, a novel cost function was proposed that meets all the objectives of MMC without the need of an outer loop or its equivalent within MPC implementation. The proposed cost function is given as follows:

$$\begin{aligned} J_j = \lambda_1(i_{v,j,ref}(k+1) - i_{v,j}(k+1))^2 + \lambda_2(i_{cir,ref} - i_{cir,j}(k+1))^2 \\ + \lambda_3(2v_{dc,ref} - v^{\Sigma}_{u,j,avg} - v^{\Sigma}_{l,j,avg})(i_{cir,ref} - i_{cir,j}(k+1)) \\ + \lambda_4(v^{\Sigma}_{u,j,avg} - v^{\Sigma}_{l,j,avg})\Delta W(k+1) \end{aligned} \quad (4.4)$$

The λ's are the weighting factors for setting the relative importance between the control objectives. The first term is to regulate the ac-side current to its reference, the second term ensures that the ac-components in the circulating current are minimized, the third and fourth term regulate the total leg voltage to $2V_{dc}$ and arm voltage difference to zero respectively. ΔW is the instantaneous energy difference between the lower and upper arm. The third and fourth term in (4.4) are the new terms that have been introduced. It is easy to see from (4.4) that the third term will have an effect only when the total leg voltage on average is not regulated to $2V_{dc}$. Similarly, the fourth term would have an effect on optimization if the average difference between the arm voltages is not regulated to zero. The average voltages are obtained through moving average filters. The third term results in an increase in the circulating current if the sum of average summation voltage of arms is less than $2V_{dc}$. As a result, the SMs capacitors will be charged more. Similarly, the third term would decrease the circulating current if the sum of average summation voltages of arms is more than $2V_{dc}$. In a similar fashion, the last term in the cost function

would try to minimize the average summation voltage difference between the arms. The change in ΔW can be expressed as [7]:

$$\frac{dW_{\Delta}}{dt} = \left(\frac{n_{u,j}}{N} v_{u,j}^{\Sigma} + \frac{n_{l,j}}{N} v_{l,j}^{\Sigma}\right) \frac{-i_{v,j}}{2} + \left(\frac{n_{u,j}}{N} v_{u,j}^{\Sigma} - \frac{n_{l,j}}{N} v_{l,j}^{\Sigma}\right) i_{cir,j} \qquad (4.5)$$

In the above expression, it is easy to see that the first term in (4.5) would be predominantly sinusoidal at the fundamental frequency. This is because the sum of voltages of both arms would be close to $2V_{dc}$ *i.e.*, a constant, if the second harmonic component is ignored and $i_{v,j}$ has a fundamental frequency sinusoidal component. The second term in (4.5) would also be predominantly sinusoidal because the voltage difference of the two arms is sinusoidal at the fundamental frequency, while $i_{cir,j}$ would be close to a dc component. Therefore, (4.5) would be a predominantly sinusoidal signal unless the first and second term cancel each other perfectly. This implies that the integral *i.e.* W_{Δ} would be a sinusoidal signal. With this in mind, it is easy to see that the last term in the objective function becomes a sinusoidal term if $v_{u,j,avg}^{\Sigma} - v_{l,j,avg}^{\Sigma}$ is not equal to zero. This sinusoidal term is then indirectly compensated by the minimization converging to a situation with a corresponding (transient) sinusoidal term in the circulating current. It is further noted that sign of q_4 needs to be reversed when active power changes direction as the sinusoidal term in (4.5) would also change phase by 180^0.

4.3.2 Summary

The working of modified reduced indirect FCS-MPC can be summarized as:

- Predict the states for the reduced set of insertion indices *i.e.* 25 options in total using (2.15).
- The option that minimizes the cost function (4.4) is selected
- Application of sorting algorithm by a local controller for capacitor voltage balancing

The flowchart for the modified reduced indirect FCS-MPC implementation is shown in Fig. 4.5.

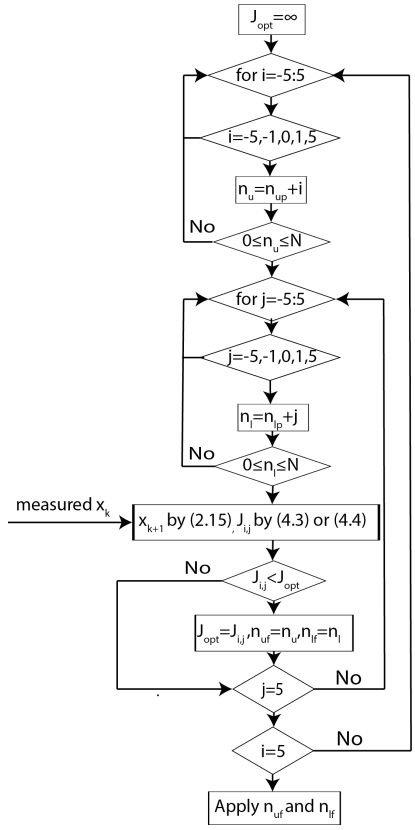

Figure 4.5: Modified Reduced Indirect FCS-MPC flowchart

4.4 Simulation Results

The performance of the proposed strategy is validated by performing simulations on a three-phase MMC with 20 SMs per arm, as shown in Fig.

4.6, and compared with the strategies proposed in [1].The synchronization of the system with grid is achieved by using a dq-frame phase locked loop (PLL). The PLL is working to align the d-axis to the grid voltage vector in steady state. All the references and measurements are sent to the proposed MPC controller which outputs the optimal insertion index for each phase. These insertion indices are then sent to the voltage balancing module which determines the gating signals for the MMC.

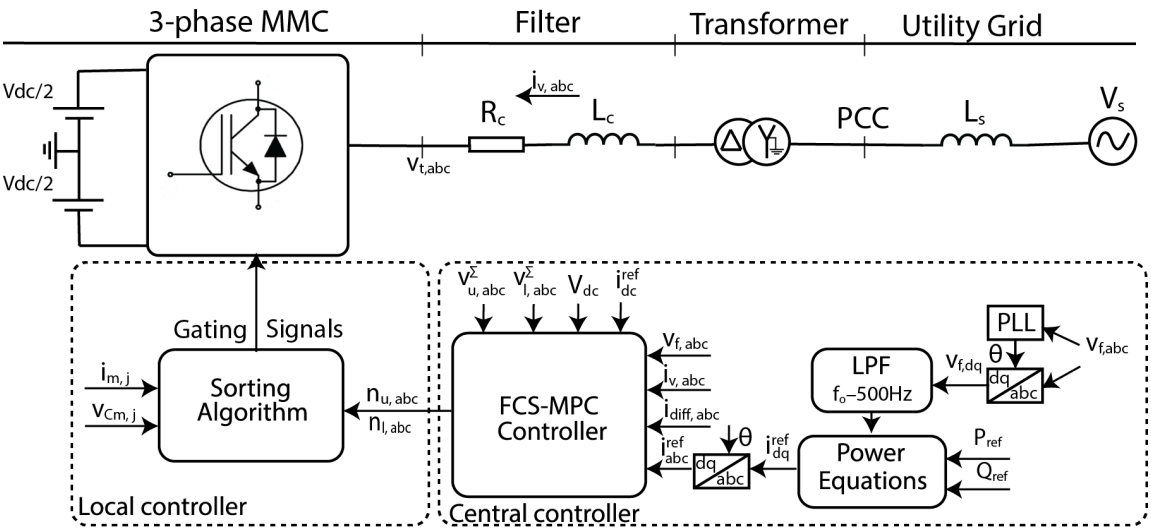

Figure 4.6: Control Block Diagram

The scenario used for simulation is such that at t=0s the reference values of active and reactive power are set to 25 MW and 0 MVar , respectively and at t = 0.5s a real power reversal command is applied by changing active power set point to −25 MW. The weighting factors of the cost function in (15) are set to $\lambda_1 = 1$, $\lambda_2 = 0.3$, $\lambda_3 = 0.016$ and $\lambda_4 = 0.0015$. The parameters used for simulation are summarized in Table 4.2.

Table 4.2: Simulation Parameters

Parameter	**Value**
MMC nominal power (base power)	50 MVA
AC system nominal voltage (base voltage)	138 kV
Short circuit ratio at PCC	5
AC source inductance (Ls)	150 mH
Nominal frequency	60 Hz
Arm inductance (L)	3 mH
Arm resistance (R)	1Ω
Submodule capacitance (C)	14000μF
Transformer voltage rating (T)	138 kV / 30 kV
Transformer power rating	55 MVA
Transformer inductance	0.05 pu
Transformer resistance	0.01 pu
Grid side converter inductance (Lc)	5 mH
Grid side converter resistance (Rc)	0.03Ω
DC side reference voltage	60 kV
Number of SMs per arm (N)	20
Sampling time (Ts)	100μs

Figure 4.7 shows the performance of all the state variables being controlled by the modified reduced indirect FCS-MPC under active power reversal command. In Fig. 4.7(a,b) the tracking of active power and accurrent is shown which indicates very good tracking. The circulating current tracking is shown in Fig. 4.7(c). It can be observed that a sinusoidal component and a small dc-component is added to circulating current under a transient till the summation voltages are balanced. This feature is due to the cost function proposed in (4.4). The summation of capacitor voltages in the lower arm of phase a are depicted in Fig. 4.7(d). It can be seen that the average value of summation voltages regulate themselves to V_{dc}. Overall it can be said that the tracking of all the state variables is very

good.

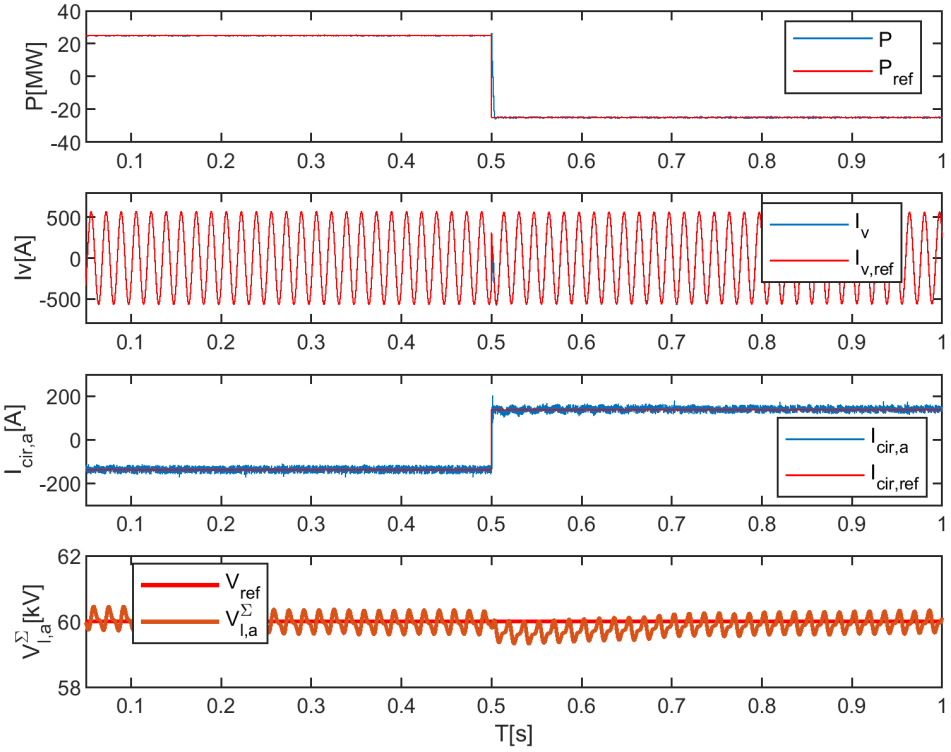

Figure 4.7: Modified reduced indirect FCS-MPC: (a) real power, (b) phase-a current, (c) phase-a circulating current, (d) summation of the capacitor voltages in the lower arm of phase a,

In Fig. 4.8 the d-axis current component of the ac-side current of the proposed method is shown in comparison with full indirect and reduced indirect FCS-MPC. This validates the superior dynamic performance of proposed modified reduced indirect FCS-MPC in comparison to the reduced

indirect FCS-MPC in [5] and shows similar dynamic performance to full indirect FCS-MPC.

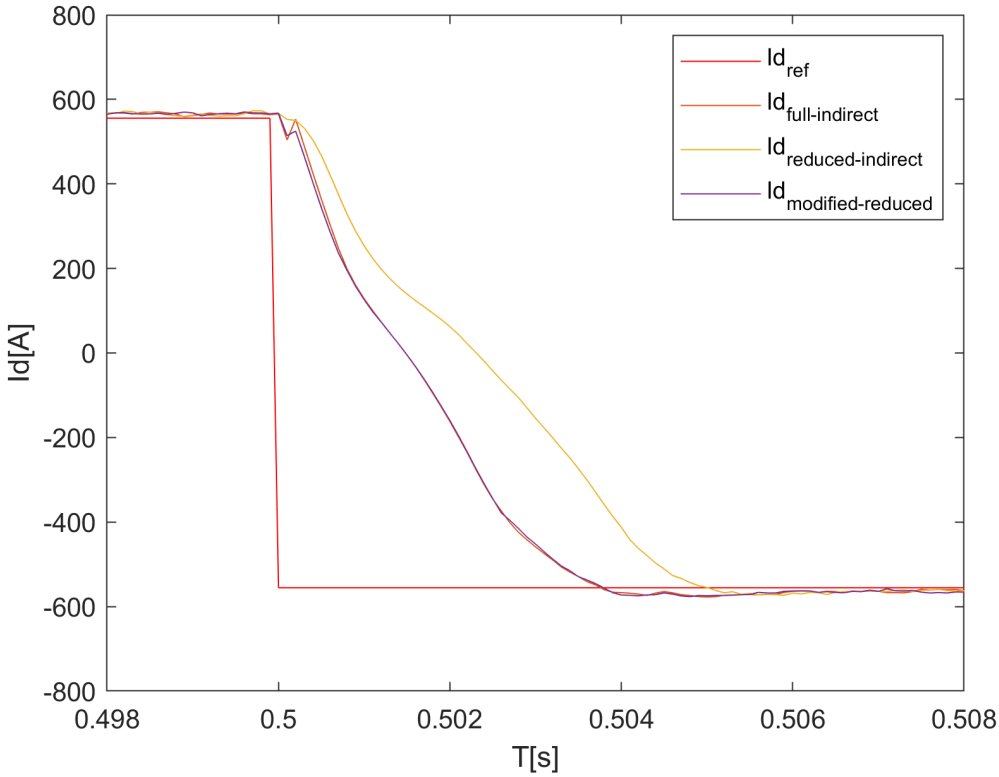

Figure 4.8: Comparison of Results for d-axis component of ac-side current

Figure 4.9 depicts the behavior of the summation capacitor voltages if cost function in (4.3) is used with constant reference of circulating current. It can be seen that on the longer run the summation voltages will become unstable as they are slowly drifting away from the reference.

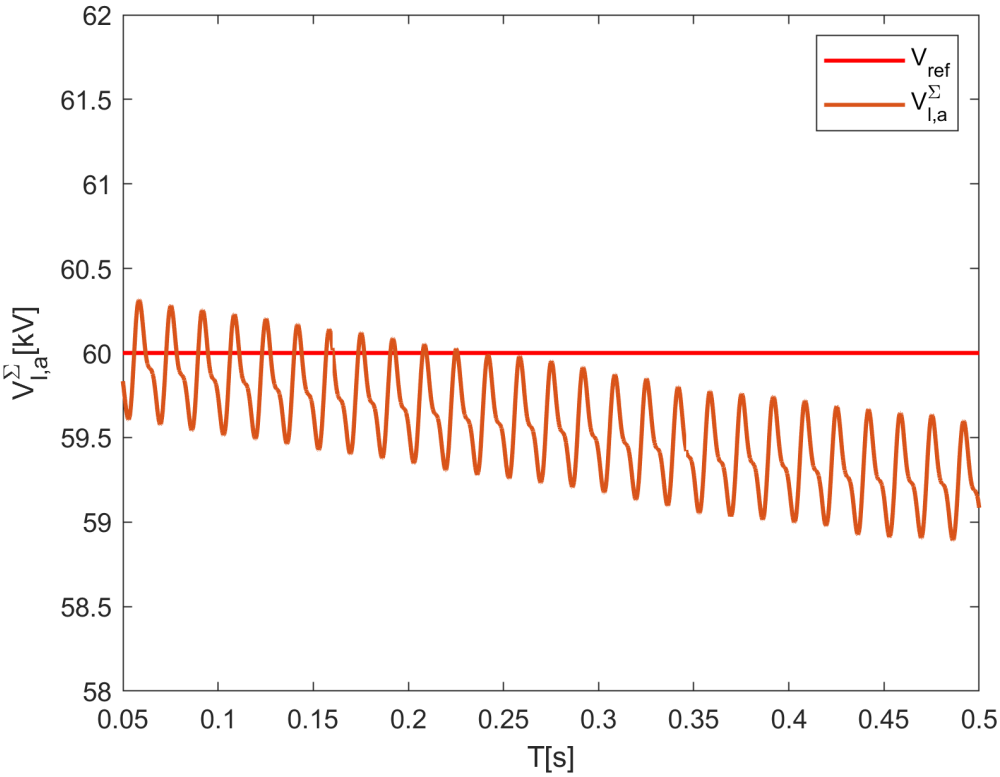

Figure 4.9: summation of the capacitor voltages in the lower arm of phase a under cost function (4.3)

Figure 4.10 shows the overall response of the system if the equivalent of outer loop on circulating current reference as proposed in [6] is used. The drawback of this approach can be seen from Fig. 4.10(c,d) *i.e.* the circulating current has ripples/adjustment even after the summation voltages have been balanced. Therefore, the equivalent of outer loop within the MPC framework as proposed in [6] is not correct because if an actual

outer loop would have been used then these ripples in circulating current would vanish as soon as the summation voltages would become balanced. The interested reader can see the results in [5] using an explicit outer loop to note that the circulating current reference becomes constant as soon as the summation voltages become balanced.

From the above discussion and results of summation voltages, it is clear that the proposed new cost function is better than the techniques in [5, 6] because it avoids the outer loop and the ripples vanish as soon as the summation voltages become balanced.

4.5 Conclusion

In this chapter, a modified reduced indirect FCS-MPC strategy was proposed for MMC with low computational complexity that achieved nearly similar dynamic performance as full indirect FCS-MPC. In addition, a novel cost function was proposed that eliminated the need of an outer loop or any kind of its equivalent within MPC framework for regulation of summation voltages. It was demonstrated that summation voltages drift slowly away from the reference if no outer loop is used. Embedding the outer loop within the MPC while using the conventional cost function (as in [6]) causes unnecessary ripples in the circulating current at steady state.

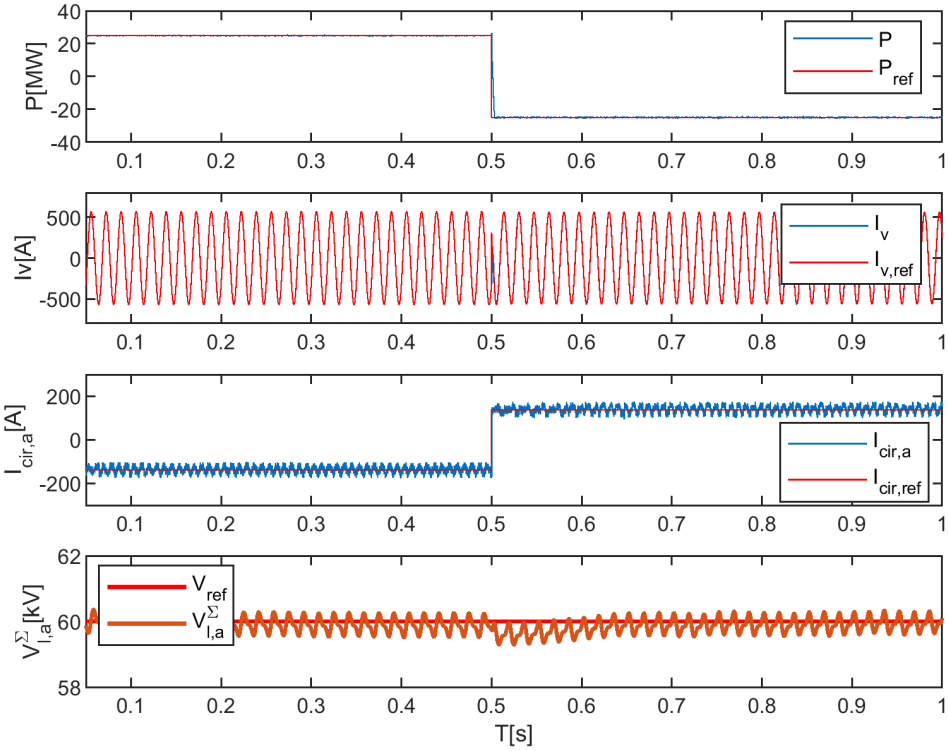

Figure 4.10: Full indirect FCS-MPC with equivalent of outer loop with in MPC [6]: (a) real power, (b) phase-a current, (c) phase-a differential current, (d) summation of the capacitor voltages in the lower arm of phase a,

Bibliography

[1] M. Vatani, B. Bahrani, M. Saeedifard and M. Hovd, "Indirect Finite Control Set Model Predictive Control of Modular Multilevel Converters," in *IEEE Transactions on Smart Grid,* vol. 6, no. 3, pp. 1520-1529, May 2015

[2] A. Yazdani and R. Iravani, *Voltage-Sourced Converters in Power Systems: Modeling, Control, and Applications.* Hoboken, NJ, USA: Wiley, 2010.

[3] M. Saeedifard and R. Iravani, "Dynamic Performance of a Modular Multilevel Back-to-Back HVDC System," *IEEE Transactions on Power Delivery,* vol. 25, no. 4, pp. 2903-2912, Oct. 2010

[4] K. Sharifabadi, L. Harnefors, H.-P. Nee, S. Norrga, and R. Teodorescu, *Design, Control and Application of Modular Multilevel Converters for HVDC Transmission Systems.* United States: Wiley-IEEE press, 2016.

[5] W. Tian, X. Gao and R. Kennel, "Model Predictive Control of Modular Multilevel Converters with Independent Arm-Balancing Control," *2019 IEEE International Symposium on Predictive Control of Electrical Drives and Power Electronics (PRECEDE),* 2019, pp. 1-5

[6] X. Chen, J. Liu, S. Song, S. Ouyang, H. Wu and Y. Yang, "Modified Increased-Level Model Predictive Control Methods With Reduced Computation Load for Modular Multilevel Converter," in *IEEE Transactions on Power Electronics,* vol. 34, no. 8, pp. 7310-7325, Aug. 2019

[7] F. Zhang, W. Li and G. Joós, "A Voltage-Level-Based Model Predictive Control of Modular Multilevel Converter," *IEEE Transactions on Industrial Electronics*, vol. 63, no. 8, pp. 5301-5312, Aug. 2016

Chapter 5

Bisection and Backstepping based Model Predictive Control for the Modular Multilevel Converter

In this chapter, two methods are proposed to make the selection of the insertion index independent from the previous sampling instant. This feature enables these methods to achieve nearly similar dynamic performance as full indirect FCS-MPC at a much lower computational burden and also removes the need to have a pre-defined large step in the insertion index as in the modified reduced FCS-MPC.

First, the bisection algorithm-based indirect FCS-MPC is presented. The proposed method greatly reduces the search space for reaching the optimal insertion index (number of submodules to be inserted) thus reducing the computational complexity. The second method that is presented here is based on backstepping and indirect FCS-MPC. In this method, backstepping is applied as the first step of modulation control in the abc reference frame for modular multilevel converters (MMCs). In the second step of both methods, reduced indirect FCS-MPC is applied where the number of

inserted modules is allowed to change by a maximum of two and one from the rounded result of the continuous outcome from bisection and backstepping, respectively. Both methods offer nearly similar dynamic performance as compared to full indirect FCS-MPC with low computational complexity. The results of the proposed methodologies are validated and compared through simulations for a 21-level MMC in MATLAB/Simulink.

5.1 Bisection Algorithm based Indirect Finite Control Set Model Predictive Control for Modular Multilevel Converters

In this method, the bisection algorithm is employed to reduce the search space for finding the optimum insertion index. The algorithm can be summarized as:

1. Evaluate $n_{u,j} = 0, n_{l,j} = N$ and $n_{u,j} = N, n_{l,j} = 0$ *i.e.* the extreme on both ends

2. if $n_{u,j} = 0, n_{l,j} = N$ gives lower cost then evaluate $n_{u,j} = N/4, n_{l,j} = N - n_{u,j}$ else evaluate $n_{u,j} = N - N/4, n_{l,j} = N - n_{u,j}$

3. Then evaluate $n_{u,j} = N/4 + N/8, n_{l,j} = N - n_{u,j}$ and $n_{u,j} = N/4 - N/8, n_{l,j} = N - n_{u,j}$ else evaluate $n_{u,j} = N - N/4 - N/8, n_{l,j} = N - n_{u,j}$ and $n_{u,j} = N - N/4 + N/8, n_{l,j} = N - n_{u,j}$

4. if from above $n_{u,j} = N/4 + N/8$ gives minimum cost then evaluate $n_{u,j} = N/4 + N/8 + N/16$ and $n_{u,j} = N/4 + N/8 - N/16$ with $n_{l,j} = N - n_{u,j}$

5. Stop this procedure when $N/(2^k)$ is $<= 1$ for some k, where k is an integer

6. Finally, once the insertion index that minimizes the cost function is found then apply reduced indirect FCS-MPC [1] with a maximum

change of two in the insertion index obtained from the bisection algorithm. This is done only for the first time step within the prediction horizon. For the following time steps, a maximum change of one is allowed in the insertion index. Note that the bisection algorithm only provides a very good estimate of the insertion index to reduced indirect FCS-MPC method and it is not applied at each time step within the prediction horizon.

Note that, if $n_{u,j} = 0, n_{l,j} = N$ gives a lower cost in step 2 then the whole region where $n_{u,j} > n_{l,j}$ does not need to be considered. Similarly, if $n_{u,j} = N, n_{l,j} = 0$ gives a lower cost in step 2 then the region where $n_{u,j} < n_{l,j}$ does not need to be evaluated. This effectively reduces the search space to half. This can be understood by keeping in mind that ac-current tracking is the most important objective. Now, the ac-current dynamics depend on the internal voltage of the MMC which is defined as:

$$e_{v,j} = \frac{n_{l,j} v_{l,j}^{\Sigma} - n_{u,j} v_{u,j}^{\Sigma}}{2N} \tag{5.1}$$

To simplify the description, it is assumed that summation voltages have no ripple and are following a constant reference *i.e.*, V_{dc}. Then (5.1) can be rewritten as:

$$e_{v,j} = \frac{(n_{l,j} - n_{u,j}) V_{dc}}{2N} \tag{5.2}$$

The above expression can be zero, positive or negative depending on the values of the insertion indices $n_{l,j}$ and $n_{u,j}$. Assuming the above expression should be positive for the accurate ac-current tracking then the combination $n_{u,j} = 0, n_{l,j} = N$ would always give a lower cost than $n_{u,j} = N, n_{l,j} = 0$. Consider the worst case *i.e.*, $e_{v,j}$ should be $+V_{dc}/2N$ for accurate ac-current tracking. Even in this case the combination $n_{u,j} = 0, n_{l,j} = N$ would have a lower cost than $n_{u,j} = N, n_{l,j} = 0$ as it is closer to the desired $e_{v,j}$. It implies that if $n_{u,j} = 0, n_{l,j} = N$ gives lower cost then $e_{v,j}$ must be positive, and the region $n_{u,j} > n_{l,j}$ does not need to be considered and vice versa.

The flowchart of the bisection algorithm is shown in Fig. 5.1 where J is the cost function. The option that minimizes the cost function is forwarded

to reduced indirect FCS-MPC where a maximum change of two is allowed from the rounded-off solution of the bisection algorithm.

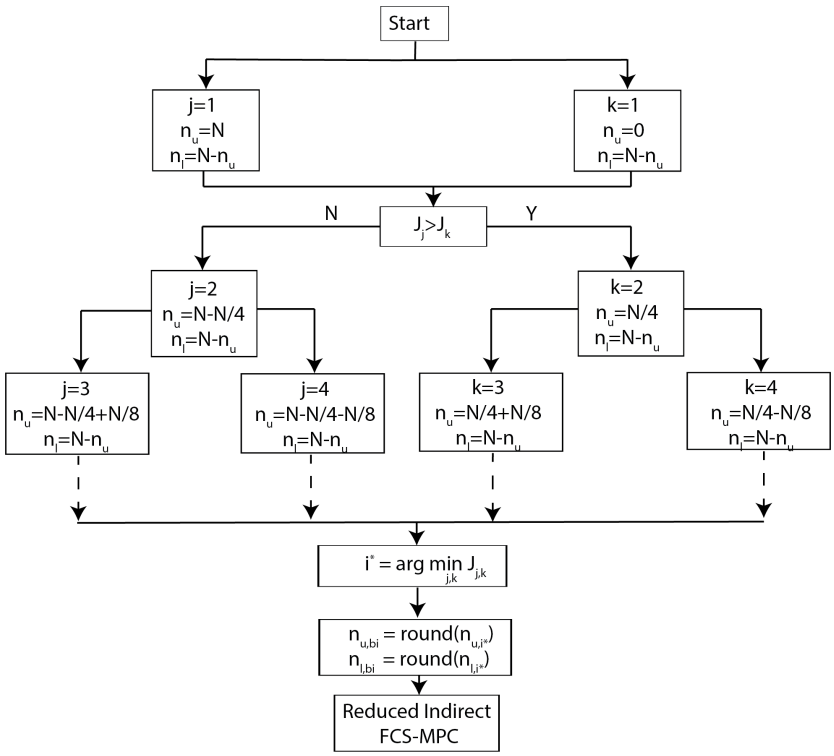

Figure 5.1: Flowchart for bisection-based indirect FCS-MPC

It is noted that in the proposed method $n_{u,j} = N/2$ is not evaluated on purpose as the algorithm will automatically converge to it if this is the optimal solution. This will happen because in the last step a maximum change of two is allowed in the insertion index. This approach significantly reduces the search space for reaching the optimal insertion index without compromising on the performance. The proposed approach has similar dynamic performance as compared to full indirect FCS-MPC which will be

demonstrated by simulations later. Moreover, this approach can easily be extended to MMCs with a large number of SMs as compared to [2] without much increase in computational burden. For instance, for $N = 100$, the number of options to be evaluated for the proposed method in the first time step will be just $13 + 25 = 38$. However, if [2] has to include even one more option in the first time step for $N = 100$ then it has to evaluate 49 options in the first time step within the prediction horizon.

The cost function (4.4) used for reduced indirect FCS-MPC implementation was presented and explained in detail in the chapter 4.

5.2 Backstepping based reduced indirect FCS-MPC

5.2.1 Backstepping Design

In this work, the ac-side current $i_{v,j}$, circulating current $i_{cir,j}$, summation of upper and lower arm capacitor voltages $v_{u,j}^{\Sigma}, v_{l,j}^{\Sigma}$ are used as the state variables. Then based on these state variables, the error variables for backstepping are given as follows:

$$e_1 = i_{cirref,j} - i_{cir,j} \tag{5.3}$$

$$e_2 = V_{dc,ref} - v_{u,j}^{\Sigma} \tag{5.4}$$

$$e_3 = V_{dc,ref} - v_{l,j}^{\Sigma} \tag{5.5}$$

$$e_4 = i_{vref,j} - i_{v,j} \tag{5.6}$$

Based on the above errors, the following four Lyapunov functions (LF) were formed for backstepping design:

$$V_1 = \frac{1}{2}e_1^2 \tag{5.7}$$

$$V_2 = V_1 + \frac{1}{2}e_2^2 \tag{5.8}$$

$$V_3 = V_2 + \frac{1}{2}e_3^2 \tag{5.9}$$

$$V_4 = V_3 + \frac{1}{2}e_4^2 \tag{5.10}$$

Before proceeding with the backstepping design, it is noted that the reference for summation voltages is constant. Moreover, the reference for circulating current is also constant for a fixed power. Therefore, their derivatives would be zero in steady state. Only the reference of ac-side current would be varying and its derivative would be non-zero.

It can be observed that the LFs are positive in (5.7-5.10). Based on Lyapunov theory, the time-based derivative of these functions must be negative to ensure stability. Using (2.12) and (2.13) and taking derivatives of the LFs the following expressions are obtained:

$$\dot{V}_1 = e_1(\frac{R}{L}i_{cir,j} + \frac{(n_{u,j}v_{u,j}^{\Sigma} + n_{l,j}v_{l,j}^{\Sigma})}{2NL} - \frac{V_{dc}}{2L}) \tag{5.11}$$

$$\dot{V}_2 = e_2(\frac{n_{u,j}\dot{i}_{v,j}}{2C} - \frac{n_{u,j}\dot{i}_{cir,j}}{C}) + \dot{V}_1 \tag{5.12}$$

$$\dot{V}_3 = e_3(-\frac{n_{l,j}\dot{i}_{v,j}}{2C} - \frac{n_{l,j}\dot{i}_{cir,j}}{C}) + \dot{V}_2 \tag{5.13}$$

$$\dot{V}_4 = e_4(\dot{i}_{vref,j} + \frac{(R+2R_c)}{L+2L_c}\dot{i}_{v,j} - \frac{n_{u,j}v_{u,j}^{\Sigma} - n_{l,j}v_{l,j}^{\Sigma}}{N(L+2L_c)} - \frac{2v_{f,j}}{L+2L_c}) + \dot{V}_3 \tag{5.14}$$

The LF in (5.14) includes the effect of all the LFs. Therefore, ensuring negativity of (5.14) would guarantee that the system is indeed stable. So, the designed controller should ensure that $\dot{V}_4$ is negative.

It is noted that there are two control inputs for each phase of the MMC *i.e.* $n_{u,j}$ and $n_{l,j}$ for each arm. However, there is only one equation *i.e.* (5.14), therefore a relation between these two controllers is required to proceed further with the design. In [3] different control choices for these controllers are shown. In this work, the following relation between the two controllers is utilized.

$$n_{u,j} = N - n_{l,j} \tag{5.15}$$

It is noted here, that (5.15) may not result in optimal performance of the MMC in the absence of an explicit modulator. This is because (5.15) is the ideal case for continuous approximation of insertion indices and does not consider the need for controlling the circulating current. Therefore, an idea from indirect FCS-MPC is presented later to deal with this. By using (5.15) in (5.14) and after some simplification the following expression is achieved.

$$\dot{V}_4 = n_{u,j}H + \frac{e_1 v_{l,j}^{\Sigma}}{2L} + e_3 N(\frac{-i_{v,j}}{2C} - \frac{i_{cir,j}}{C}) + \frac{e_4 v_{l,j}^{\Sigma}}{L+2L_c} + e_1(\frac{R}{L}i_{cir,j} - \frac{V_{dc}}{2L}) + e_4(\dot{i}_{vref,j} + \frac{(R+2R_c)}{L+2L_c}i_{v,j} - \frac{2v_{f,j}}{L+2L_c}) \quad (5.16)$$

where

$$H = \frac{e_1 v_{u,j}^{\Sigma}}{2NL} + e_2(\frac{i_{v,j}}{2C} - \frac{i_{cir,j}}{C}) - \frac{e_4 v_{u,j}^{\Sigma}}{N(L+2L_c)} - \frac{e_1 v_{l,j}^{\Sigma}}{2NL} - e_3(\frac{-i_{v,j}}{2C} - \frac{i_{cir,j}}{C}) - \frac{e_4 v_{l,j}^{\Sigma}}{N(L+2L_c)} \quad (5.17)$$

So, now the control law $n_{u,j}$ that will guarantee system stability and negative time derivative of the LF is selected as:

$$n_{u,j} = \frac{1}{H}(-\frac{e_1 v_{l,j}^{\Sigma}}{2L} - e_3 N(\frac{-i_{v,j}}{2C} - \frac{i_{cir,j}}{C}) - \frac{e_4 v_{l,j}^{\Sigma}}{L+2L_c} - e_1(\frac{R}{L}i_{cir,j} - \frac{V_{dc}}{2L}) - e_4(\dot{i}_{vref,j} + \frac{(R+2R_c)}{L+2L_c}i_{v,j} - \frac{2v_{f,j}}{L+2L_c}) - c_1 e_1^2 - c_2 e_2^2 - c_3 e_3^2 - c_4 e_4^2) \quad (5.18)$$

The above control law will give the following expression:

$$\dot{V}_4 = -c_1 e_1^2 - c_2 e_2^2 - c_3 e_3^2 - c_4 e_4^2 \quad (5.19)$$

Therefore, to ensure that (5.19) is negative all the coefficients c_i must be positive. These coefficients can also impact the control design. In this work,

no specific criteria is used to determine them. However, it was noted that by increasing the values of these coefficients (up to a certain limit) the errors were reduced. In this paper, all coefficients are kept equal to a value of 250 as increasing beyond this value resulted in an increase in the errors. It is also noted that if the expression for H results in a very small number then there is a possibility of using excessively large control inputs. On analyzing H, it is noted that only e_4 terms will have a significant contribution. Therefore, whenever the absolute value of e_4 is small, its absolute value is increased by 1 or -1 depending on the sign of e_4, to avoid excessively large input values. It is also worth mentioning here that the above design can be simplified further by only considering e_1 and e_4 and setting e_2, e_3 equal to zero. This can be seen from (2.12) where the summation voltages are depending on the other two state variables and control input. Therefore, if the other two state variables are well regulated then summation voltages should automatically regulate themselves. The same is done in this work. This simplifies (5.18) significantly. However, this requires the use of a modified cost function as presented in the previous chapter to ensure regulation of the average of summation voltages or the use of an outer loop or its equivalent within MPC.

The controllers returned by the above design would be continuous. However, the voltage levels of the MMC can only be discrete without an explicit modulator. Therefore, the above solutions are rounded off to the nearest integer. Then (5.15) can be utilized to find the other controller. However, as previously mentioned, (5.15) will not necessarily result in optimal performance. Thus, the idea from indirect FCS-MPC is utilized.

5.2.2 Reduced Indirect FCS-MPC Stage

Again the cost function (4.4) is used. However, as opposed to the bisection algorithm, the maximum change in the rounded-off insertion index obtained from the backstepping stage is set to one instead of two. Therefore, this approach just has to consider 9 options for the FCS-MPC stage and results in nearly similar dynamic performance as full indirect FCS-MPC. The flowchart of the overall proposed approach is shown in Fig. 5.2.

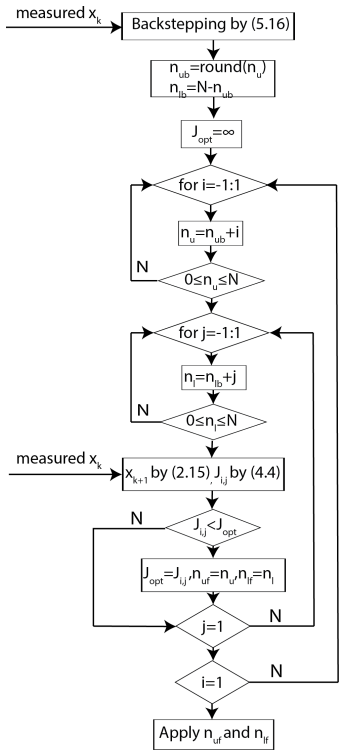

Figure 5.2: Flowchart for backstepping based indirect FCS-MPC

5.3 Discussion and Comparison of the Strategies

The computational requirement comparison between the different FCS-MPC strategies is shown in Table 5.1. It can be observed that the least number of control options evaluated are for reduced indirect FCS-MPC and backstepping-based indirect FCS-MPC. However, the added advantage of backstepping-based indirect FCS-MPC strategy is that it provides nearly similar dynamic performance as full indirect FCS-MPC while reduced indirect FCS-MPC has a sluggish dynamic response. Then the modified re-

duced indirect FCS-MPC strategy has a low number of computations which are nearly similar to bisection-based indirect FCS-MPC. The advantage of the bisection-based method is that its number of computations increases slowly as compared to modified reduced indirect FCS-MPC with the increase in the number of SMs of MMC.

Table 5.1: Number of possible control options for different FCS-MPC strategies (p=3, 20 SMs/arm)

Methodology (N=20)	**No. of Control Options p=3**
Full Indirect FCS-MPC	85,766,121
Reduced Indirect FCS-MPC	729
Modified Reduced Indirect FCS-MPC	2025
Bisection based Indirect FCS-MPC	2592
Backstepping based Indirect FCS-MPC	729

Note that the calculation of backstepping control input is insignificant compared to the evaluation of a control option for indirect FCS-MPC. However, to provide some details the comparison in terms of the total number of floating point operations (FLOPS) is made. The total number of FLOPS required for the backstepping based method is 1413 whereas the FLOPS for just implementing the reduced indirect FCS-MPC method is 1242. In terms of elapsed time, the backstepping method takes 3.5 ms and the reduced indirect FCS-MPC method takes 3.4 ms. It is noted that both these comparisons are made for a prediction horizon of 1 and the elapsed time was calculated using MATLAB R2019b on Intel® Core i7, 3.20 GHz, with 16 GB RAM

5.4 Simulation Results

Similar scenarios and simulation parameters as in the previous chapter are used. Figs. 5.3 and 5.4 show the overall performance of bisection and backstepping based indirect FCS-MPC respectively. It can be observed that all the state variables are being tracked very well.

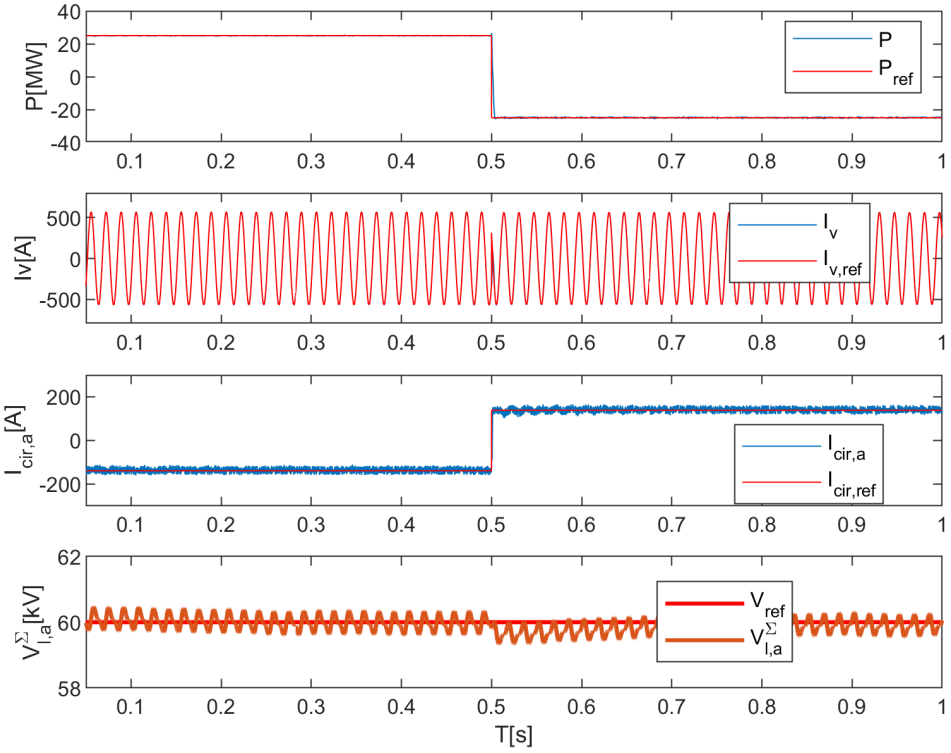

Figure 5.3: Bisection-based indirect FCS-MPC: (a) real power, (b) phase-a current, (c) phase-a circulating current, (d) summation of the capacitor voltages in the lower arm of phase a,

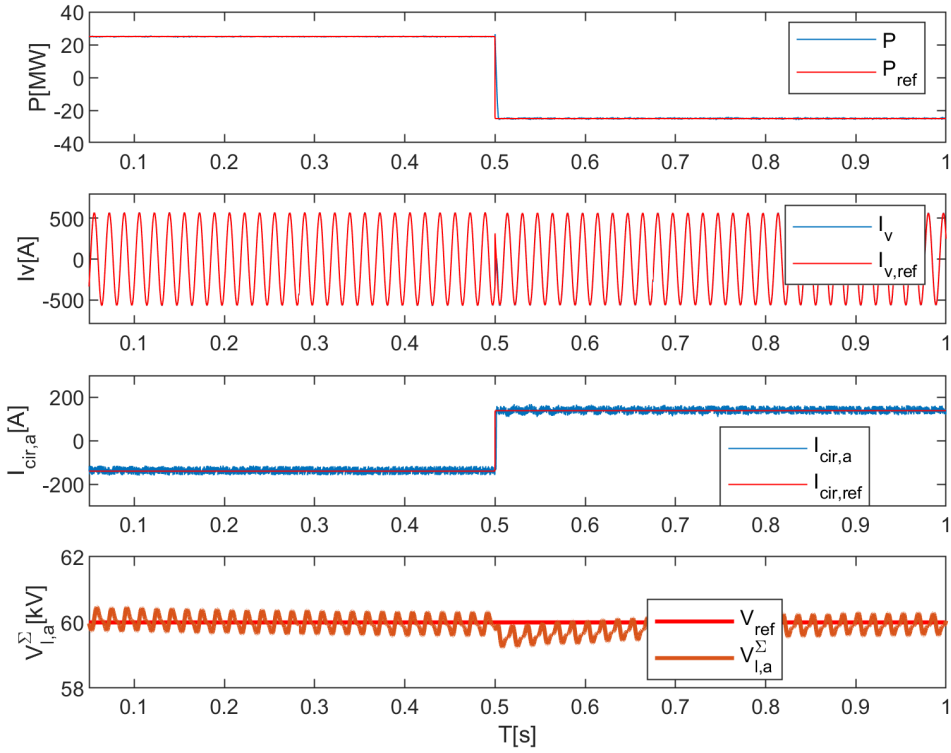

Figure 5.4: Backstepping based indirect FCS-MPC: (a) real power, (b) phase-a current, (c) phase-a circulating current, (d) summation of the capacitor voltages in the lower arm of phase a,

Figure 5.5 shows that the dynamic response of both backstepping and bisection-based indirect FCS-MPC strategies is nearly similar to the full indirect FCS-MPC strategy. It appears that the bisection method has a slightly better dynamic response than the backstepping method. This is due to the coefficients c_i. A different selection of $c_i's$ improves the performance

of the backstepping method which is shown in Fig. 5.6.

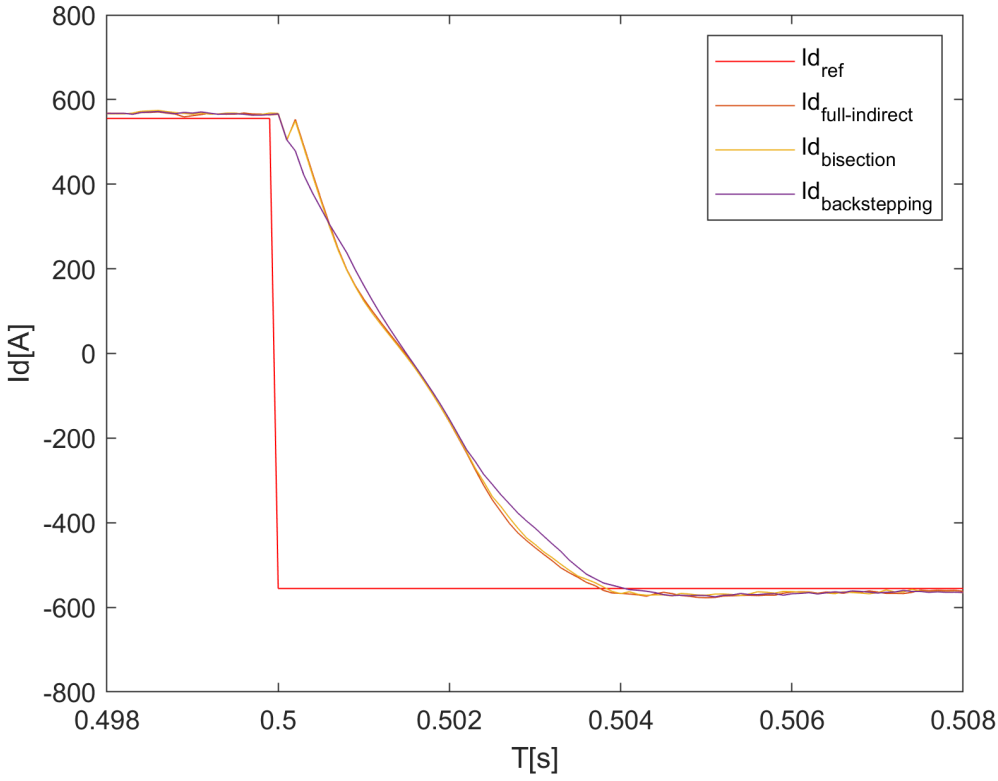

Figure 5.5: Comparison of Results for d-axis component of ac-side current

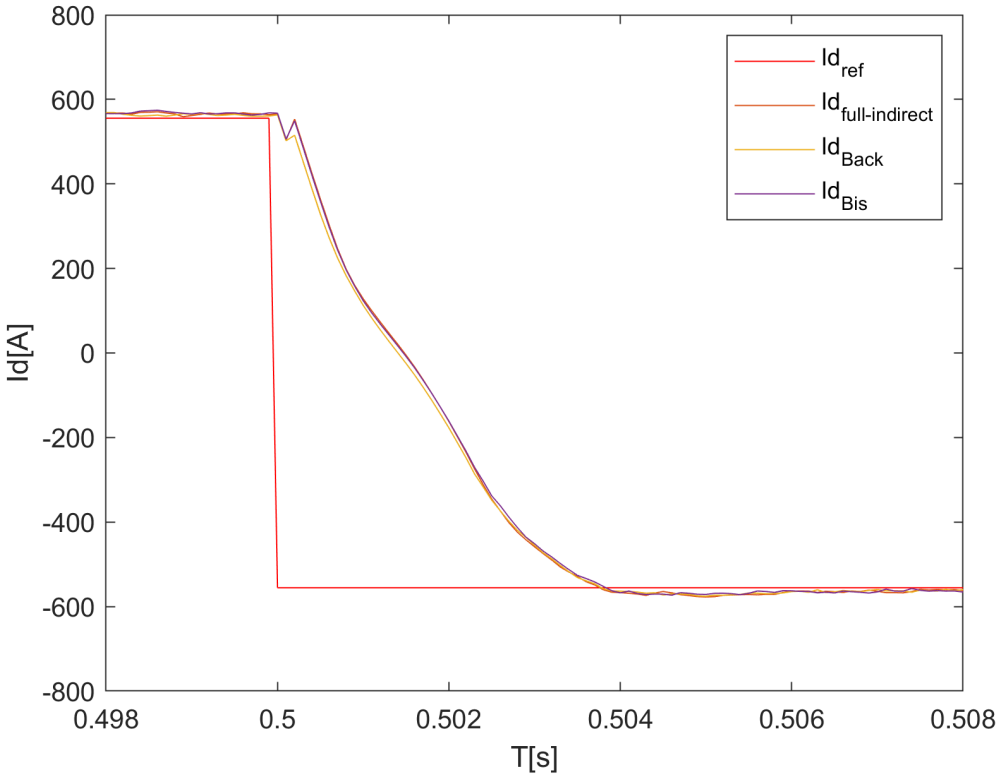

Figure 5.6: Comparison of Results for d-axis component of ac-side current

5.5 Conclusion

In this chapter, two methods based on reduced indirect FCS-MPC using a bisection algorithm and backstepping were presented. Both methods make the selection of the insertion index independent from the previous sampling instant. This independence resulted in a nearly similar dynamic performance as a full indirect FCS-MPC strategy with low computational

complexity. In addition, both methods can be easily extended for MMCs with a high number of SMs without much increase in computational complexity.

Bibliography

[1] M. Vatani, B. Bahrani, M. Saeedifard and M. Hovd, "Indirect Finite Control Set Model Predictive Control of Modular Multilevel Converters," in *IEEE Transactions on Smart Grid,* vol. 6, no. 3, pp. 1520-1529, May 2015

[2] S. Hamayoon, M. Hovd, J. A. Suul and M. Vatani, "Modified Reduced Indirect Finite Control Set Model Predictive Control of Modular Multilevel Converters," *2020 IEEE 21st Workshop on Control and Modeling for Power Electronics (COMPEL),* 2020, pp. 1-6

[3] F. Zhang, W. Li and G. Joós, "A Voltage-Level-Based Model Predictive Control of Modular Multilevel Converter," *IEEE Transactions on Industrial Electronics*, vol. 63, no. 8, pp. 5301-5312, Aug. 2016,

Chapter 6

Active Set Method based Modulated Model Predictive Control for Modular Multilevel Converters

The computational complexity of finite control set model predictive control (FCS-MPC) for modular multilevel converters (MMCs) is dependent on the number of submodules (SMs) per arm. Moreover, the steady-state performance of FCS-MPC is slightly degraded due to the absence of a modulator. In this chapter, a modulated model predictive control based on the enumeration of all active sets is proposed. A per-phase model of MMC is considered, therefore the valid active sets are just nine irrespective of the number of SMs. The proposed method offers better steady-state and dynamic performance as compared to full indirect FCS-MPC with much lower computational complexity and is independent of the number of SMs. The steady-state and dynamic response of the proposed method is verified by both simulations and experiments.

6.1 Introduction

The FCS-MPC techniques suffer from degraded steady-state performance due to their discrete nature and the absence of modulator. In addition, their computational complexity is dependent on the number of SMs. In order to address both of these issues, continuous control set model predictive control (CCS-MPC) can be used. However, many of the methods based on CCS-MPC rely on linearization of the MMC model [1,3] in order to make the real-time application simple. Unfortunately, linearization leads to errors. The real-time application of the methods based on non-linear model predictive control [2,4] is complicated due to high computational complexity resulting from a non-convex optimization problem and very short sampling times.

The steady-state performance of indirect FCS-MPC methods has been improved by developing modulated MPC methods [5,6]. In these methods, the two or three voltage levels that minimize a pre-defined cost function are first identified and then duty cycles are calculated for each voltage level. However, in the aforementioned methods circulating current control is not very good, due to the limitation of the duty cycle of the selected voltage levels. Although these methods improve the steady-state response, the computational complexity is still dependent on the number of SMs.

Another method based on modulated MPC having computational complexity independent of the number of SMs was proposed by Wang et al. [7]. This method first determines two voltage levels to control the ac-current and circulating current at the same time but without evaluating all voltage levels. Then it determines the arm voltage modulation references.

In order to address both issues *i.e.*, steady-state performance and computational complexity, a modulated model predictive control is applied using the active set method which is widely used in non-linear optimization problems. This work considers a per-phase model of MMC and therefore, the total number of valid active sets is just nine. The conditions for these nine cases are solved offline and equations are formed for each case. The case which satisfies the KKT conditions online is then used to implement the modulated MPC. The proposed method's computational complexity is independent of the number of SMs and it also offers a better steady-

state response due to the presence of a modulator. It is noted that the active set method always results in an optimal solution and respects the constraints. Thus, both the steady-state and dynamic performance of the proposed method outperforms full indirect FCS-MPC.

It is worth mentioning here that there are some methods based on active set enumeration [8,9] but they are for a three-phase model of MMC. Hence, they still have high computational complexity.

6.2 Problem Formulation

The minimization of the cost function (4.4) subject to the model (2.15) and constraints on the insertion index for the upper and lower arm can be expressed as:

$$\begin{aligned} \min_{u} \quad & J_j \\ \text{s.t.} \quad & x_{k+1} = Ax_k + \sum_{i=1}^{2}(B_{ix}u_i) + d \\ & 0 \leq u_1 \leq N \\ & 0 \leq u_2 \leq N \end{aligned} \tag{6.1}$$

where $u = [u_1 \quad u_2]^T = [n_{u,j} \quad n_{l,j}]^T$, $B_{ix} = \begin{bmatrix} B_1 x_k & B_2 x_k \end{bmatrix}$ and definitions of A, B_1, B_2, d can be found in (2.15).

From (6.1), it is observed that each input is bounded below from 0 and bounded above by N. The upper arm input can have the following three cases:

- Upper bound is active constraint (denoted by $UB_{u,j}$)
- Lower bound is active constraint (denoted by $LB_{u,j}$)
- Both upper and lower bounds are inactive constraints (denoted by $NB_{u,j}$)

Similarly, the input for the lower arm can have the above three cases. Therefore, the total number of active sets would be nine for each phase. The list of active sets is as follows:

1. $NB_{u,j}$,$NB_{l,j}$
2. $UB_{u,j}$,$UB_{l,j}$
3. $UB_{u,j}$,$LB_{l,j}$
4. $UB_{u,j}$,$NB_{l,j}$
5. $LB_{u,j}$,$UB_{l,j}$
6. $LB_{u,j}$,$LB_{l,j}$
7. $LB_{u,j}$,$NB_{l,j}$
8. $NB_{u,j}$,$UB_{l,j}$
9. $NB_{u,j}$,$LB_{l,j}$

Before the formulation of the Lagrangian function, it is clarified that the equality constraints (the model equations (2.15)) have been substituted into the cost function (4.4). Let the resulting cost function be denoted by $J_{s,j}$. Then the optimization problem can be rewritten as:

$$\begin{aligned} \min_{u} \quad & J_{s,j} \\ & 0 \leq u_1 \leq N \\ & 0 \leq u_2 \leq N \end{aligned} \tag{6.2}$$

Now, the Lagrangian can be formulated as follows:

$$\mathcal{L}_j = J_{s,j} - q_1 n_u + q_2(n_u - N) - q_3 n_l + q_4(n_l - N) \tag{6.3}$$

where q_i are Lagrange multipliers. In the proposed method, all the active sets are evaluated and the active set which satisfies the KKT condition

is then used to implement modulated MPC. The KKT conditions are given as follows:

$$\begin{aligned}
&\frac{\partial L}{\partial n_u} = 0 \\
&\frac{\partial L}{\partial n_l} = 0 \\
&q_1(0 - n_u) = 0 \\
&q_2(n_u - N) = 0 \\
&q_3(0 - n_l) = 0 \\
&q_4(n_l - N) = 0 \\
&0 \leq u \leq N, q_i \geq 0
\end{aligned} \tag{6.4}$$

Now, the conditions in (6.4) can be set up and solved for the unknown variables for each case. It is noted that the prediction horizon is one. The explicit expressions for $n_{u,j}$ and $n_{u,j}$ and Lagrange multipliers for each case are provided below:

6.2.1 Case 1 $(q_1 = q_2 = q_3 = q_4 = 0)$

$$n_{u,j} = -\left(\frac{A_1 B_4 - A_2 B_2}{B_1 B_4 - B_2 B_3}\right) \tag{6.5a}$$

$$n_{l,j} = -\left(\frac{A_1 B_3 - A_2 B_1}{B_2 B_3 - B_1 B_4}\right) \tag{6.5b}$$

6.2.2 Case 2 $(n_u = n_l = N, \quad q_1 = q_3 = 0)$

$$q_2 = -\frac{A_1 + A_2 + (B_1 + B_2 + B_3 + B_4)N}{2} v_{u,j}^{\Sigma} \tag{6.6a}$$

$$q_4 = -\frac{A_1 - A_2 + (B_1 + B_2 - B_3 - B_4)N}{2} v_{l,j}^{\Sigma} \tag{6.6b}$$

6.2.3 Case 3 $(n_u = N, n_l = 0, \quad q_1 = q_4 = 0)$

$$q_2 = -\frac{A_1 + A_2 + (B_1 + B_3)N}{2} v_{u,j}^{\Sigma} \tag{6.7a}$$

$$q_3 = \frac{A_1 - A_2 + (B_1 - B_3)N}{2} v_{l,j}^{\Sigma} \tag{6.7b}$$

6.2.4 Case 4 $(n_u = N, \quad q_1 = q_3 = q_4 = 0)$

$$n_{l,j} = -\frac{A_1 - A_2 + (B_1 - B_3)N}{B_2 - B_4} \tag{6.8a}$$

$$q_2 = -(A_1 + B_1 N + B_2 n_{l,j}) v_{u,j}^{\Sigma} \tag{6.8b}$$

6.2.5 Case 5 $(n_u = 0, n_l = N, \quad q_2 = q_3 = 0)$

$$q_1 = \frac{A_1 + A_2 + (B_2 + B_4)N}{2} v_{u,j}^{\Sigma} \tag{6.9a}$$

$$q_4 = -\frac{A_1 - A_2 + (B_2 - B_4)N}{2} v_{l,j}^{\Sigma} \tag{6.9b}$$

6.2.6 Case 6 $(n_u = n_l = 0, \quad q_2 = q_4 = 0)$

$$q_1 = \frac{A_1 + A_2}{2} v_{u,j}^{\Sigma} \tag{6.10a}$$

$$q_3 = \frac{A_1 - A_2}{2} v_{l,j}^{\Sigma} \tag{6.10b}$$

6.2.7 Case 7 $(n_u = 0, \quad q_2 = q_3 = q_4 = 0)$

$$n_{l,j} = -\frac{A_1 - A_2}{B_2 - B_4} \tag{6.11a}$$

$$q_1 = (A_1 + B_2 n_{l,j}) v_{u,j}^{\Sigma} \tag{6.11b}$$

6.2.8 Case 8 $(n_l = N, \quad q_1 = q_2 = q_3 = 0)$

$$n_{u,j} = -\frac{A_1 + A_2 + (B_2 + B_4)N}{B_1 + B_3} \tag{6.12a}$$

$$q_4 = (A_2 + B_3 n_{u,j} + B_4 N) v_{l,j}^{\Sigma} \tag{6.12b}$$

6.2.9 Case 9 $(n_l = 0, \quad q_1 = q_2 = q_4 = 0)$

$$n_{u,j} = -\frac{A_1 + A_2}{B_1 + B_3} \tag{6.13a}$$

$$q_3 = (A_1 + B_1 n_{u,j}) v_{l,j}^{\Sigma} \tag{6.13b}$$

where

$A_3 = \left(i_{v,j,ref}(k+1) - i_{v,j}(k) + T_s \frac{R+2R_c}{L+2L_c} i_{v,j}(k) - \frac{2V_f(k)T_s}{L+2L_c}\right) \frac{2T_s}{N(L+2L_c)}$

$B_3 = \left(i_{cir,ref}(k+1) - i_{cir,j}(k) + \frac{T_s R}{L} i_{cir,j}(k) - \frac{V_{dc}T_s}{2L}\right) \frac{\lambda_2 T_s}{NL}$

$C_1 = \lambda_3 \left(2V_{dc,ref} - v_{u,j,avg}^{\Sigma}(k) - v_{l,j,avg}^{\Sigma}(k)\right) \frac{T_s}{2NL}$

$D = \lambda_4 \left(v_{u,j,avg}^{\Sigma}(k) - v_{l,j,avg}^{\Sigma}(k)\right)$

$E = \frac{2T_s^2}{N(L+2L_c)}$

$F = \frac{2\lambda_2 T_s^2}{2NL}$

$A_1 = 2B_3 + 2C_1 + DT_s i_{v,j}(k)$

$A_2 = -2A_3 - 2DT_s i_{cir,j}(k)$

$B_1 = \frac{F v_{u,j}^{\Sigma}(k)}{NL} - \frac{DCT_s^2}{v_{u,j}^{\Sigma}(k)} \left(\frac{-i_{v,j}(k)}{2C} + \frac{i_{cir,j}(k)}{C}\right)^2$

$B_2 = \frac{F v_{l,j}^{\Sigma}(k)}{NL} + \frac{DCT_s^2}{v_{l,j}^{\Sigma}(k)} \left(\frac{i_{v,j}(k)}{2C} + \frac{i_{cir,j}(k)}{C}\right)^2$

$B_3 = \frac{2E v_{u,j}^{\Sigma}(k)}{N(L+2L_c)} - \frac{DCT_s^2}{v_{u,j}^{\Sigma}(k)} \left(\frac{-i_{v,j}(k)}{2C} + \frac{i_{cir,j}(k)}{C}\right)^2$

$B_4 = \frac{-2E v_{l,j}^{\Sigma}(k)}{N(L+2L_c)} - \frac{DCT_s^2}{v_{l,j}^{\Sigma}(k)} \left(\frac{i_{v,j}(k)}{2C} + \frac{i_{cir,j}(k)}{C}\right)^2$

The equation for each case can be evaluated with measurement data when the system is running. Then the equation among these nine cases that

satisfy KKT conditions is used for the modulation stage. It is to be noted here that the solution obtained from the above process will be continuous and therefore a PWM stage is required. In this case, SM unified pulse width modulation (SUPWM) is utilized where PWM is only applied to one SM in each arm. As a result, of this PWM stage, the steady-state response of the proposed method is better than finite control set MPC methods for MMCs.

It is further noted here that the evaluation of all the nine cases is the worst case scenario *i.e.* if any case satisfies the KKT conditions, then it is the optimal solution and then there is no need to evaluate the other cases. In the author's opinion mostly just one case is evaluated during normal/steady-state operation *i.e.* case 1 which corresponds to the unconstrained solution. During a transient, more cases are evaluated and the case satisfying KKT conditions is then used for the modulation stage. It is further noted that the optimal solution is guaranteed by the proposed method and the computational complexity is independent of the number of SMs.

6.2.10 Summary

The overall strategy is summarized as below:

- Evaluation of all the active set cases for KKT conditions (6.4)
- Selection of the case which satisfies KKT condition
- Perform modulation and capacitor voltage balancing task based on SUPWM and sorting algorithm

6.3 Simulation Results

Similar scenarios and simulation parameters as in the previous chapter are used. Fig. 6.1 show the overall performance of the proposed method. It can be observed that all the state variables are being tracked very well.

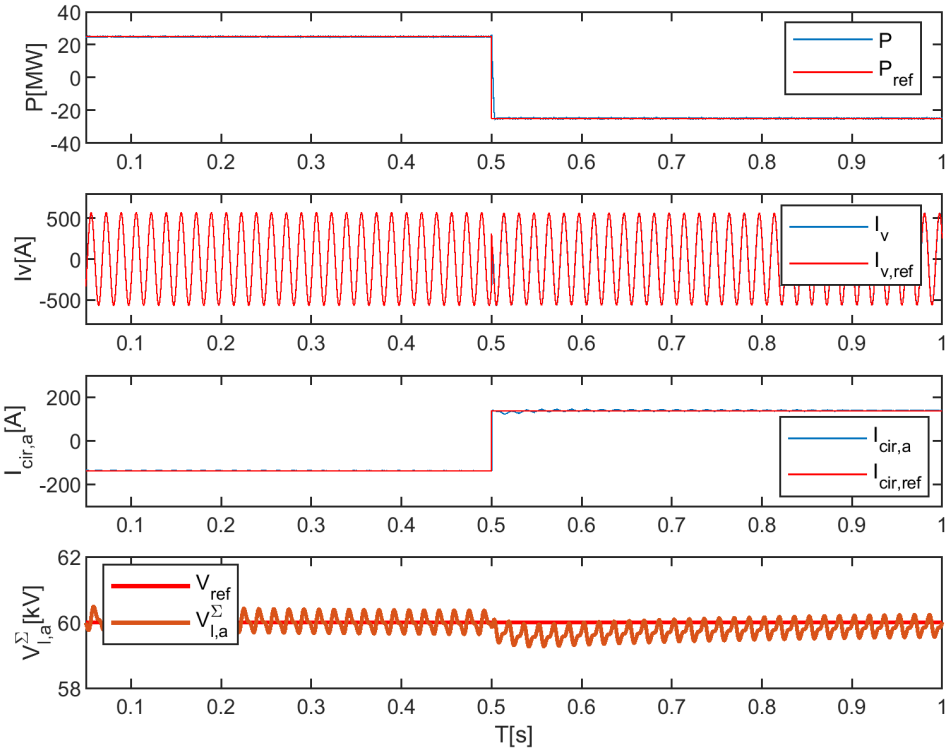

Figure 6.1: Active Set Method based Modulated Model Predictive Control: (a) real power, (b) phase-a current, (c) phase-a circulating current, (d) summation of the capacitor voltages in the lower arm of phase a,

Figure 6.2 shows the dynamic response of the active set method in comparison with full indirect FCS-MPC strategy and unconstrained saturated solution *i.e.*, Case 1 saturated to either N (when higher than N) or 0 (when less than 0) whenever it violates the constraints. It can be observed that active set method overlaps full-indirect FCS-MPC. However,

the unconstrained saturated solution is slightly slower. This shows that the unconstrained saturated solution is not optimal during the transients. Moreover, there is no guarantee of optimal solution with unconstrained saturated solution and it may lead to undesirable operating points in some other application.

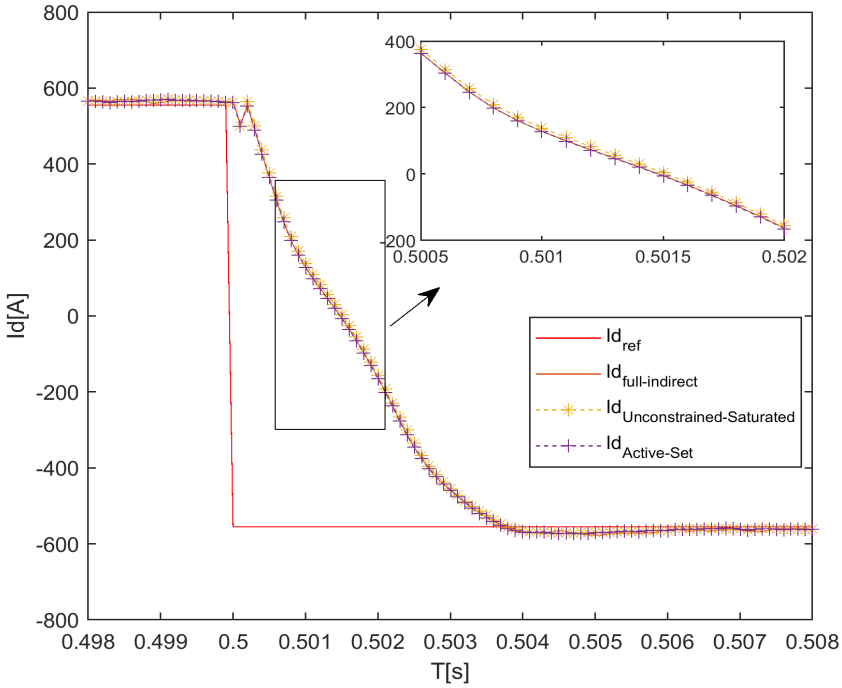

Figure 6.2: Comparison of Results for d-axis component of ac-side current

The THDs are already very low for both full-indirect FCS-MPC and active set methods. Still, the active set method offers better THD because PWM is applied to one SM. The THD for the active set and full-indirect FCS-MPC are 0.38% and 0.61% respectively as shown in Fig. 6.3 & 6.4.

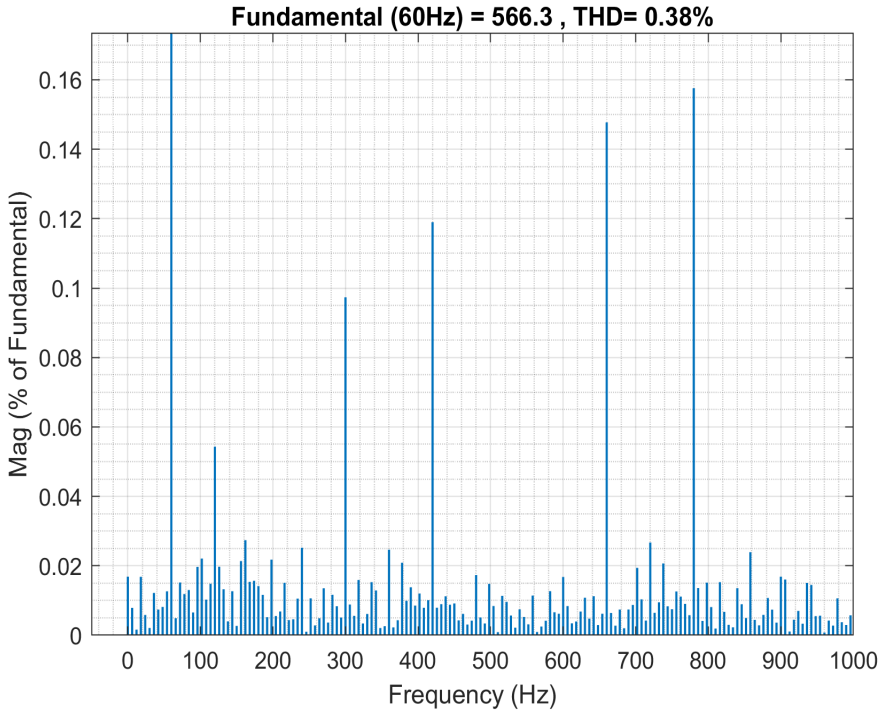

Figure 6.3: THD of Proposed Active Set Method

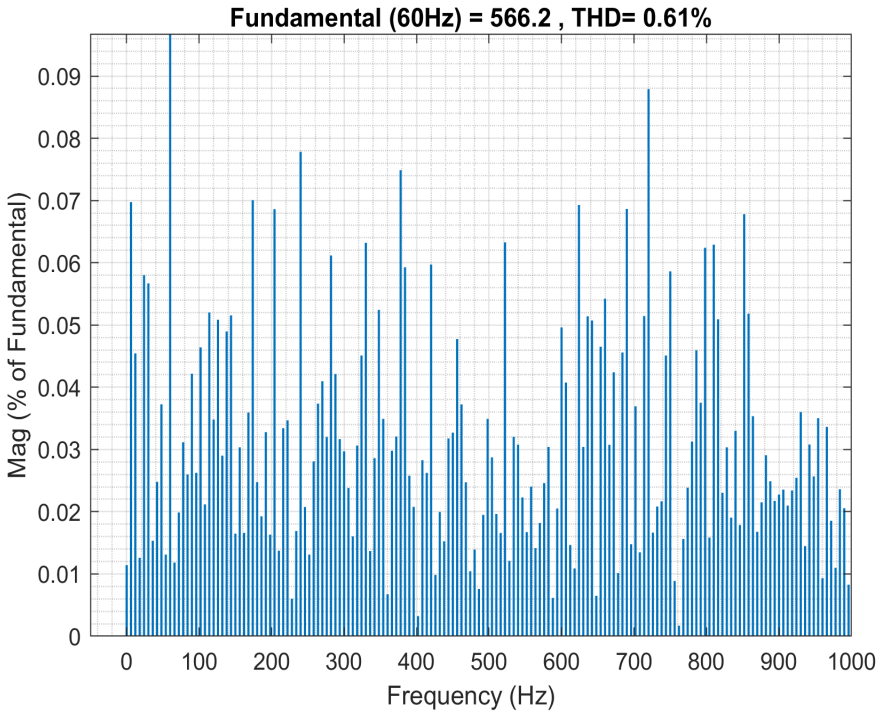

Figure 6.4: THD of Full Indirect FCS-MPC

6.4 Conclusion

A method based on an exhaustive enumeration of the active set was presented for the per-phase model of MMC. The proposed method made the computational complexity independent of the number of SMs, and can therefore be applied to MMCs with any number of SMs. The method presented offered better steady-state and similar dynamic performance as compared to full indirect FCS-MPC at a much lower computational burden.

Bibliography

[1] G. Darivianakis, T. Geyer and W. van der Merwe, "Model predictive current control of modular multilevel converters," *2014 IEEE Energy Conversion Congress and Exposition (ECCE),* 2014, pp. 5016-5023

[2] S. Fuchs and J. Biela, "Impact of the Prediction Error on the Performance of Model Predictive Controllers with Long Prediction Horizons for Modular Multilevel Converters - Linear vs. Nonlinear System Models," *2018 20th European Conference on Power Electronics and Applications (EPE'18 ECCE Europe),* 2018, pp. P.1-P.9.

[3] S. Fuchs, M. Jeong and J. Biela, "Long Horizon, Quadratic Programming Based Model Predictive Control (MPC) for Grid Connected Modular Multilevel Converters (MMC)," *IECON 2019 - 45th Annual Conference of the IEEE Industrial Electronics Society,* 2019, pp. 1805-1812

[4] S. Hamayoon, M. Hovd and J. A. Suul, "Non-Linear Model Predictive Control for Modular Multilevel Converters," *2022 International Power Electronics Conference (IPEC-Himeji 2022- ECCE Asia)*, 2022, pp. 562-568

[5] H. Mahmoudi, M. Aleenejad, and R. Ahmadi, "Modulated model predictive control of modular multilevel converters in VSC-HVDC systems," *IEEE Trans. Power Del.*, vol. 33, no. 5, pp. 2115–2124, Oct. 2018.

[6] D. Zhou, S. Yang, and Y. Tang, "Model predictive current control of modular multilevel converters with phase-shifted pulse-width modulation," *IEEE. Trans. Ind. Electron.*, vol. 66, no. 6, pp. 4368–4378, Jun. 2019.

[7] J. Wang, X. Liu, Q. Xiao, D. Zhou, H. Qiu and Y. Tang, "Modulated Model Predictive Control for Modular Multilevel Converters With Easy Implementation and Enhanced Steady-State Performance," *IEEE Transactions on Power Electronics*, vol. 35, no. 9, pp. 9107-9118, Sept. 2020

[8] X. Gao, W. Tian, Q. Yang and R. Kennel, "Model Predictive Control for Modular Multilevel Converters based on a Box-constrained Quadratic Problem Solver," *2020 IEEE 9th International Power Electronics and Motion Control Conference (IPEMC2020-ECCE Asia), 2020,* pp. 3068-3072

[9] X. Gao et al., "Modulated Model Predictive Control of Modular Multilevel Converters Operating in a Wide Frequency Range," in *IEEE Transactions on Industrial Electronics,* 2022

Chapter 7

Circulating Current Reference Based on Average and Instantaneous Information of Summation Voltages

In this chapter, first it is analytically shown that model predictive control (MPC) with the conventional cost function for modular multilevel converters without an outer loop or additional control over circulating current reference results in a marginally stable system. Note that this marginal stability is shown by using the results of a previous work. As a result, long term stability of summation voltages cannot be guaranteed. Then a proper circulating current reference based on the average and instantaneous information of summation voltages is proposed to ensure summation voltages stability. The proposed method does not require an explicit outer loop, nor knowledge of amplitude and phase angle of the ac current. Finally, this reference is used in the conventional cost function to show that summation voltages are regulated by the proposed circulating current reference. The

steady-state and dynamic response is verified by simulations.

7.1 Introduction

This work identifies an issue in the indirect FCS-MPC strategies. The cost function in many of the indirect FCS-MPC strategies just include ac-current and circulating current tracking as objectives [1–7] with constant circulating current reference. As shown in earlier chapters, with constant circulating current reference these methods cannot ensure long term stability of summation voltages. Now, this will be shown analytically in this chapter. It is noted that there are some other works with the same cost function but with an outer loop on circulating current reference [8–11]. These works regulate the summation voltages accurately but have the disadvantage of using an outer loop where the phase information of each phase is required.

It is further noted that there are also works based on indirect FCS-MPC which include summation voltages or the energy of each arm as objectives in the cost function [12–15]. These terms are based on instantaneous summation voltages/energy whereas their reference is set as average summation voltages/energy. Therefore, these works need a very long prediction horizon. It would have to be long enough to cover a significant fraction of the slow time constants *i.e.*, the slow dynamics of the summation voltages. Assuming a 50Hz grid, a horizon of 5 to 10ms might be required. However, the techniques based on indirect FCS-MPC for MMC have a very high computational complexity and cannot be extended easily for such long prediction horizons. It was earlier shown in Fig. 4.9 that these cost functions with a shorter horizon cannot ensure stability of summation voltages.

In this chapter, a method to determine the circulating current reference without an explicit outer loop is proposed. The reference is determined from average and instantaneous information of summation voltages and does not require the phase information of ac-current in each phase. This reference is used with conventional cost function of indirect FCS-MPC and it is shown that all the states of MMC are well regulated.

7.2 Proposed Approach

7.2.1 Analytical Proof of Marginal Stability when using the Conventional Cost Function with indirect FCS-MPC for MMC

The conventional cost function under consideration can be given as follows:

$$J_j = \lambda_1(i_{v,j,ref}(k+1) - i_{v,j}(k+1))^2 + \lambda_2(i_{cir,ref} - i_{cir,j}(k+1))^2 \quad (7.1)$$

Ignoring the constraints of the MMC, it is clear that the unconstrained minimum of (7.1) is 0. This can only happen if:

$$i_{v,j,ref}(k+1) - i_{v,j}(k+1) = 0 \quad (7.2a)$$
$$i_{cir,ref} - i_{cir,j}(k+1) = 0 \quad (7.2b)$$

Solving (7.2) using discrete model of the MMC in (2.15) results in the following expression of the controllers:

$$n_{u,j} = \frac{H_1}{2v_u^{\Sigma}} \quad (7.3a)$$
$$n_{l,j} = \frac{H_2}{2v_l^{\Sigma}} \quad (7.3b)$$

where

$$H_1 = D_1 + D_2 \quad (7.4a)$$
$$H_2 = D_2 - D_1 \quad (7.4b)$$

and

$$D_1 = \frac{(L+2L_c)N}{T_s}(i_{v,ref}(k+1) - i_v(k)) + i_v(k)(R+2R_c)N - 2v_f N \quad (7.5)$$

$$D_2 = \frac{2NL}{T_s}(i_{cir}(k) - i_{cir,ref}(k+1)) - 2RNi_{cir}(k) + NV_{dc} \tag{7.6}$$

The controllers (7.3) would lead to a marginal stable system. This can be understood by substituting (7.3) into (2.15). As a result, summation voltages would completely disappear from the dynamics of the ac-current and circulating current as they will be cancelled by the denominator of the controllers [16]. Although marginal stability is claimed in [16, 17], no formal proof has been given. However, observations from simulations verify the claim of marginal stability of summation voltages. Therefore, an open loop control approach (based on estimated summation voltages instead of measured) or a closed loop approach based on an outer loop for the circulating current reference are required to achieve asymptotic stability [17].

7.3 Proposed Circulating Current Reference

It is well known that it is the circulating current that acts as a driving agent to regulate the summation voltages to their reference [16]. There are two control goals with respect to summation voltages *i.e.*, first being the regulation of leg voltage in each phase to $2V_{dc}$ on average and second being the regulation of average arm voltage difference in each phase to 0.

The first objective can be met by adding a dc-component into the circulating current reference, while the second objective can be met by adding a fundamental frequency component to the circulating current reference [18, 19]. Therefore, these two components must be added to the otherwise constant circulating current reference *i.e.* $I_{dc}/3$ which is responsible for power transfer between the ac and dc side of the converter.

This is achieved as follows in the proposed work:

$$i_{cir,ref,j} = \frac{I_{dc}}{3} + q_1\left(2V_{dc} - v^{\Sigma}_{u,avg,j} - v^{\Sigma}_{l,avg,j}\right) + q_2\left(v^{\Sigma}_{u,avg,j} - v^{\Sigma}_{l,avg,j}\right)\Delta W_j \tag{7.7}$$

where $q_i's$ are the weighting factors/gains for the two objectives and ΔW_j is the instantaneous energy difference between the upper and lower arm of phase j and is given as:

$$\frac{dW_\Delta}{dt} = \frac{C}{2}\left(v_{u,j}^{\Sigma}(k)^2 - v_{l,j}^{\Sigma}(k)^2\right) \tag{7.8}$$

The second term in (7.7) adds the dc component whereas the third term adds the ac-component which will be explained later. For the following discussion it is important to keep in mind that (7.1) will be used as a cost function later in the MPC stage. Now, coming to the second term of (7.7) it can be seen that if the total leg voltage is less than $2V_{dc}$ then the cost function would only decrease if the circulating current increases. This increase will result in more charging of the capacitors thus increasing the average summation voltages as required. Similarly, if the total leg voltage is higher than $2V_{dc}$ then the cost function would only decrease if the circulating current decreases.

To explain the third term, the following representation of arm energy difference is considered.

$$\frac{dW_\Delta}{dt} = \left(\frac{n_{u,j}}{N}v_{u,j}^{\Sigma} + \frac{n_{l,j}}{N}v_{l,j}^{\Sigma}\right)\frac{-i_{v,j}}{2} + \left(\frac{n_{u,j}}{N}v_{u,j}^{\Sigma} - \frac{n_{l,j}}{N}v_{l,j}^{\Sigma}\right)i_{cir,j} \tag{7.9}$$

In this expression, it is easy to see that the first term would be predominantly sinusoidal at the fundamental frequency. This is because the sum of voltages of both arms would be close to $2V_{dc}$ *i.e.*, a constant, if the second harmonic component is ignored and $i_{v,j}$ has a fundamental frequency sinusoidal component. The second term would also be predominantly sinusoidal because the voltage difference of the two arms is sinusoidal at the fundamental frequency, while $i_{cir,j}$ would be close to a dc component in normal operation. Therefore, (7.9) would be a predominantly sinusoidal signal unless the first and second term cancel each other perfectly. This implies that the integral *i.e.* W_Δ would be a sinusoidal signal. With this in mind, it is easy to see that the last term in (7.9) becomes a sinusoidal term if $v_{u,j,avg}^{\Sigma} - v_{l,j,avg}^{\Sigma}$ is not equal to zero. Therefore, this term adds the required ac-component in circulating current reference. It is further noted that the sign of q_4 needs to be reversed when active power changes direction as the sinusoidal term in (7.9) would also change phase by 180^0.

It is noted that the added sinusoidal component should be in phase with the corresponding phase. This can be achieved by delaying (7.8) by 90 degrees as the voltages in the arms would lead the currents by 90 degrees due to the inductor.

It should be added that the second and third terms in (7.7) would only act when the summation voltages are not regulated to V_{dc}. Finally, it is noted that the modified reduced indirect FCS-MPC method is used for verification.

7.3.1 Summary

The overall strategy is summarized as below:

- One step ahead prediction with delay compensation using the modified reduced indirect FCS-MPC method *i.e.*, for only 25 control options at the initial time step, followed by nine control options at next time steps using (2.15). This makes the total control options for a prediction horizon (denoted by p) $= 25 \cdot (3)^{2(p-1)}$
- The correct reference determination for circulating current using (7.7)
- Selection of insertion indices which minimize the cost function (7.1) , with circiulationg current reference as specified above.
- Perform capacitor voltage balancing task based on some sorting algorithm and the selected insertion indices.

7.4 Simulation Results

The same scenario and simulation parameters are used as in chapters Chapters 4,5,6. Figure 7.1 shows that the steady-state and dynamic performance of the active power and ac-current tracking is very good. In Fig. 7.2 circulating current tracking along with summation voltages is shown. It is noted here that due to the proposed reference, the circulating current adjusts itself whenever the summation voltages are not balanced. For example, the

sinusoidal component in circulating current is clearly visible at the transient and as soon as summation voltages balance themselves this component vanishes completely. It can also be observed that the average of the summation voltages of each arm is at their reference. Thus the total leg voltage is regulated to $2V_{dc}$ on average and arm voltage difference is regulated to zero on average. This is in contrast to Fig. 4.9 where the constant circulating current reference was used with conventional quadratic cost function and without any outerloop. It can be seen in Fig. 4.9 that the summation voltages are diverging away from the reference. The dynamic response of the summation voltages can be further improved by increasing q_2 in (7.7). However, this will result in an increased ripple in circulating current during the transient.

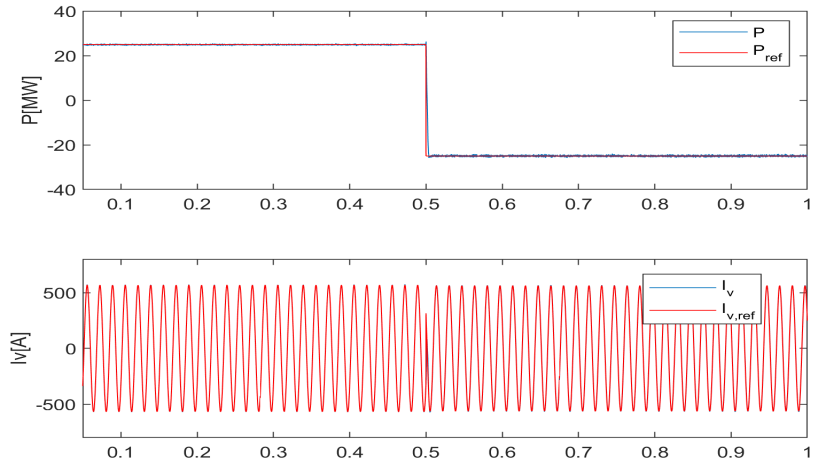

Figure 7.1: Proposed Method: (a) real power, (b) phase-a current,

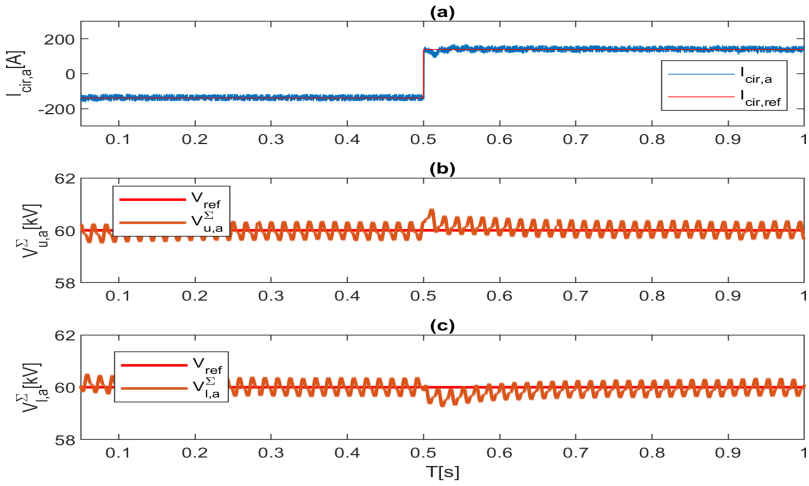

Figure 7.2: Proposed Method: (a) phase-a circulating current, (b) summation of the capacitor voltages in the lower arm of phase a, and (c) summation of the capacitor voltages in the upper arm of phase a

7.5 Conclusion

In this work, it is shown that a proper reference for the circulating current is required when using conventional cost function (7.2) (without any outer PI loop) with predictive control techniques to ensure regulation of summation voltages. A constant circulating current reference leads to a marginally stable system and leads to summation voltages that slowly diverge away from their reference. Therefore, a new reference for circulating current based on instantaneous and average summation voltages was proposed that regulates the average summation voltages to their reference without the need of outer loop.

Bibliography

[1] Z. Gong, P. Dai, X. Yuan, X. Wu and G. Guo, "Design and Experimental Evaluation of Fast Model Predictive Control for Modular Multilevel Converters," *IEEE Transactions on Industrial Electronics,* vol. 63, no. 6, pp. 3845-3856, June 2016

[2] J. Huang et al., "Priority Sorting Approach for Modular Multilevel Converter Based on Simplified Model Predictive Control," *IEEE Transactions on Industrial Electronics,* vol. 65, no. 6, pp. 4819-4830, June 2018

[3] Nguyen, M.H.; Kwak, S. "Improved Indirect Model Predictive Control for Enhancing Dynamic Performance of Modular Multilevel Converter." *Electronics* 9(9), 1405, 2020.

[4] F. Zhang and G. Joos, "A predictive nearest level control of modular multilevel converter," *2015 IEEE Applied Power Electronics Conference*

and Exposition (APEC), 2015, pp. 2846-2851

[5] J. Yin, J. I. Leon, L. G. Franquelo, S. Vazquez and A. Marquez, "Generating the Arm Voltage References of Modular Multilevel Converters Employing Predictive Technique," *IECON 2018 - 44th Annual Conference of the IEEE Industrial Electronics Society,* 2018, pp. 3949-3954

[6] M. H. Nguyen, S. Kwak and T. Kim, "Phase-Shifted Carrier Pulse-Width Modulation Algorithm With Improved Dynamic Performance for Modular Multilevel Converters," in *IEEE Access,* vol. 7, pp. 170949-170960, 2019

[7] H. Mahmoudi, M. Aleenejad and R. Ahmadi, "Modulated Model Predictive Control of Modular Multilevel Converters in VSC-HVDC Systems," in *IEEE Transactions on Power Delivery,* vol. 33, no. 5, pp. 2115-2124, Oct. 2018

[8] M. Li, X. Chang, N. Dong, S. Liu, H. Yang and R. Zhao, "Arm-Current-Based Model Predictive Control for Modular Multilevel Converter Under Unbalanced Grid Conditions," in *IEEE Journal of Emerging and Selected Topics in Power Electronics,* vol. 10, no. 3, pp. 3195-3206, June 2022

[9] J. Wang, Y. Tang, P. Lin, X. Liu and J. Pou, "Deadbeat Predictive Current Control for Modular Multilevel Converters With Enhanced Steady-State Performance and Stability," in *IEEE Transactions on Power Electronics,* vol. 35, no. 7, pp. 6878-6894, July 2020

[10] W. Tian, X. Gao and R. Kennel, "Model Predictive Control of Modular Multilevel Converters with Independent Arm-Balancing Control," *2019 IEEE International Symposium on Predictive Control of Electrical Drives and Power Electronics (PRECEDE),* 2019, pp. 1-5

[11] Y. Jin et al., "A Novel Sliding-Discrete-Control-Set Modulated Model Predictive Control for Modular Multilevel Converter," in *IEEE Access,* vol. 9, pp. 10316-10327, 2021

[12] M. Vatani, B. Bahrani, M. Saeedifard and M. Hovd, "Indirect Finite Control Set Model Predictive Control of Modular Multilevel Converters," *IEEE Transactions on Smart Grid,* vol. 6, no. 3, pp. 1520-1529, May 2015

[13] M. H. Nguyen and S. Kwak, "Simplified Indirect Model Predictive Control Method for a Modular Multilevel Converter," *IEEE Access,* vol. 6, pp. 62405-62418, 2018

[14] P. Liu, Y. Wang, W. Cong and W. Lei, "Grouping-Sorting-Optimized Model Predictive Control for Modular Multilevel Converter With Reduced Computational Load," *IEEE Transactions on Power Electronics,* vol. 31, no. 3, pp. 1896-1907, March 2016

[15] B. Gutierrez and S. Kwak, "Modular Multilevel Converters (MMCs) Controlled by Model Predictive Control With Reduced Calculation Burden," *IEEE Transactions on Power Electronics,* vol. 33, no. 11, pp. 9176-9187, Nov. 2018

[16] K. Sharifabadi, L. Harnefors, H.-P. Nee, S. Norrga, and R. Teodorescu, *Design, Control and Application of Modular Multilevel Converters for HVDC Transmission Systems.* United States: Wiley-IEEE press, 2016

[17] L. Harnefors, S. Norrga, A. Antonopoulos and H. Nee, "Dynamic modeling of modular multilevel converters," *Proceedings of the 2011 14th European Conference on Power Electronics and Applications,* 2011, pp. 1-10.

[18] A. Antonopoulos, L. Angquist and H. Nee, "On dynamics and voltage control of the Modular Multilevel Converter," *2009 13th European Conference on Power Electronics and Applications,* 2009, pp. 1-10

[19] L. Harnefors, A. Antonopoulos, S. Norrga, L. Angquist and H. Nee, "Dynamic Analysis of Modular Multilevel Converters," in *IEEE Transactions on Industrial Electronics,* vol. 60, no. 7, pp. 2526-2537, July 2013

Chapter 8

Nonlinear Model Predictive Control of Modular Multilevel Converters

In this chapter, non-linear model predictive control (NMPC) without an explicit modulator is presented for modular multilevel converters (MMCs). To avoid the modulator, two strategies are presented to handle the continuous solution of NMPC. In the first strategy, the number of submodules (SMs) to be inserted for each arm is obtained by rounding the continuous solution for the insertion index from the NMPC to the nearest integer value. In the second strategy, the optimal solution obtained from the NMPC is further evaluated by rounding it up and down for both arms. This leads to evaluating the cost function (same as NMPC stage cost) for four discrete cases, independently from the number of SMs per arm. This evaluation is conducted only for the initial time step within the prediction horizon. Then the solution that minimizes the cost function is applied to the MMC. It is demonstrated that both strategies offer almost identical dynamic and steady-state results as full indirect FCS-MPC.

8.1 Introduction

Contrary to FCS-MPC based methods, the computational complexity of continuous control set model predictive control (CCS-MPC) is independent of the number of SMs and can be easily extended for longer prediction horizons. Previous works based on CCS-MPC for MMC [1–3] are mostly based on the linearized model of MMC and use explicit PWM modulators.

In this paper, a non-linear model predictive control (NMPC) is proposed for the MMC with delay compensation. To avoid the explicit modulator, two strategies have been proposed to deal with the continuous solution of NMPC. In the first strategy, the solution from NMPC is simply rounded off and sent to the balancing algorithm. In the second strategy, the solution obtained is tested by rounding it down and rounding it up for both the upper and lower arms. The second strategy requires only four simulations per time step, independently of the number of SMs/arm. Both strategies offer similar steady-state and dynamic performance as compared to full-indirect FCS-MPC.

8.2 Proposed Approach

8.2.1 Problem Formulation

The references for all the state variables are the same as presented in Section 4.1.1 and the cost function used for this work is (4.4)

The constraints on the inputs of the system are linear and given as:

$$\begin{aligned} 0 \leq u_1 \leq N \\ 0 \leq u_2 \leq N \\ u_1 + u_2 \leq N + 2 \\ u_1 + u_2 \geq N - 2 \end{aligned}$$

where N is the total number of SMs in each arm of the MMC. The first two constraints are physical constraints *i.e.*, the number of inserted modules per arm cannot be negative and cannot be more than the total

number of SMs in that arm. The other two constraints ensure that the total number of switched-on modules is not too far from N because in normal operation the total number of voltage levels should be near N. Note that the reference of summation voltages is fixed to V_{dc} for this work. If the reference is not fixed then constraints three and four need to be modified. Moreover, in addition to the constraints defined above, linear constraints can also be imposed on state variables.

The optimization problem can then be written as:

$$\begin{aligned} \min_{u} \quad & \sum_{n=1}^{p} J_j \\ \text{s.t.} \quad & \dot{x}(t) = Ax(t) + \sum_{i=1}^{2}(B_{ix}u_i) + d(t) \\ & 0 \leq u_1 \leq N \\ & 0 \leq u_2 \leq N \\ & u_1 + u_2 \leq N + 2 \\ & u_1 + u_2 \geq N - 2 \end{aligned} \tag{8.1}$$

where the model in (2.14) is discretized by the Runge-Kutta 4 method, p is the prediction horizon, and the control horizon is kept equal to the prediction horizon.

With the above problem, NMPC is applied using CasADi in MATLAB to get the continuous optimal solution. In order to avoid the modulator, two strategies are presented to deal with the continuous solution of the NMPC. In the first strategy (Case I), this solution is simply rounded off to the nearest integer and is sent to the voltage balancing module. In the second strategy (Case II), the solution obtained from NMPC for both arms is rounded up and rounded down. This leads to evaluating the cost function (4.4) for four discrete cases, independently from the number of SMs per arm. It is noted here that the rounding operations are only performed for the solution in the first step of the prediction horizon.

Case I can be summarized as:

1. Continuous-valued optimal insertion index based on the minimization of the cost function (4.4) is obtained by NMPC

2. Round off the solution to the nearest integer from step 1

3. Perform capacitor voltage balancing using the sorting algorithm

Case II can be summarized as:

1. Continuous optimal insertion index based on the minimization of the cost function (4.4) is obtained by NMPC

2. Round up and down the solution from 1

3. Select the insertion index from 2 that minimizes the cost function (4.4)

4. Perform capacitor voltage balancing in voltage balancing module

8.3 Simulation Results

Similar scenarios and simulation parameters as in the previous chapter are used. Figures 8.1 & 8.2 shows the overall response for all states using Case I and II respectively. It can be observed that both methods offer almost identical performance.

The dynamic response comparison of both methods to full indirect FCS-MPC is shown in Fig. 8.3 which shows that both methods result in identical dynamic performance as full indirect FCS-MPC.

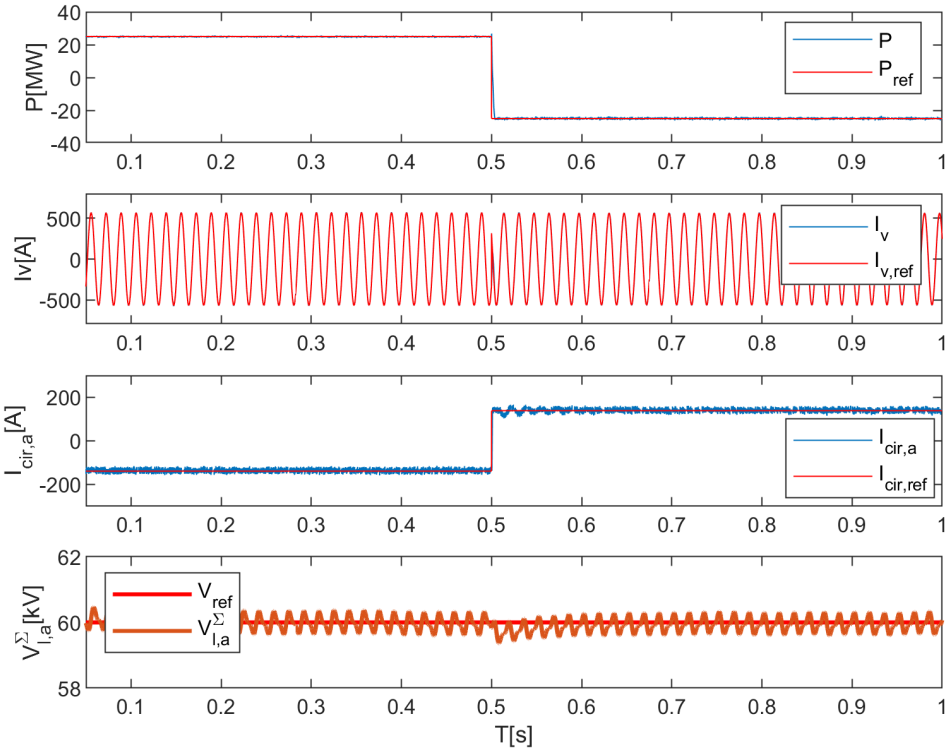

Figure 8.1: Proposed Method-Case I: (a) real power, (b) phase-a current, (c) phase-a circulating current, (d) summation of the capacitor voltages in the lower arm of phase a,

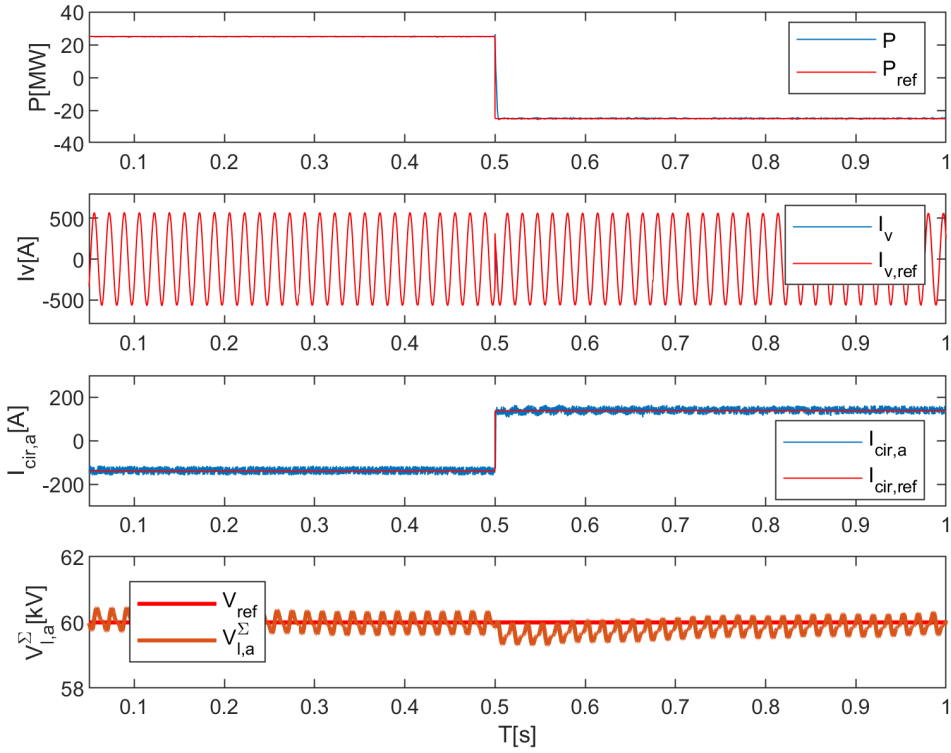

Figure 8.2: Proposed Method-Case II: (a) real power, (b) phase-a current, (c) phase-a circulating current, (d) summation of the capacitor voltages in the lower arm of phase a,

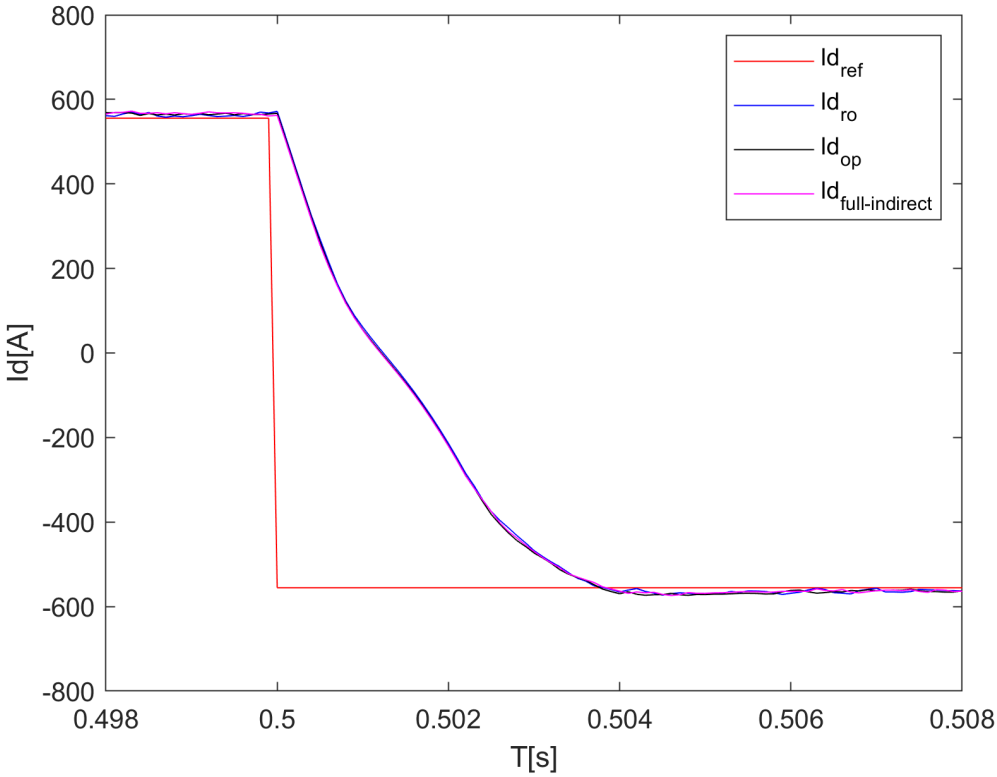

Figure 8.3: Comparison of Results for d-axis component of ac-side current: Id_{ro}: Case-I, Id_{op}: Case-II, $Id_{full-indirect}$:Full-indirect FCS-MPC

8.3.1 Computational Requirements Discussion

Simulations

The simulations were made using MATLAB R2019b on Intel® Core i7, 3.20 GHz, with 16 GB RAM. The time taken by full indirect FCS-MPC and NMPC for a one-time step for 18SMs/arm and a prediction horizon

$p = 2$ are on average 0.9321 and 0.5401 seconds respectively. It can be observed that the time taken by FCS-MPC is almost twice that of NMPC in this scenario. Therefore, for longer prediction horizons, NMPC should be the automatic choice. However, for $p = 1$ full indirect FCS-MPC ($0.0185s$) is faster as compared to NMPC ($0.4997s$). Therefore, due to the bilinear model and short sampling time, the computational complexity of NMPC for MMC is high thus complicating its real-time application. It is expected that with ongoing research the computational complexity of NMPC will be reduced in the near future.

Dedicated Hardware Platform

The time taken by both FCS-MPC and NMPC is expected to be much shorter with efficient implementation on a dedicated real-time platform (without much of the overhead of the operating system on a general-purpose computer). Although the experimental results are discussed in the next chapter, some computational loading is discussed here.

It is noted that for the experiments the loading on the system includes both the loading by the conventional PI control and by the MPC methods. The following summarizes how much the system was loaded with a $T_s = 100\mu s$.

Table 8.1: System Loading Comparison

Methodology	**System Loading**
Conventional PI based Control	52%
PI + Modified Reduced indirect FCS-MPC	71%
PI + Nonlinear Model Predictive Control	128%

The comparison in Table 8.1 shows that the conventional PI-based control implementation requires around $52\mu s$ for one time step, whereas modified reduced indirect FCS-MPC (MRI-FCS-MPC) requires an additional $19\mu s$ and nonlinear model predictive control (NMPC) requires an additional

$76\mu s$ as compared to PI-based control. This means that if implemented alone then MRI-FCS-MPC and NMPC would require $19\mu s$ and $76\mu s$ for one time step (horizon 1). However, NMPC experiments could not be implemented in the lab with $T_s = 100\mu s$ as PI based control was required for start up.

8.4 Conclusion

In this work, an NMPC strategy without an explicit modulator is proposed for MMC. Two methods were presented to deal with the continuous solution of NMPC. It was shown that it is enough to simply round off the solution from NMPC to avoid the explicit modulator. The NMPC problem was formulated and solved using CasADi in MATLAB with a per-phase cost function and linear constraints. Simulations demonstrate that the proposed method gives similar performance as full indirect FCS-MPC. Moreover, as compared to indirect FCS-MPC techniques the proposed method can easily be extended for longer prediction horizons. It should be noted, though, that a longer prediction horizon will require longer calculation times also for NMPC. However, for NMPC this increase can be expected to be much less than for full indirect FCS-MPC.

Bibliography

[1] G. Darivianakis, T. Geyer and W. van der Merwe, "Model predictive current control of modular multilevel converters," *2014 IEEE Energy Conversion Congress and Exposition (ECCE),* 2014, pp. 5016-5023

[2] S. Fuchs, M. Jeong and J. Biela, "Long Horizon, Quadratic Programming Based Model Predictive Control (MPC) for Grid Connected Modular Multilevel Converters (MMC)," *IECON 2019 - 45th Annual Conference of the IEEE Industrial Electronics Society,* 2019, pp. 1805-1812

[3] S. Fuchs and J. Biela, "Impact of the Prediction Error on the Performance of Model Predictive Controllers with Long Prediction Horizons for Modular Multilevel Converters - Linear vs. Nonlinear System Models," *2018 20th European Conference on Power Electronics and Applications (EPE'18 ECCE Europe),* 2018, pp. P.1-P.9.

Chapter 9

Experimental Verification

In this chapter, the necessary modifications in the proposed methods for experimental verification will be presented. The modifications include delay compensation i.e. forward and feedback delays. In total, a delay of $6T_s$ is compensated. In the existing literature, only a computational (forward) delay of $1T_s$ is considered. The extended delay compensation leads to a problem in ac-side voltage prediction. This problem is detailed and as a remedy for that, a very simple method for grid voltage estimation or a virtual ac side voltage approach is proposed as an alternative to using measured ac-side voltage. The steady-state and dynamic response is verified and compared with PI-based control both by simulations and in laboratory setup using an MMC with 18 half-bridge sub-modules per arm.

9.1 Introduction

The methods proposed in previous chapters addressed different issues, however only simulation results were presented and no practical delays were considered.

The existing papers in the literature consider only a computational delay of one sampling instant and handle it by finding the state variables at $k+2$ instant instead of $k+1$ [1]. However, a solution closer to reality should

consider both the forward (control) delay and the feedback (measurement) delay. The forward delay compromises two delays *i.e.*, the delay from the central controller to arm level control and the delay from arm level control to module level modulation output.

In this chapter, the works presented in earlier chapters are extended by incorporating actual experimental time delays and compensating for them. A total time delay of $6T_s$ is compensated. The performance is evaluated both by simulations and experiments. The cost function adopted is given in (4.4). In addition, a problem with ac-side voltage prediction was encountered when considering such a large time delay compensation. This issue is also presented and as a remedy for that, a very simple method for grid voltage estimation or a virtual ac side voltage approach is proposed.

9.2 Proposed Method

9.2.1 Delay Compensation

As already mentioned, the existing papers on time delay compensation for FCS-MPC only compensate for a time delay of one sampling instant *i.e.* the computational time delay. However, in the actual experimental setup, there are other delays that need to be considered as well. In this work, all such time delays are considered and compensated for. The total delay compensated in this paper is $6T_s$. The details of each delay are discussed later in the hardware setup section.

The delay compensation method is similar to as detailed in [2]. However, due to a longer time delay, it is modified as follows:

- measurement received x(k-1)
- application of u(k-6) to find x(k)
- application of u(k-5) to find x(k+1)
- application of u(k-4) to find x(k+2)
- application of u(k-3) to find x(k+3)

- application of u(k-2) to find x(k+4)
- application of u(k-1) to find x(k+5)
- prediction of states x(k+6) using any one of the proposed methods
- evaluation of cost function for each insertion index
- selection of insertion index that minimizes the cost function

9.2.2 Problem with Prediction of AC-side Voltage

Before explaining the prediction problem associated with ac-side voltage, it is important to highlight that in practice the MMC is mostly connected in a three-phase three-wire system. Therefore, zero sequence voltage cannot cause zero sequence current. However, the model in (2.14) was derived for a three-phase four-wire system. As a result, zero sequence current would appear. Hence, zero sequence voltage compensation is required. It is noted that zero sequence voltage compensation is only required for the delay compensation part *i.e.,* for the actual execution of MPC per-phase model given by (14) will be used. The detailed derivation for this compensated term can be found in [3]. The modified ac-current dynamics after compensation can be given as:

$$\frac{di_{v,j,comp}}{dt} = \frac{di_{v,j}}{dt} + V_{comp} \tag{9.1}$$

where

$$V_{comp} = \frac{1}{3N(L+2L_c)}(\sum_{i=a}^{c} E_{v,i}) \tag{9.2}$$

and

$$E_{v,j} = n_{l,j}v_{l,j}^{\Sigma} - n_{u,j}v_{u,j}^{\Sigma} \tag{9.3}$$

Coming back to the problem with the prediction of ac-side voltage, it is noted that to reach $x(k+6)$, the prediction model of ac-side voltage v_f is also required. A simple sinusoidal model cannot be used for predicting v_f in

the presence of grid/ac-side impedance. This is due to the discrete nature of MPC that results in an instantaneous step in v_f whenever the total number of inserted SMs will change. It is noted here that this problem does not appear with the existing MPC techniques in literature because they only consider delay compensation of $1T_s$. Therefore, ignoring a single step in v_f does not have a significant effect on the performance of the system. However, because the actual real system delay is longer (in this case $6T_s$) so there would be a step in v_f for each compensation (six times) and the sinusoidal model would fail to accurately predict v_f six steps ahead.

To understand this better, it is first assumed that there is no transformer between the grid and MMC. It is noted here that L_c is the equivalent grid inductance and the measured ac voltage is $v_{t,j}$ as indicated in Fig. 2.1 for this simplified case. The MMC output voltage can be written as:

$$v_{t,j} = \frac{R}{2} i_{v,j} + \frac{L}{2} \frac{di_{v,j}}{dt} - \frac{(\sum_{i=a}^{c} E_{v,i})}{6N} + \frac{n_{l,j} v_{l,j}^{\Sigma} - n_{u,j} v_{u,j}^{\Sigma}}{2N} \tag{9.4}$$

For the purpose of simplification, the internal voltage of MMC (last term in above equation) is denoted by $e_{v,j}$. After some simplification and using $e_{v,j}$, (9.4) can be rewritten as:

$$v_{t,j} = \frac{R}{2} i_{v,j} + \frac{L}{2} \frac{di_{v,j}}{dt} - \frac{(\sum_{i=a}^{c} e_{v,i})}{3} + e_{v,j} \tag{9.5}$$

Now, the instantaneous change in MMC output voltage under the change in insertion index using (9.5) can be expressed as:

$$\Delta v_{t,j} = \left(\frac{L}{2}\right) \frac{\Delta di_{v,j}}{dt} + \Delta e_{v,j} - \frac{(\sum_{i=a}^{c} \Delta e_{v,i})}{3} \tag{9.6}$$

The first term in (9.5) will have negligible contribution in $\Delta v_{t,j}$ because the current will not have a significant change instantaneously. Now, to find an exact expression for $\Delta v_{t,j}$, it is required to find an expression for $\frac{\Delta di_{v,j}}{dt}$. Using (9.1), this can be expressed as:

$$\frac{\Delta di_{v,j}}{dt} = \left(\frac{2}{L + 2L_c}\right) \left(\frac{(\sum_{i=a}^{c} \Delta e_{v,i})}{3} - \Delta e_{v,j}\right) \tag{9.7}$$

Following the same reasoning, the first and last term of (2.13a) will have negligible contribution in $\frac{\Delta di_{v,j}}{dt}$ under the change in insertion index because the grid voltage and current will not have significant change instantaneously. Now, substituting (9.7) into (9.6) following is obtained:

$$\Delta v_{t,j} = \left(\frac{L}{L+2L_c}\right)\left(\frac{(\sum_{i=a}^{c}\Delta e_{v,i})}{3} - \Delta e_{v,j}\right) + \left(\Delta e_{v,j} - \frac{(\sum_{i=a}^{c}\Delta e_{v,i})}{3}\right) \tag{9.8}$$

So, the instantaneous change in MMC output voltage can be represented by the above equation. Once this change has occurred, then the MMC output voltage follows a sinusoidal model until another change of insertion index occurs. Therefore, it is important to take this instantaneous change into account while predicting the ac-side voltage of MMC. It can be noted that if $L_c = 0$ then there would be no instantaneous jump in ac-side voltage.

In the above derivation, it was assumed that there is no transformer between the MMC and the grid. The only modification required in (9.8) to include the impact of the transformer is to add the transformer equivalent inductance into L_c.

Therefore, in order to predict ac-side voltage accurately the instantaneous change in (9.8) needs to be accommodated. The method described above would work fine for the delay compensation part as the change in insertion indices is known from the past. However, a problem would arise when predicting the state x(k+6) for the possible insertion indices. This can be seen from (9.8) *i.e.*, the instantaneous jump depends on the change of insertion index in all phases. As a result, one cannot use independent cost functions for each phase. The use of a single cost function would require evaluating all the combinations of insertion indices among the phases thus resulting in a very high computational complexity *i.e.*, $(N+1)^6$.

In order to avoid the above problem, an estimated grid voltage or a virtual ac-side voltage can be used instead of measured ac-voltage. These voltages would follow a sinusoidal path and are independent of the changes in insertion indices of MMC. Hence, they can be predicted very accurately using a sinusoidal model.

9.2.3 Estimated Grid Voltage

Within the MPC framework, it is very simple to estimate the grid voltage. The discretized version of the grid voltage using (9.1) can be given as:

$$v_{g,j}(k) = (i_{v,j}(k+1) - i_{v,j}(k))\,\frac{L+2L_c}{2T_s} + \frac{R}{2} i_{v,j}(k) + \frac{\left(n_{u,j} v^{\Sigma}_{u,j}(k) - n_{l,j} v^{\Sigma}_{l,j}(k)\right)}{2N} + \frac{V_{comp}(k)(L+2L_c)}{2T_s} \quad (9.9)$$

It is noted that L_c is the equivalent grid side impedance. In (9.9), if the actual measured value for $i_{v,j}(k+1)$ is known then the grid voltage can be estimated very accurately. However, there is no way to know the measured value of $i_{v,j}(k+1)$ before its measurement. Therefore, the past values of the ac-current, summation voltages, and zero sequence voltage are stored. Then using measured value $i_{v,j}(k)$ and the stored past values $i_{v,j}(k-1)$, $v^{\Sigma}_{u,j}(k-1)$, $v^{\Sigma}_{l,j}(k-1)$, $V_{comp}(k-1)$, $n_{u,j}(k-1)$ and $n_{l,j}(k-1)$, it is very easy to find the estimated grid voltage at $(k-1)$ instant. Once this is known, a sinusoidal model is used to predict it into the future. The ninety-degree delayed version of the estimated grid voltage is given as feedback to MPC for the sinusoidal model to work. It is noted that the estimate of the grid voltage is updated at each sampling instant. An issue associated with the presented grid voltage estimation is its sensitivity to measurement noise. Therefore, a bandpass filter [4] is used on (9.9) to eliminate the measurement noise.

9.2.4 Virtual AC-Side Voltage

Another method to avoid the problem with the prediction of AC-side voltage is to create a virtual AC-side voltage (denoted by $V_{f,vt}$). This is achieved by setting $L_c = 0$ in (9.9). It is noted that the value obtained for $V_{f,vt}$ is also for the $(k-1)$ time instant, and a sinusoidal model is used to predict it into the future. Again a bandpass filter is essential to nullify the impact of measurement noise and the steps in ac-side voltage.

This method is better than the estimated grid voltage approach as the equivalent grid side impedance knowledge is generally not available and this impedance in itself is estimated. Therefore, in this work, the virtual ac-side voltage approach is utilized.

9.3 Hardware Setup for Experimental Validation

The tests are performed in the laboratory on a reduced-scale MMC prototype with controllable ac- and dc-side voltage sources. A brief description of the hardware setup is provided next.

9.3.1 Hardware Setup

The validation of the proposed method is done on an experimental setup consisting of an MMC with 18 modules per arm. The MMC operating limits for ac and dc voltage are 400 V and 700 V respectively [5]. The SMs are rated for a dc voltage up to 80V and MOSFETs are used as switching devices.

The main control loops of the MMC are implemented on an OPAL-RT OP5600 real-time simulation platform used for rapid prototyping of the control system. For the conventional control, these loops consist of a circulating current suppression controller and grid current regulator. The circulating current controller is based on [6]. The ac-side currents are controlled by using a standard decoupled dq current control in the synchronously rotating reference frame [6]. In the case of MPC, only a MATLAB function block is used which receives the measurements from the actual system. It is also to be noted here that MPC is working in the abc reference frame.

The modulation of each arm and the processing of the individual cell voltage measurements are handled by a distributed control system based on FPGAs [5, 7]. The sorting algorithm as described in [10] is used to perform the SM capacitor voltage balancing task in combination with SM unified PWM (SUPWM) where only one SM is modulated. Based on the direction of arm currents, the appropriate SM capacitor is inserted or bypassed. The modulation technique used compensates for cell voltages [8].

9.3.2 Delays

The different delays that exist for an MMC experimental setup considered in this work are summarized as follows:

- Forward delay – from a central controller (OPAL-RT) to arm-level control (Zync control board): $2T_s$
- Forward delay – from arm-level control (Zync) to module-level modulation output: $2T_s$ ($1T_s$ for communication and $1T_s$ for the modulation)
- Feedback delay – from capacitor voltage measurements to OPAL-RT: $2T_s$
- Feedback delay – from arm current measurements to OPAL-RT: $1T_s$

This implies that there is a total delay of $4T_s + 2T_s$ (forward + feedback) in addition to a one-time step for actuation. However, the voltage dynamics are quite slow as compared to current dynamics. Therefore, the feedback delay is considered to be $1T_s$ *i.e.*, it is assumed that there is no significant change in the capacitor voltages within $1T_s$.

9.4 Results

9.4.1 Simulation Results

The performance of the system is validated by performing simulations on a three-phase MMC with 18 SMs per arm, as shown in Fig. 9.1 using the strategies proposed in earlier chapters and compared with the conventional PI based control.The synchronization of the system with grid is achieved by using a dq-frame phase locked loop (PLL). The PLL is working to align the d-axis to the grid voltage vector in steady state. All the references and measurements are sent to the MPC controller which outputs the optimal insertion index for each phase. These insertion indices are then sent to

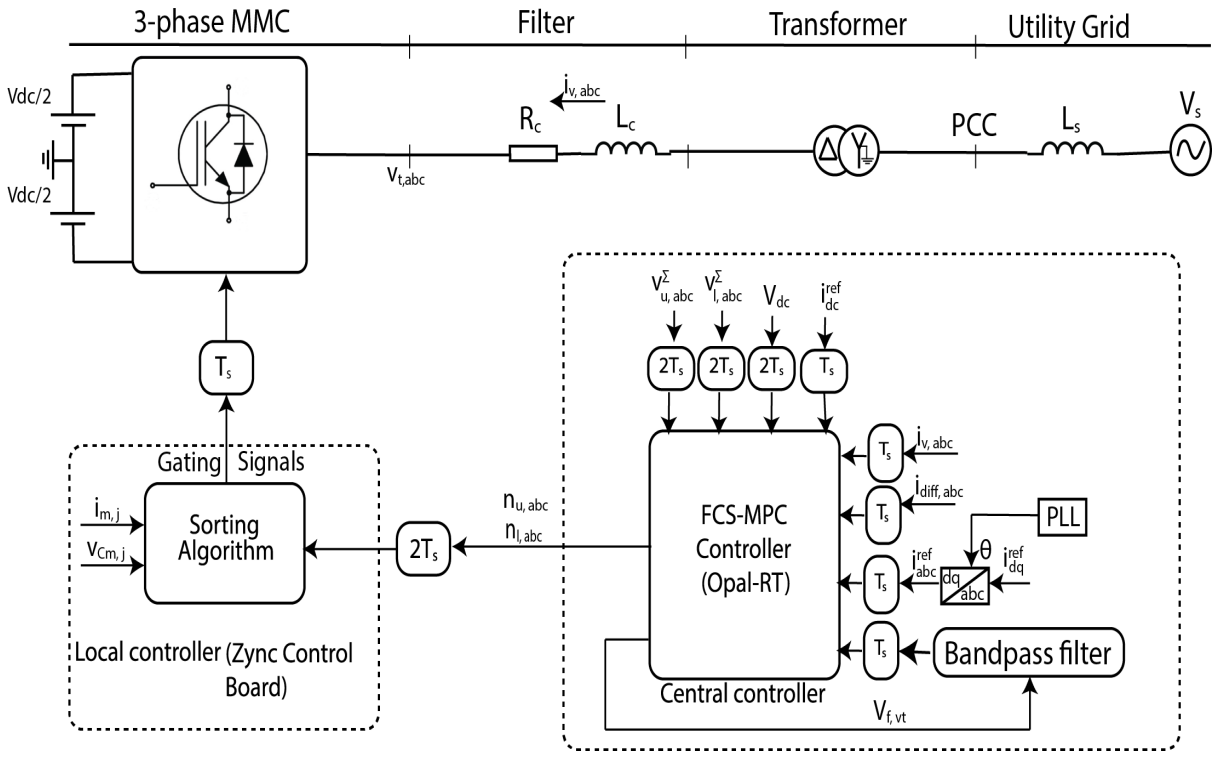

Figure 9.1: Control Block Diagram

the voltage balancing module which determines the gating signals for the MMC.

The scenario used for simulation is such that at t=0s the reference values of d and q component of current are set to 50 A and 0 A respectively, and at t = 0.3s the reference for d-component of current is changed to -50 A and finally at t=0.6s the reference is changed back to 50 A. The parameters used for simulation are summarized in Table 9.1.

Table 9.1: Simulation Parameters

Parameter	**Value**
MMC nominal power (base power)	50 kVA
AC system nominal voltage (base voltage)	400 V
Nominal frequency	50 Hz
Arm inductance (L)	1.55 mH
Arm resistance (R)	0.01Ω
Submodule capacitance (C)	20000μF
Transformer voltage rating (T)	400 V / 400 V
Transformer power rating	50 kVA
Transformer inductance	0.04 pu
Transformer resistance	0.006 pu
DC side reference voltage	700 V
Number of SMs per arm (N)	18
Sampling time (Ts)	70μs

To start with the overall response of modified reduced indirect FCS-MPC in comparison with PI based control [9] is shown in Fig. 9.2. The figure shows the performance of all the state variables being controlled by the proposed method and PI-based control. It can be observed from the results that the proposed method has better dynamic response for all the state variables. For instance, in Fig. 9.2(b) the PI-based control has large overshoots at transient in one direction and is slow to settle at the reference in the other direction. Whereas the proposed method has fast

dynamic response without overshoots in both directions. The circulating current tracking comparison can be seen from Fig. 9.2(c). Here again, the PI-based control has large ripples at transients which die out slowly thus resulting in a slower dynamic response of summation voltages tracking as shown in Fig. 9.2(d). On the other hand, with the proposed method, a dc and sinusoidal component is only introduced at the transient momentarily before settling at the new reference. Therefore, with the proposed method the summation voltages are also regulated fast as compared to PI-based control. The ripple in circulating current with the proposed method is introduced due to the use of the third and fourth terms in the cost function (4.4).

The overall response of all the other methods presented in previous chapters are more or less the same as MRI-FCS-MPC. Their results will be presented in the experimental results section. However, each method has certain advantages. As highlighted in Chapter 5, the added advantage of bisection and backstepping methods is reduced computational complexity and easy scaling up for MMCs with high number of SMs. Then, the active set method advantages are improvement of steady-state response and making computational complexity independent of the number of SMs. The method presented in Chapter 7 can be used with any of the proposed methods and its main advantage is the utilization of simple quadratic cost function as compared to 4.4. Finally, the advantage of NMPC is that it can be extended easily for longer prediction horizons. It is noted that the proposed active set method is only for a prediction horizon of one as it would be impossible to get the analytical expressions for higher prediction horizons due to the bilinear model of MMC.

Therefore, the main comparisons with PI-based control for each of the proposed methods would be same. The other meaningful comparison that can be made is of the dynamic response and total harmonic distortion (THD) with PI-based control. The dynamic response comparison of all the methods except Chapter 7 along with PI-based control is shown in Fig. 9.3 where

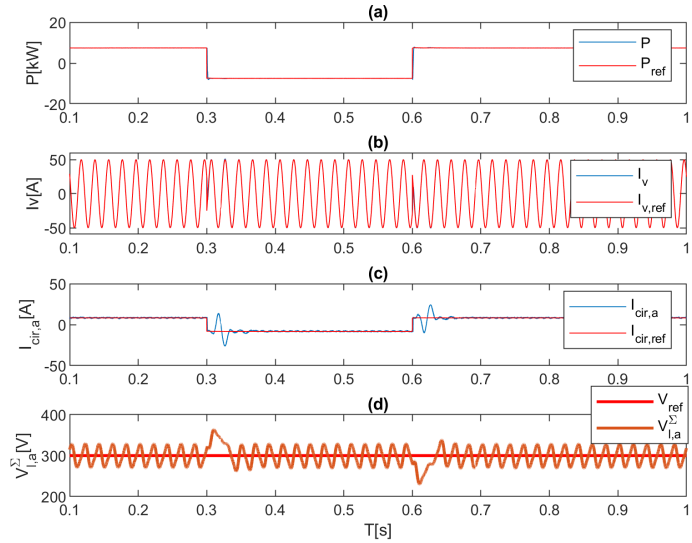

(i) MRI-FCS-MPC

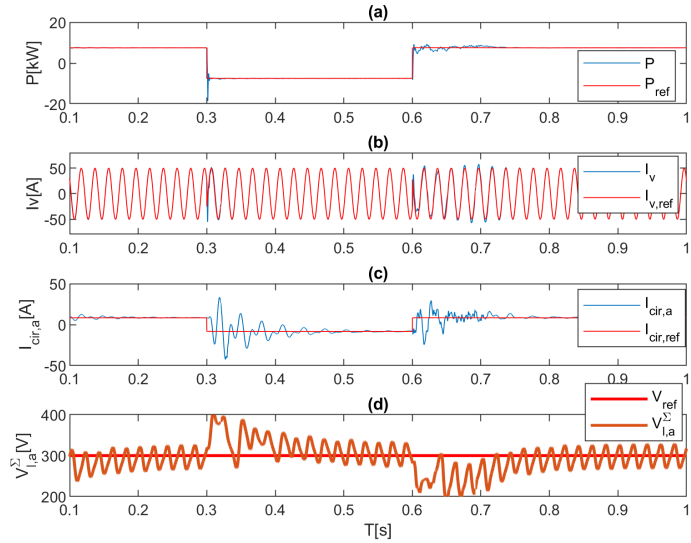

(ii) PI Based Method

Figure 9.2: MRI-FCS-MPC vs PI Based Method: (a) real power, (b) phase-a current, (c) phase-a circulating current, (d) summation of the capacitor voltages in the lower arm of phase a

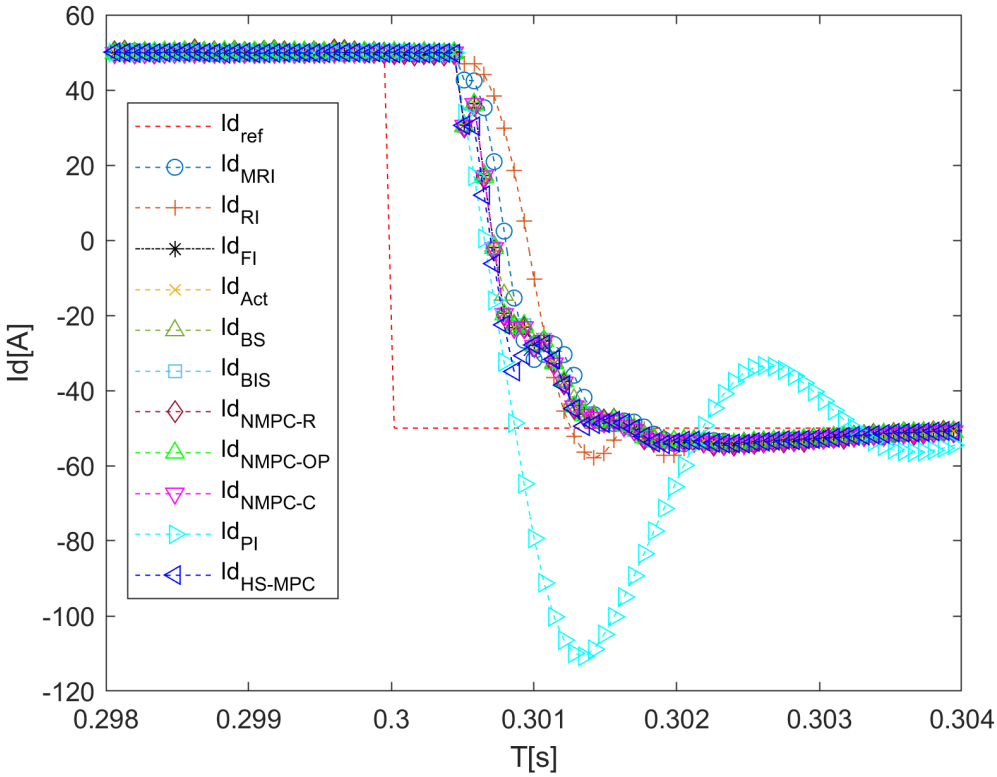

Figure 9.3: Comparison of Results for d-axis component of ac-side current

$Id_{ref} : Reference \quad Current$
$Id_{MRI} : Modified \quad Reduced \quad Indirect \quad FCS - MPC$
$Id_{RI} : Reduced \quad Indirect \quad FCS - MPC$
$Id_{FI} : Full \quad Indirect \quad FCS - MPC$
$Id_{Act} : Active \quad Set \quad Method$
$Id_{BS} : Backstepping \quad Method$
$Id_{BIS} : Bisection \quad Method$

$Id_{NMPC-R} : Nonlinear \quad Model \quad Predictive \quad Control - CaseII$
$Id_{NMPC-OP} : Nonlinear \quad Model \quad Predictive \quad Control - CaseI$
$Id_{NMPC-C} : Nonlinear \quad Model \quad Predictive \quad Control - Continuous$
$Id_{PI} : PI \quad based \quad Control$
$Id_{HS-MPC} : Higher \quad steps \quad based \quad method$

Before, discussing this figure a comment is made on the Id_{HS-MPC} i.e., higher steps based method. This method has not been explicitly presented in the thesis before. This method overcomes the disadvantage of modified reduced indirect FCS-MPC i.e., having the changes other than 0,+/-1 fixed to +/-5. In HS-MPC an estimate of what should be the larger steps than 0,+/-1,+/-2 is obtained by using the unconstrained solution and comparing it with the insertion index of the previous sampling instant. This difference is then used as a larger step. As a result, the large step is no longer fixed but it has become dynamic. In normal (steady-state) conditions, this difference would not be higher than 1 or 2. At transients, it could take higher values. Therefore, the computational complexity of this method becomes independent from the number of SMs.

As expected, reduced indirect FCS-MPC has the slowest dynamic response among the MPC based methods followed by modified reduced indirect FCS-MPC (MRI-FCS-MPC). All the other MPC based methods almost overlap with the full indirect FCS-MPC (where all the discrete voltage levels are considered). The MRI-FCS-MPC fails to achieve identical performance as full indirect FCS-MPC because the changes other than 0,+/-1 are fixed to +/-5 as explained earlier. Finally, coming to the PI based control. It appears that PI based control has the fastest dynamic response but this fast rate results in a large overshoot resulting in a slow convergence to the reference. Therefore, the response of all MPC based methods is better than the PI based method.

The THD of all the proposed methods are presented in Table 9.2. As claimed earlier the THD of active set method and nonlinear model predictive control are the best because they output continuous insertion index. These methods THDs are even better than the PI based method with the SUPWM method. There is no significant difference between the THDs of

Table 9.2: THD Comparison

Method	THD
Reduced Indirect FCS-MPC	0.36%
Modified Reduced Indirect FCS-MPC	0.33%
Full Indirect FCS-MPC	0.33%
Active Set Method	0.15%
Backstepping Method	0.33%
Bisection Method	0.33%
Non linear Model Predictive Control-Continuous	0.16%
PI based Method	0.24%
Higher Steps Method	0.34%

all the other methods which shows that in steady-state all of them have approximately same performance.

9.4.2 Experiment Results

The only difference between the simulation parameters and the experiment parameters is of the sampling time i.e., a sampling time of $100\mu s$ is used for experiments instead of $70\mu s$.

Here, again the overall response of the HS-FCS-MPC and MRI-FCS-MPC technique is presented in comparison with PI based control as shown in Figs. 9.4 and 9.5. As noted in simulations, it can again be noted that the MPC based methods offer better dynamic performance for each state variable. Moreover, the MPC based methods have little to no overshoots whereas the PI based method has overshoots and it also does not have a good performance when the reference is changed from -50 A to 50 A i.e., it takes a long time before settling at the desired reference as compared to MPC based methods. Regarding the comparison of HS-FCS-MPC and MRI-FCS-MPC it can be observed through Fig. 9.4 that the HS-FCS-MPC method has a slightly better dynamic response. This difference would have

been more visible if an MMC with a large number of SMs was used.

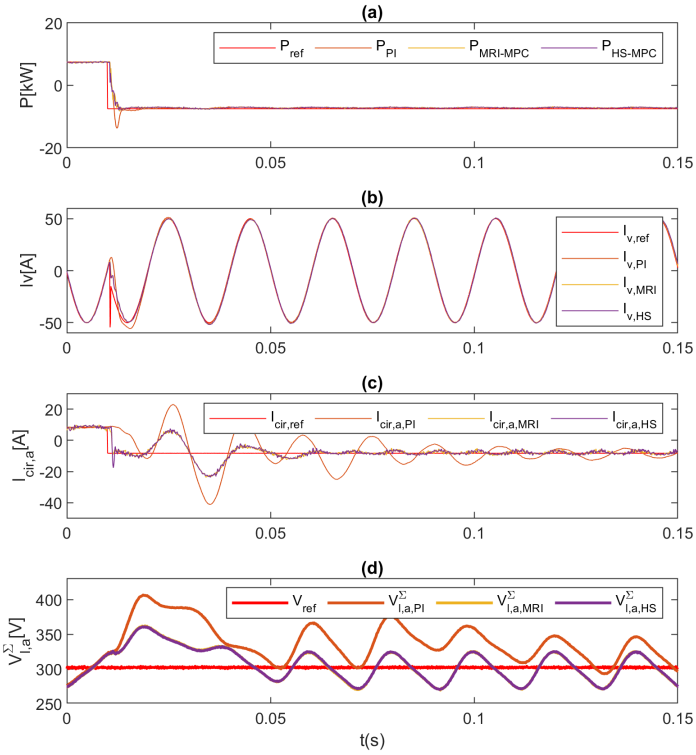

Figure 9.4: MRI-FCS-MPC vs HS-MPC vs PI based Control for change in $I_{d,ref}$ from 50 A to -50 A (a) real power, (b) phase-a current, (c) phase-a circulating current, (d) summation of the capacitor voltages in the lower arm of phase a

Now, the overall results for all the other proposed methods are presented. First the results of backstepping and bisection methods are shown in Figs. 9.6 and 9.7. It can be observed that both the methods have almost overlapping results which shows that both methods are equally good. The main reason behind the overlapping results is that both methods make the

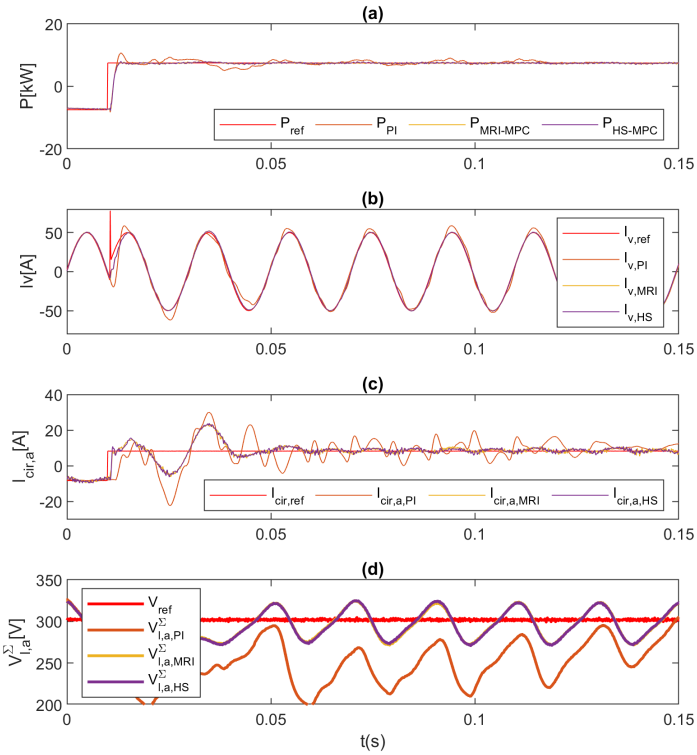

Figure 9.5: MRI-FCS-MPC vs HS-MPC vs PI based Control for change in $I_{d,ref}$ from -50 A to 50 A (a) real power, (b) phase-a current, (c) phase-a circulating current, (d) summation of the capacitor voltages in the lower arm of phase a

selection of the insertion index independent from the previous sampling instant and provide a very good continuous estimate of the insertion index in the first stage. Finally, in the second stage they look in a small neighborhood around this rounded estimate to find the discrete optimal insertion index.

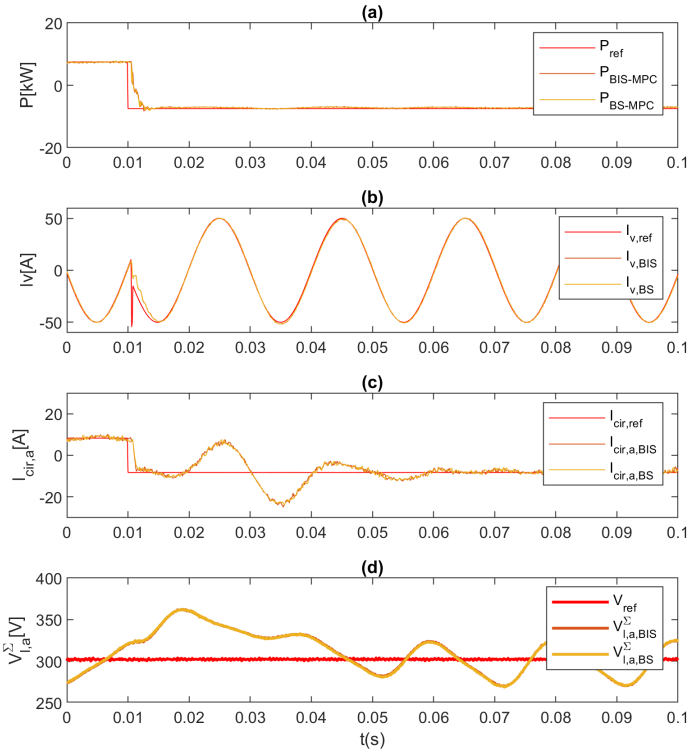

Figure 9.6: Bisection and Backstepping based MPC for change in $I_{d,ref}$ from 50 A to -50 A: (a) real power, (b) phase-a current, (c) phase-a circulating current, (d) summation of the capacitor voltages in the lower arm of phase a

Next, the overall results for the active set method and the unconstrained

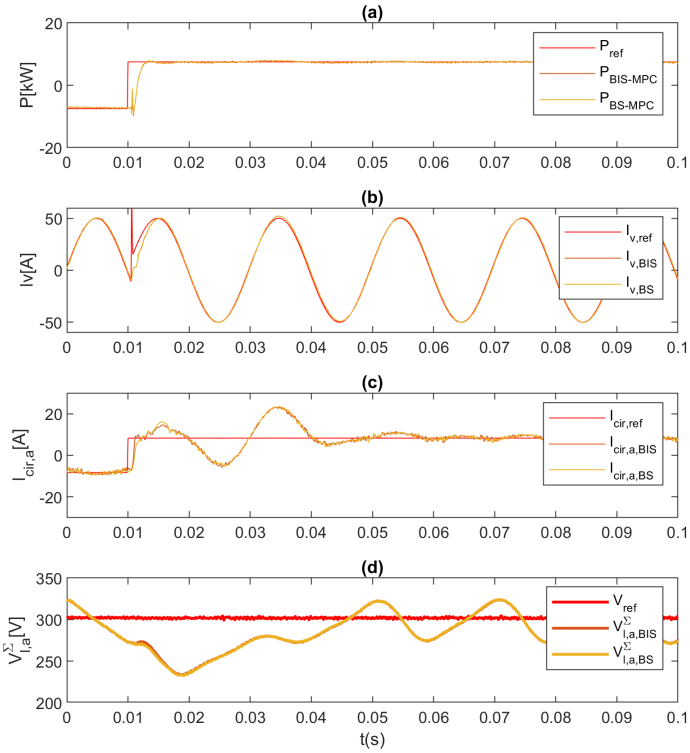

Figure 9.7: Bisection and Backstepping based MPC for change in $I_{d,ref}$ from -50 A to 50 A: (a) real power, (b) phase-a current, (c) phase-a circulating current, (d) summation of the capacitor voltages in the lower arm of phase a

saturated solution method are presented in Figs. 9.8 and 9.9. Here, as expected both methods have overlapping results in the steady-state as it is the unconstrained solution that will be followed in steady-state.

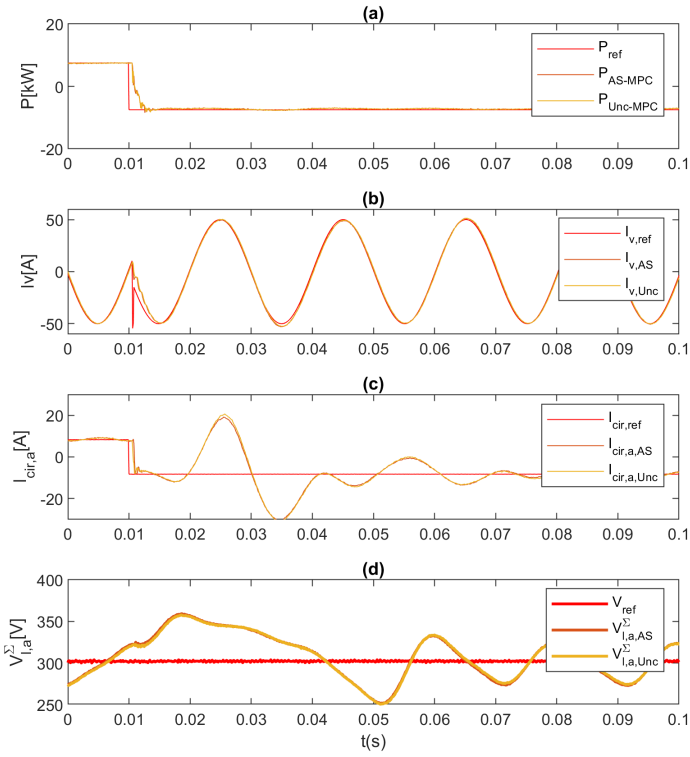

Figure 9.8: Active Set Vs Unconstrained Saturated Solution for change in $I_{d,ref}$ from 50 A to -50 A: (a) real power, (b) phase-a current, (c) phase-a circulating current, (d) summation of the capacitor voltages in the lower arm of phase a

To illustrate the difference between the active set method and the unconstrained saturated solution method the d-component of ac-current is shown in Fig. 9.10.

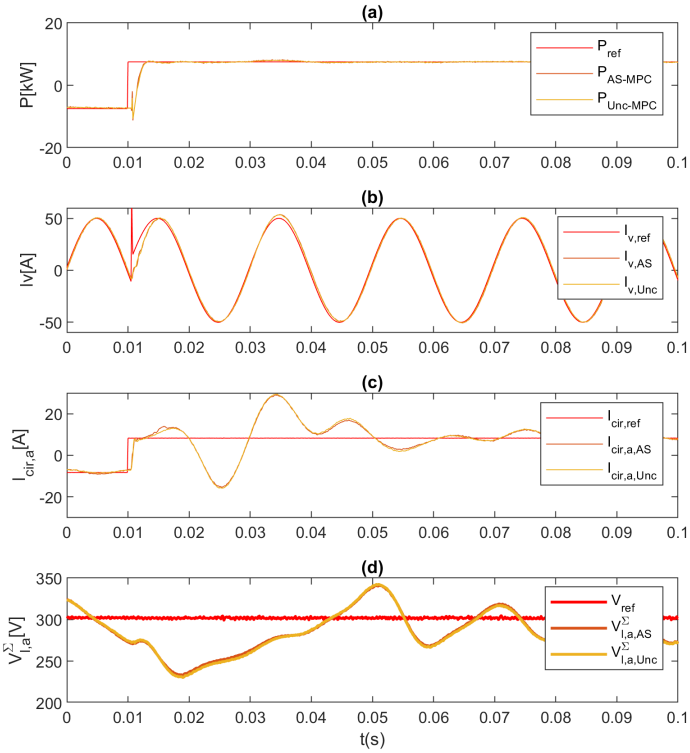

Figure 9.9: Active Set Vs Unconstrained Saturated Solution for change in $I_{d,ref}$ from -50 A to 50 A: (a) real power, (b) phase-a current, (c) phase-a circulating current, (d) summation of the capacitor voltages in the lower arm of phase a

Here one can see that the active set method offers slightly better dynamic response which confirms the fact that the unconstrained saturated solution is not the optimal one. In comparison to MRI-FCS-MPC, bisection and backstepping based methods, the active set method offers better steady state performance as it results in continuous insertion index and SUPWM is being used at modulation stage. However, the ripple in the circulating current at the transient is higher in the active set or unconstrained satu-

rated solution method as compared to the MRI-FCS-MPC, bisection and backstepping based methods.

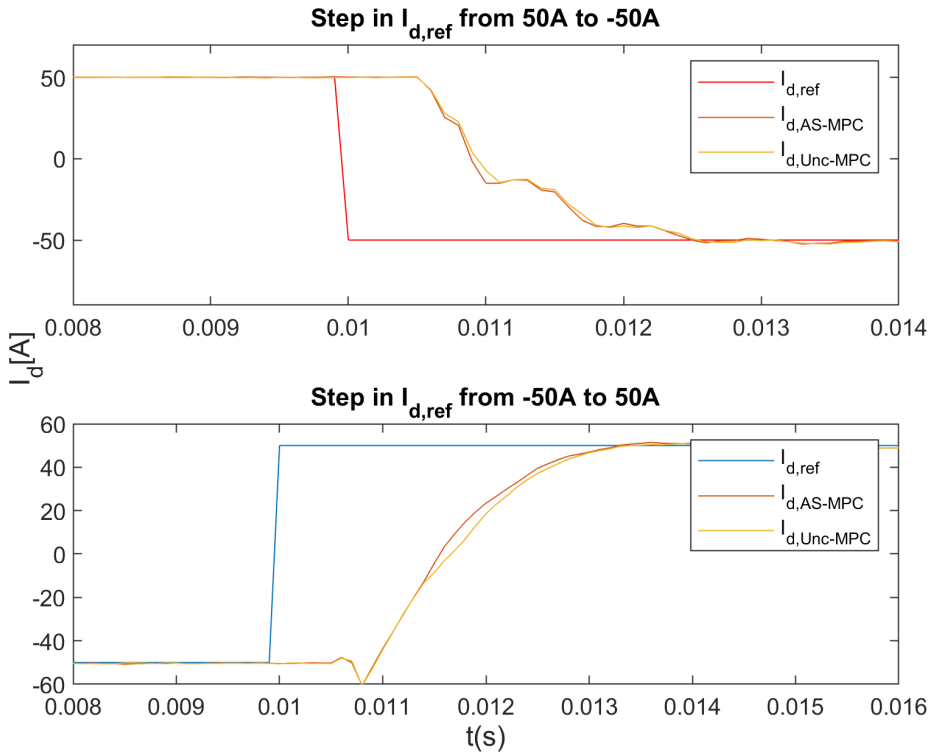

Figure 9.10: Active Set Vs Unconstrained Saturated Solution: Comparison of Results for d-axis component of ac-side current

The results for the method presented in Chapter 7 are shown in Figs. 9.11 and 9.12. The method successfully regulates the summation voltages at their reference with a simple quadratic cost function and all the other state variables tracking is also good. As compared to MRI-FCS-MPC, bisection and backstepping methods this method has a slightly large ripple in circulating current at transient and also takes a bit more time to settle

at the constant reference for circulating current. The circulating current response can be improved by tuning the q_1 and q_2 terms in (7.7).

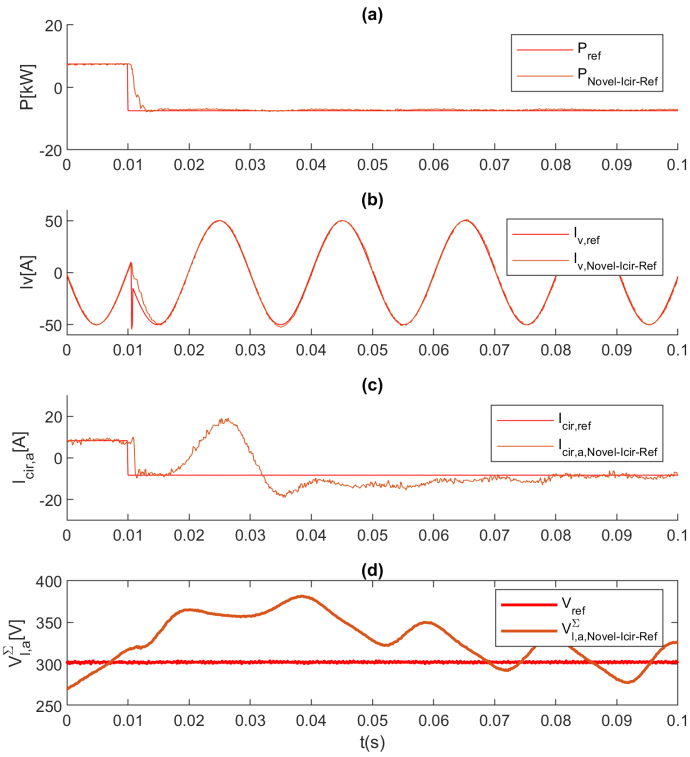

Figure 9.11: Novel Circulating Current Reference Method for change in $I_{d,ref}$ from 50 A to -50 A: (a) real power, (b) phase-a current, (c) phase-a circulating current, (d) summation of the capacitor voltages in the lower arm of phase a

The experimental results for d-component of ac-current for all the methods are shown in Fig. 9.13 to show dynamic response comparison. Similar conclusions as from simulation results can be made here.

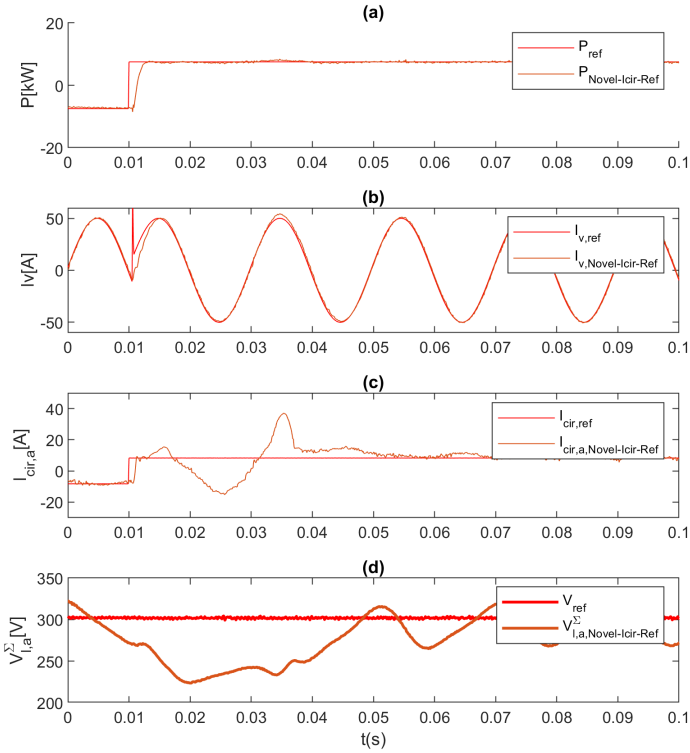

Figure 9.12: Novel Circulating Current Reference Method for change in $I_{d,ref}$ from -50 A to 50 A: (a) real power, (b) phase-a current, (c) phase-a circulating current, (d) summation of the capacitor voltages in the lower arm of phase a

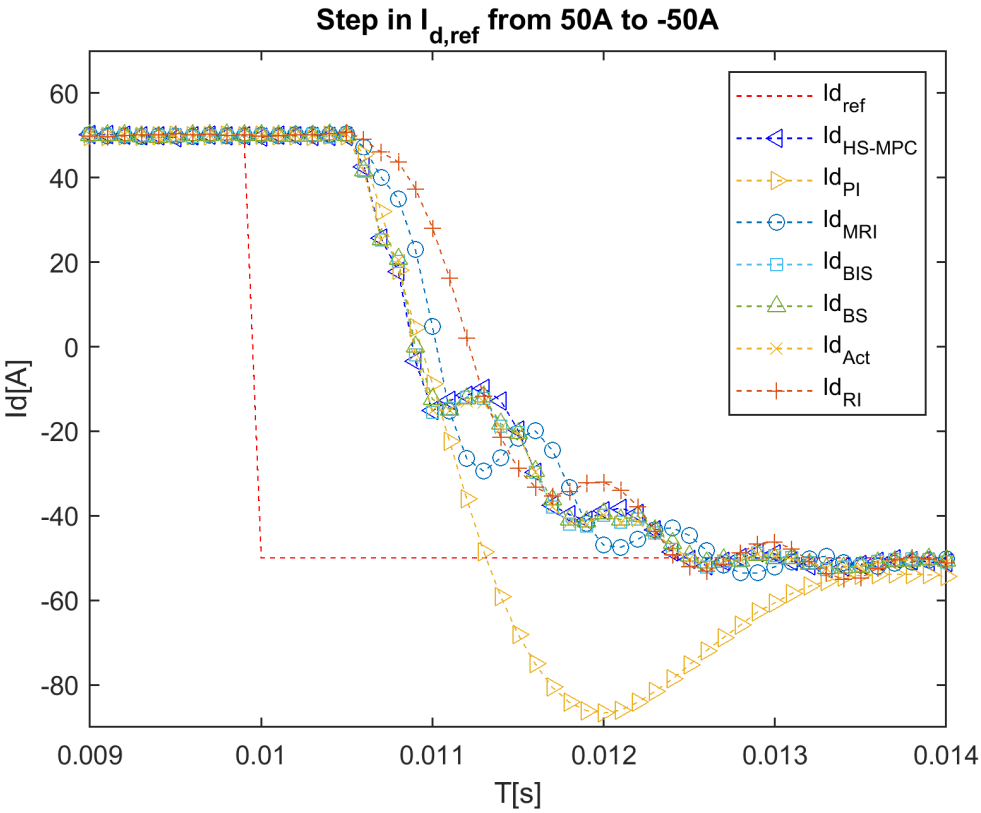

Figure 9.13: Comparison of Results for d-axis component of ac-side current

9.5 Discussion on Experimental Verification of NMPC

The experimental verification of NMPC method was not successful. Initially, the method had very high computational complexity for a sampling time of $100\mu s$ and was causing significant overruns when tested in real time. After that, some efforts were made to successfully reduce the computational complexity and avoid overruns at startup.

However, the developed algorithm did not give overruns only for a range of input voltage. The method starts to give significant overruns as soon as the input DC voltage is increased beyond a certain range. In this author's opinion, the most probable reason for this behavior is numerical issues in the C code generated by CasADi and not due to the computational complexity of the method. This reasoning is supported by the fact that the same algorithm works without overruns for a range of input values. If the issue was linked to the computational complexity of the method then the system should have reported overruns for all values.

In this author's opinion, these issues might be resolved by providing stable states to the NMPC algorithm at startup. Because the supplied dc voltage in the lab increases as a ramp and that might result in very large derivatives/jacobians calculated by the C code generated by CasADi. So, enabling NMPC when the DC voltage has stabilized might resolve this issue. Efforts and debugging are still being done to identify the exact source of the problem.

9.6 Summary

The key aspects of different MPC methods in this thesis are presented and compared as shown in Table 9.3.

9.7 Conclusion

In this chapter, the required modifications in the proposed methods for experimental verification were highlighted. A very simple method for grid voltage estimation or virtual ac-side voltage was proposed to deal with the problem of ac-side voltage prediction with long time delays. Finally, both simulation and experimental results of the proposed methods in this thesis are compared with the conventional PI-based control and it is shown that the dynamic response of the proposed methods is far better than the conventional control. A comparison of all the methods suggest that nonlinear model predictive control with explicit modulator is the best method,

however, its real-time implementation is complicated due to its very high computational complexity. Therefore, from a practical point of view, the proposed active set method can be considered as the best.

Bibliography

[1] B. S. Riar, T. Geyer and U. K. Madawala,"Model Predictive Direct Current Control of Modular Multilevel Converters: Modeling, Analysis, and Experimental Evaluation," in *IEEE Transactions on Power Electronics,* vol. 30, no. 1, pp. 431-439, Jan. 2015

[2] P. Cortes, J. Rodriguez, C. Silva and A. Flores, "Delay Compensation in Model Predictive Current Control of a Three-Phase Inverter," in *IEEE Transactions on Industrial Electronics,* vol. 59, no. 2, pp. 1323-1325, Feb. 2012

[3] Z. Xu, B. Li, S. Wang, S. Zhang and D. Xu, "Generalized Single-Phase Harmonic State Space Modeling of the Modular Multilevel Converter With Zero-Sequence Voltage Compensation," *IEEE Transactions on Industrial Electronics,* vol. 66, no. 8, pp. 6416-6426, Aug. 2019

[4] P. Rodriguez, A. Luna, I. Etxeberria, J. R. Hermoso and R. Teodorescu, "Multiple second order generalized integrators for harmonic synchronization of power converters," *2009 IEEE Energy Conversion Congress and Exposition,* 2009, pp. 2239-2246

[5] K. Ljøkelsøy and G. Guidi, "Development of a scaled model of a modular multilevel converter," *Energy Procedia*, vol. 137, pp. 505–513, Oct. 2017.

[6] G. Bergna-Diaz, J. Freytes, X. Guillaud, S. D'Arco, and J. A. Suul, "Generalized voltage-based state-space modeling of modular multilevel converters with constant equilibrium in steady state," *IEEE J. Emerg. Sel. Topics Power Electron.*, vol. 6, no. 2, pp. 707–725, Jun. 2018

[7] S. D'Arco, G. Guidi, and J. A. Suul, "Operation of a modular multilevel converter controlled as a virtual synchronous machine," in *Proc.Int. Power Electron. Conf. (IPEC-Niigata–ECCE Asia)*, May 2018, pp. 20–24.

[8] G. Guidi, S. D'Arco, K. Nishikawa and J. A. Suul, "Load Balancing of a Modular Multilevel Grid-Interface Converter for Transformer-Less Large-Scale Wireless Electric Vehicle Charging Infrastructure," in *IEEE Journal of Emerging and Selected Topics in Power Electronics*, vol. 9, no. 4, pp. 4587-4605, Aug. 2021

[9] S. Hamayoon, M. Hovd, J. A. Suul and M. Vatani, "Modified Reduced Indirect Finite Control Set Model Predictive Control of Modular Multilevel Converters," *IEEE COMPEL 2020*, Aalborg, Denmark, pp. 1-6,

[10] M. Saeedifard and R. Iravani, "Dynamic Performance of a Modular Multilevel Back-to-Back HVDC System," *IEEE Transactions on Power Delivery,* vol. 25, no. 4, pp. 2903-2912, Oct. 2010

Table 9.3: Comparison of Different Strategies

Method	**Computational Complexity /Burden**	**Steady-State Performance**	**Dynamic Performance**	**Explicit Modulator OR Only Sorting Algorithm**	**Remarks**
RI-FCS-MPC	3^{2p}	Good	Slow	Sorting	Computationally efficient but suffers from reduced dynamic performance
MRI-FCS-MPC	$25 \cdot 3^{2(p-1)}$	Good	Fast	Sorting	Dynamic response is not as good as the following methods because the large step is fixed to +/-5. Computational complexity will increase with increased # of SMs. This would result due to the need to include more steps.
FI-FCS-MPC	$(N+1)^2$	Good	Very Fast	Sorting	Very good performance but suffers from high computational complexity and reduced steady state performance (if # of SMs are low)
BS-FCS-MPC	3^{2p}	Good	Very Fast	Sorting	As good as FI-FCS-MPC with much lower computational burden. Computational complexity may increase slightly with increased # of SMs
BIS-FCS-MPC	$25 \cdot 3^{2(p-1)}$	Good	Very Fast	Sorting	As good as FI-FCS-MPC with much lower computational burden. Computational complexity may increase slightly with increased # of SMs
A-MPC	9	Very Good	Very Fast	Requires Modulator	As good as FI-FCS-MPC with much lower computational burden with added advantage of improved steady-state performance but requires explicit PWM modulator. Can only be used for horizon of 1.
NMPC-C	-	Very Good	Very Fast	Requires Modulator	This is the only method that can be extended easily for higher prediction horizons, offers similar dynamic performance as FI-FCS-MPC and better steady-state performance. But requires explicit PWM modulator. Computational complexity is independent of # of SMs but very high which makes real time implementation complicated.
NMPC-R	-	Good	Very Fast	Sorting	Can be extended easily for longer prediction horizons, avoids explicit modulator, offers similar dynamic and steady-state performance as FI-FCS-MPC. Computational complexity is independent from # of SMs but very high which makes real time implementation complicated
NMPC-OP	-	Good	Very Fast	Sorting	Can be extended easily for longer prediction horizons, avoids explicit modulator, offers similar dynamic and steady-state performance as FI-FCS-MPC. Computational complexity is independent from # of SMs but very high which makes real time implementation complicated
HS-MPC	$25 \cdot 3^{2(p-1)}$	Good	Very Fast	Sorting	Makes the calculation of large step dynamic as opposed to MRI-FCS-MPC. Therefore, offers identical dynamic and steady-state performance as FI-FCS-MPC

Chapter 10

Modified Sorting Algorithm

In this chapter, a modified sorting algorithm is proposed that ensures an equal switching frequency for each SM on average, in addition to reducing the switching frequency as compared to the conventional sorting algorithm thus distributing the losses equally among the SMs. Simulations are performed to validate the performance of the proposed methods compared to the conventional and reduced switching frequency sorting algorithms.

10.1 Introduction

An issue with the MPC strategies for MMC is the variable (if an explicit PWM modulator is not used) and high (with conventional sorting) switching frequency. Many solutions have been proposed to address the issue of high switching frequency [1–5]. For instance, in [1] it is proposed to sort only the bypassed SMs if more SMs need to be inserted and sort only the inserted SMs in the previous sampling instant if some SMs need to be removed. The methods in [3–5] are based on maximum and minimum SM capacitor voltages. These methods may suffer from reduced dynamic performance as they limit the change in SMs to be one or two.

Although the methods mentioned above address the issue of high switching frequency but they do not consider the variability issue. Also, a draw-

back of these methods is that they lead to an individual imbalance between the capacitor voltages if some tolerance band is not considered. The methods that ensure fixed switching frequency require PWM modulators such as phase-shifted carrier PWM (PSC-PWM). A drawback of these methods is that for each SM a separate carrier is allocated. Therefore, the number of carriers grows proportionally with the number of SMs, and generating the precise phase difference between carriers can become a problem for hardware implementation.

In this work, a modified sorting algorithm without an explicit modulator is proposed that not only results in reduced switching frequency but also ensures fixed switching frequency for each SM over an average of a few cycles. As a result, the losses are evenly distributed among the SMs.

10.2 Modified Sorting Algorithm

To achieve low switching frequency, the same method as in [1] is applied where only the bypassed SMs and the inserted SMs in the previous sampling instant are considered if a new SM is to be inserted and if an SM is to be removed, respectively. For achieving a fixed switching frequency on an average of a few cycles the following is proposed:

- keep track of previously inserted and bypassed SMs
- Keep a count of the number of commutations of each SM
- If a new SM is to be inserted
  - Sort the bypassed SMs in ascending order according to the number of commutations
  - if the number of commutations of first $|\Delta SM_{on}|$ are unique then insert these and no need to do voltage sorting
  - Else insert the first 'n' sorted SMs with unique commutation number. For $|n - \Delta SM_{on}|$ SMs under consideration having the same commutation number do voltage sorting according to arm current direction and SM voltages

- if an SM is to be removed

  - Sort the inserted SMs in ascending order according to the number of commutations
  - if the number of commutations of first $|\Delta SM_{on}|$ are unique then bypass these and no need to do voltage sorting
  - Else bypass the first 'n' sorted SMs with unique commutation number. For $|n - \Delta SM_{on}|$ SMs under consideration having the same commutation number do voltage sorting according to arm current direction and SM voltages

where $\Delta SM_{on} = SM_{on} - SM_{on,p}$ and SM_{on} are the number of SMs to be inserted and $SM_{on,p}$ are the number of SMs that were inserted in the previous sampling instant.

With the proposed approach, after a few cycles, each switch would have the same number of commutations and on average the switching frequency would be fixed for each SM. It is noted here that the individual capacitor voltages will not be far from their reference and will be approximately balanced among themselves because each SM average switching frequency over a few cycles would be fixed. This will be demonstrated in the results section. Note that for long-term operations, the number of commutations will eventually overflow. Therefore, the number of commutations of each SM is set back to zero after 20 cycles.

It is noted that the count of commutations of each SM can easily be kept by monitoring if the SM has changed its state from the previous sampling instant. The proposed modified sorting algorithm is shown in Fig. 10.1. It is important to highlight that voltage sorting based on arm current direction is still required because if the count of commutations for SMs is the same then the SMs with the least or highest voltage according to arm current direction should be selected.

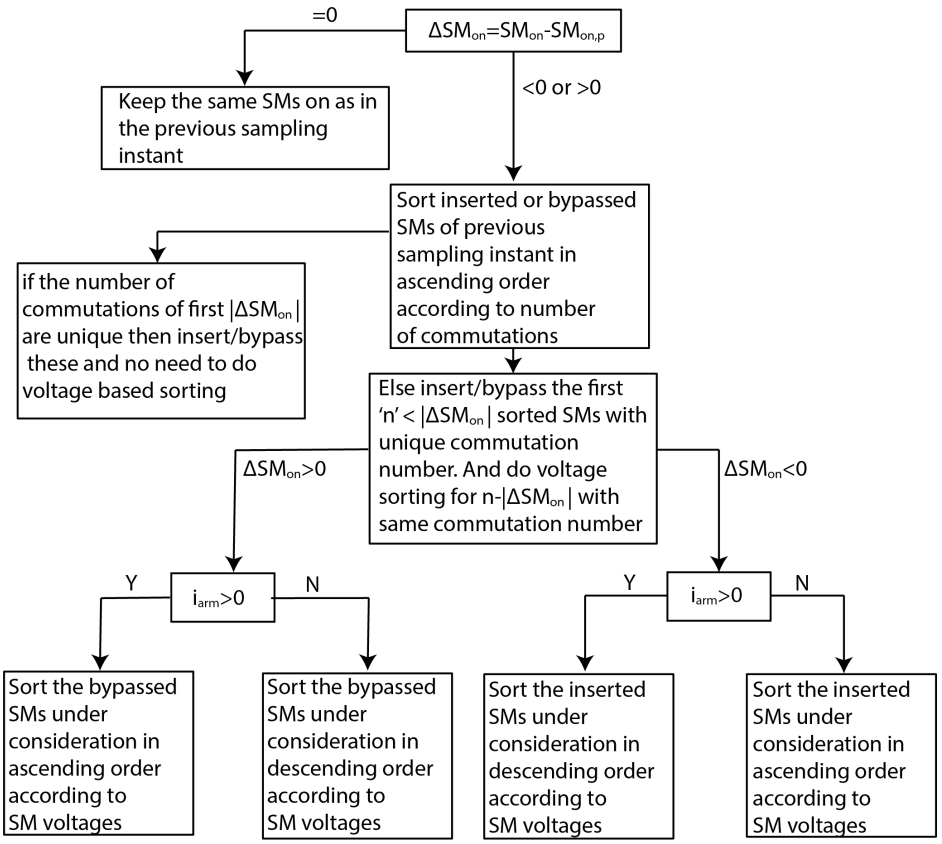

Figure 10.1: Modified Sorting Algorithm

10.3 Simulation Results

The results of the proposed sorting method are compared with the conventional sorting algorithm and the method of [1] that only considers the bypassed/sorted SMs from the previous sampling instant. The average switching frequency over 20 cycles for all the SMs in the upper arm of phase a for the conventional sorting algorithm is shown in Fig. 10.2. Whereas

the proposed modified sorting algorithm in comparison with [1] is shown in Fig. 10.3. It can be observed that the proposed sorting algorithm not only reduces the switching frequency but also ensures that every SM is switching at approximately the same frequency in the long run as compared to the conventional sorting algorithm. It is to be highlighted here that this equal switching frequency is attained without the use of phase-shifted carrier PWM or other modulation techniques. It is also noted that if the number of cycles to calculate the average switching frequency is increased then the proposed sorting algorithm would result in even more close and the same switching frequency of all the SMs. The method of [1] on the other hand only results in reduced switching frequency. Therefore, the switching frequency of SMs is not balanced among themselves with [1].

In Fig. 10.4, the switching states of two random SMs *i.e.*, SM_5 in the upper arm of phase a and SM_{12} in the lower arm of phase a are shown for the proposed and reduced switching frequency method of [1] for one cycle. It can be observed that both methods offer lower switching frequencies.

Figure 10.5 demonstrates the behavior of the individual capacitors in each arm for the proposed, reduced switching frequency and conventional sorting method. As expected the best balancing is achieved with the conventional sorting algorithm. There does not seem much difference between the proposed and reduced switching frequency method [1]. However, the reduced switching frequency methods such as [1] require a tolerance band in the long run whereas the proposed method would not require that because every SM is switching approximately at a similar frequency. Therefore, no SM capacitor voltage can diverge farther away from other SMs with the proposed method.

10.4 Conclusion

In this chapter, a modified sorting algorithm was proposed that resulted in a nearly fixed switching frequency of each SM without the use of an explicit modulator in addition to reduced switching frequency thus resulting in

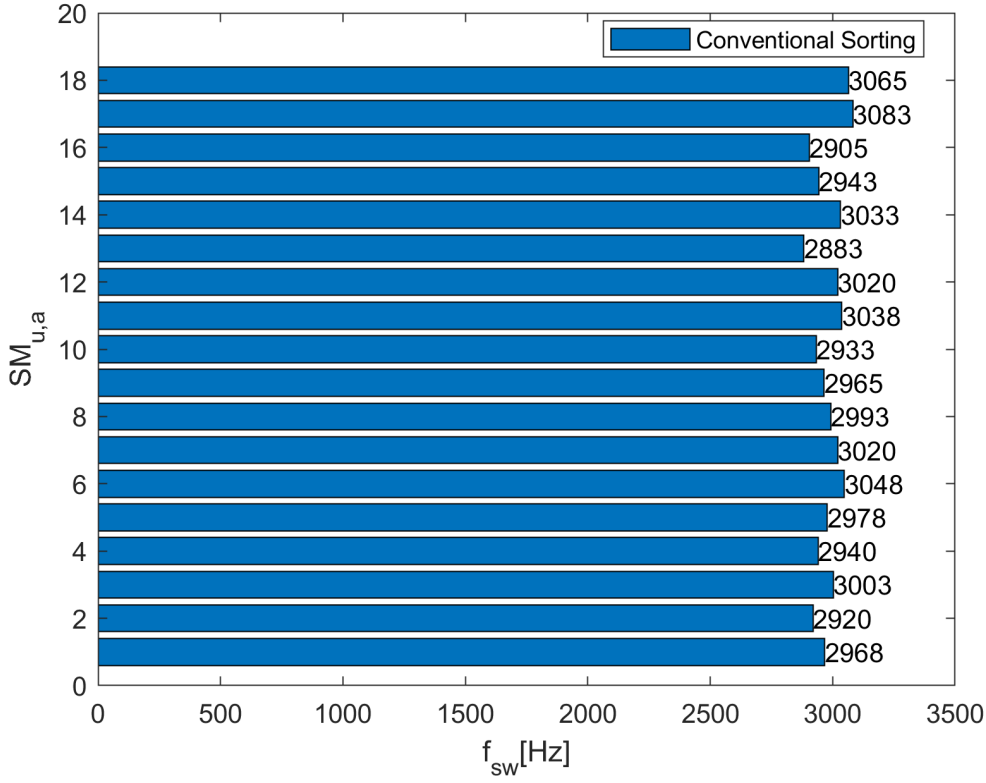

Figure 10.2: Average Switching Frequency over 20 cycles of all the SMs in the upper arm of phase a using Conventional Sorting Algorithm

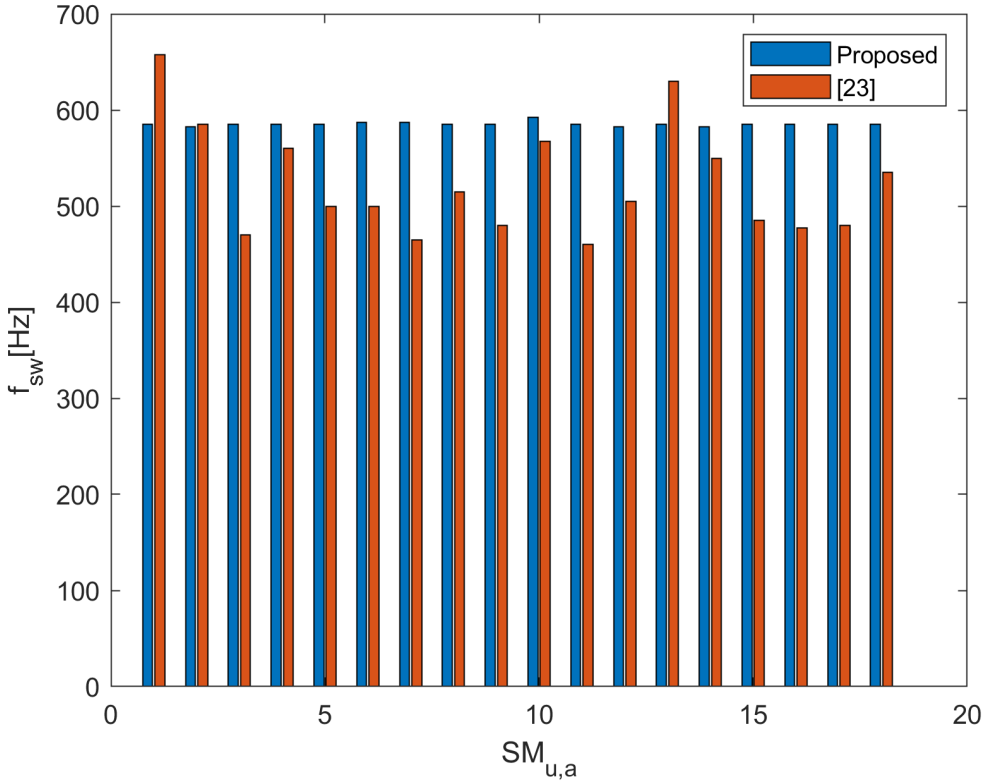

Figure 10.3: Average Switching Frequency over 20 cycles of all the SMs in the upper arm of phase a using Modified Sorting Algorithm and [1]

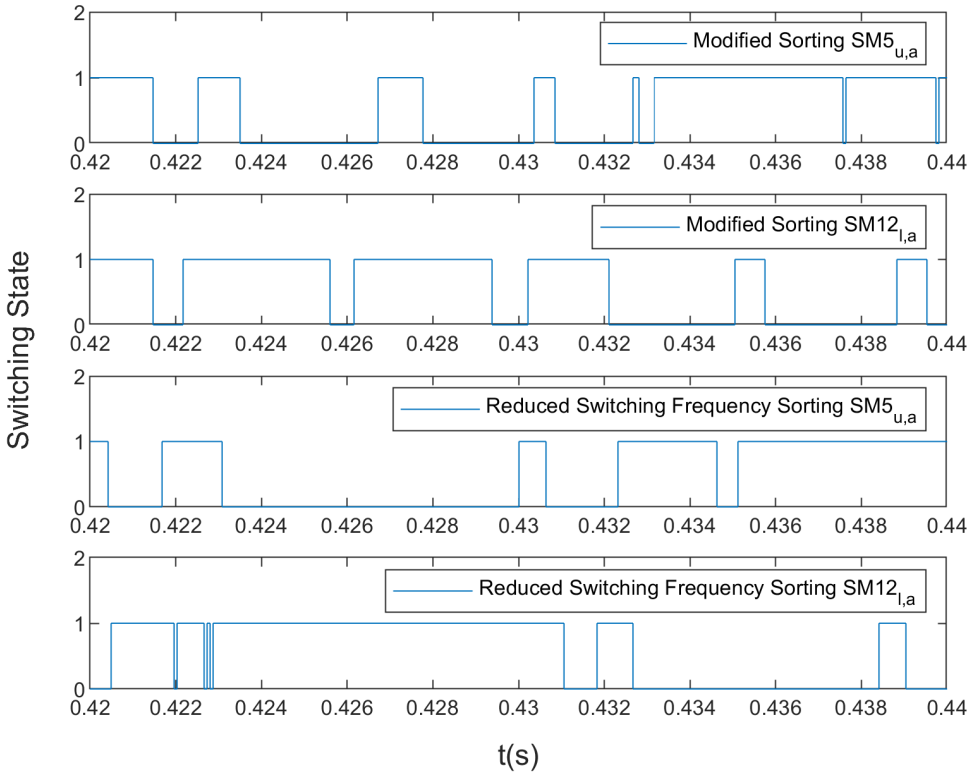

Figure 10.4: Switching States of two randomly picked SMs under proposed method and [1]

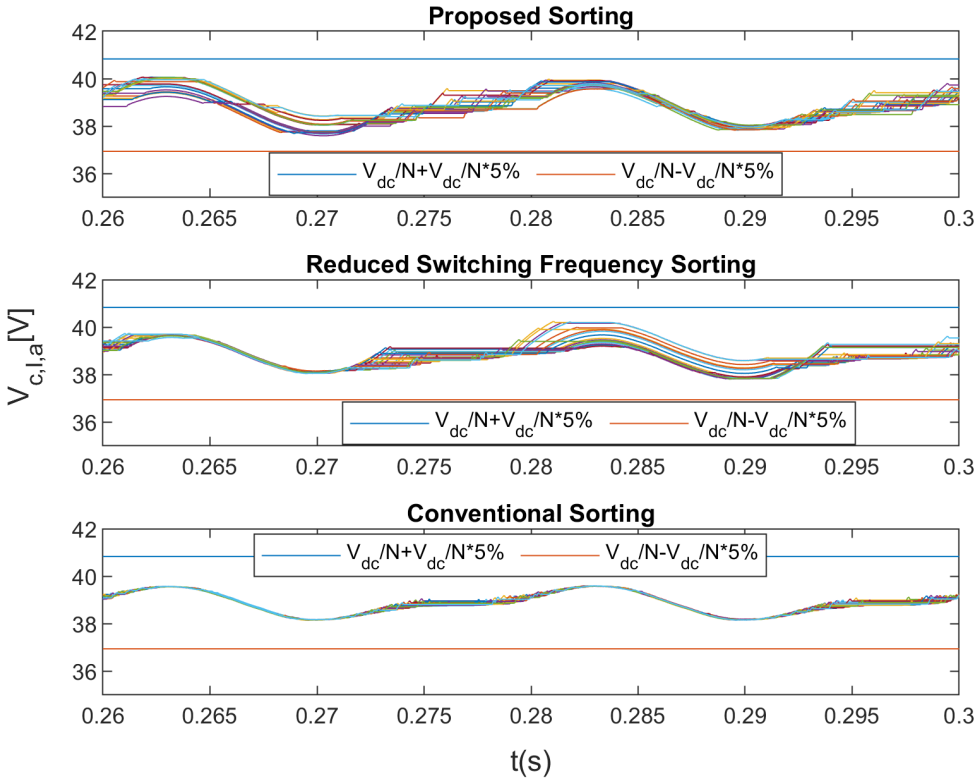

Figure 10.5: Individual capacitor voltages in the lower arm of phase under proposed method, [1] and conventional sorting

equal distribution of losses among the SMs.

Bibliography

[1] Q. Tu, Z. Xu and L. Xu, "Reduced Switching-Frequency Modulation and Circulating Current Suppression for Modular Multilevel Converters," in *IEEE Transactions on Power Delivery,* vol. 26, no. 3, pp. 2009-2017, July 2011

[2] J. Qin and M. Saeedifard, "Reduced Switching-Frequency Voltage-Balancing Strategies for Modular Multilevel HVDC Converters," in *IEEE Transactions on Power Delivery,* vol. 28, no. 4, pp. 2403-2410, Oct. 2013

[3] S. Fan, K. Zhang, J. Xiong and Y. Xue, "An Improved Control System for Modular Multilevel Converters with New Modulation Strategy and Voltage Balancing Control," in *IEEE Transactions on Power Electronics,* vol. 30, no. 1, pp. 358-371, Jan. 2015

[4] H. Saad, X. Guillaud, J. Mahseredjian, S. Dennetière and S. Nguefeu, "MMC Capacitor Voltage Decoupling and Balancing Controls," in *IEEE Transactions on Power Delivery,* vol. 30, no. 2, pp. 704-712, April 2015

[5] D. Siemaszko, "Fast Sorting Method for Balancing Capacitor Voltages in Modular Multilevel Converters," in *IEEE Transactions on Power Electronics,* vol. 30, no. 1, pp. 463-470, Jan. 2015

Chapter 11

Enhancement of Steady State Response of Indirect Finite Control Set Model Predictive Control

In this chapter, a simple method is presented to improve the steady-state response of indirect finite control set model predictive control (I-FCS-MPC) techniques. The I-FCS-MPC methods return the discrete optimal solution, and this solution will be closest to its continuous counterpart in steady-state i.e., at maximum ± 0.5 *away from the actual continuous solution. Based on this observation, a few more continuous options within the range* ± 0.5 *are evaluated on the solution from I-FCS-MPC. Then the option among these which gives the minimum cost is used for the modulation stage. Simulations demonstrate that for a 19-level modular multilevel converter, the total harmonic distortion is reduced by 56% by the proposed method as compared to full I-FCS-MPC and 55% as compared to one of the computationally efficient versions of I-FCS-MPC.*

11.1 Introduction

A short background is presented below to make this chapter independent. Readers who have covered the preceding chapters may go directly to section 11.2.

Model predictive control (MPC) has emerged as a promising control technique as it can easily handle multi-input multi-output systems, nonlinearity, time delays, and constraints [1]. For power converters, typically finite control set model predictive control (FCS-MPC) is used [2]. In FCS-MPC, all the possible switching states are evaluated with a predefined cost function, and the state that minimizes this cost function is then applied to the power converter. FCS-MPC is suitable for power converters with a low number of switches as its computational complexity grows exponentially with the increase in the number of switching states. Therefore, indirect finite control set model predictive control (I-FCS-MPC) techniques have been proposed in literature [3–5]. In I-FCS-MPC optimization is performed over voltage levels instead of switching states. As a result, I-FCS-MPC has a much lower computational burden as compared to direct FCS-MPC. However, an issue common to both direct and indirect FCS-MPC is the reduced steady-state response because of the discrete nature of these algorithms and the absence of an explicit modulator.

This issue can be resolved by using MPC methods such as continuous control set MPC (CCS-MPC) [6–8] and deadbeat predictive control [9] that generate a continuous solution and can easily incorporate the modulator. However, CCS-MPC has high computational complexity which makes its real-time application complicated, and deadbeat predictive control does not employ a cost function and therefore cannot handle multiple objectives. Therefore, modulated FCS-MPC techniques have also been investigated [10–12]. In these techniques, the two or three voltage levels that minimize a predefined cost function are first identified and then duty cycles are calculated for each voltage level. Finally, these duty cycles are applied to a suitable modulator.

In this chapter, a method to improve the steady-state response without the explicit calculation of duty cycles is proposed. The proposed method is

based on the idea that the discrete solution generated by the I-FCS-MPC method will be closest to its continuous counterpart *i.e.*, at maximum ± 0.5 away from the actual continuous solution in steady-state. Based on this observation, a few more continuous options are evaluated within ± 0.5 of the solution returned by I-FCS-MPC. Note that, these additional options are independent both from the prediction horizon and the total number of voltage levels. Therefore, the total computations would just increase by the number of these options. The option among these which gives the minimum cost is used for the modulation stage. The proposed method is applied to a 19-level modular multilevel converter (MMC).

11.2 Proposed Method

The discrete solution from I-FCS-MPC is at a maximum ± 0.5 away from the solution that would be obtained by an MPC treating the insertion index as a continuous variable. This is clearly valid for full indirect FCS-MPC where all the voltage levels are considered. For example, if the actual continuous solution was $n_u = 12.345$ and $n_l = 5.655$ for $N = 18$ then the discrete solution returned by full indirect FCS-MPC would be $n_u = 12$ and $n_l = 6$ as all the other discrete combinations would give higher cost. If modified reduced I-FCS-MPC as in [13] is applied where only a neighborhood of voltage levels w.r.t the previous sampling instant are considered, then the validity of this observation may be questioned. However, in the steady state, the solution from both [3] and [13] would be approximately the same as in the steady state the voltage level does not change significantly from one sampling instant to the next. Therefore, this observation is good enough, as will be demonstrated by the simulation results.

Based on the above discussion, further continuous options are considered on the solution obtained from the I-FCS-MPC methods. Let the insertion indices obtained from I-FCS-MPC methods be denoted as n_{uf} and n_{lf} then the extra options evaluated for both arms are given as follows:

$$n_{uf}, n_{uf} \pm 0.5, n_{uf} \pm 0.375, n_{uf} \pm 0.25, n_{uf} \pm 0.125 \tag{11.1a}$$

$$n_{lf}, n_{lf} \pm 0.5, n_{lf} \pm 0.375, n_{lf} \pm 0.25, n_{lf} \pm 0.125 \tag{11.1b}$$

The total number of combinations between upper and lower arm insertion indices resulting from (11.1) would be 81. It is noted that these options would only be evaluated on the solution of the first step within the prediction horizon from the I-FCS-MPC method. Further note that the proposed method does not lead to the exact continuous solution. Therefore, more options such as ± 0.0625 and others can be added in (11.1) to get closer to the actual continuous solution.

Let the number of extra continuous voltage levels evaluated by the proposed method be denoted by n_{extra}. Then the total extra options evaluated are $(n_{extra}+1)^2-1$ since the combination (n_{uf}, n_{lf}) has already been calculated in the I-FCS-MPC.

In this work, only eight additional voltage levels are considered because simulations showed that there is little to gain by adding more voltage levels. Therefore, the total number of evaluated options by the proposed method applied to [13] would be $25 \cdot 3^{2(p-1)} + 80$ where p is the prediction horizon and $25 \cdot 3^{2(p-1)}$ are the number of options evaluated by [6], 80 are the additional options evaluated by the proposed method. Similarly, for full I-FCS-MPC [3] the total number of options evaluated will be $(N+1)^{2p} + 80$ where N is the total number of submodules (SMs) in each arm of MMC. The option among these 80 that minimizes the cost function is then sent to the modulator. In this work, SM unified PWM (SUPWM) where only one SM is in PWM mode is used [14]. Note that the SM in PWM mode is not fixed and changes based on the sorting algorithm at each time step. The comparison of the number of control options considered by different I-FCS-MPC strategies with and without the proposed method is shown in Table-I for a prediction horizon of three steps for an MMC with 20 SMs per arm. From Table 11.1 it can be concluded that additional evaluations added by the proposed method are negligible.

The flowchart for the proposed method is shown in Fig. 11.1 where $n_{ud,opt}$ and $n_{ld,opt}$ are the discrete optimal insertion indices returned by I-FCS-MPC and $J_{i,j}$ is the cost function to be minimized.As indicated in Fig. 11.1 the discrete solution obtained from I-FCS-MPC will be further evaluated. The implementation shown in the flowchart can easily be implemented using a nested for loop. Each option of the upper arm as shown

Table 11.1: Number of possible control options for different I-FCS-MPC strategies with and without Proposed Method

Method	CB without Proposed Method	CB with Proposed Method
FI-FCS-MPC	85,766,121	85,766,201
RI-FCS-MPC	729	809
MRI-FCS-MPC	2025	2105

* FI=Full Indirect, RI=Reduced Indirect, MRI=Modified Reduced Indirect, CB=Computational Burden

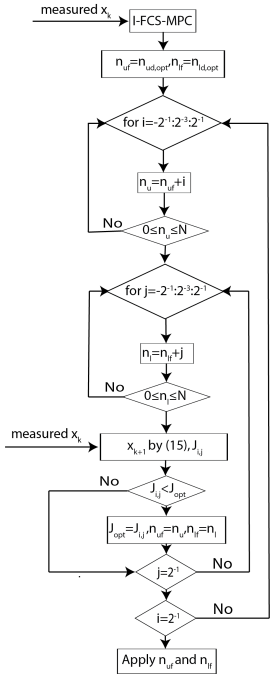

Figure 11.1: Flowchart for the proposed method

in (11.1) would be tested in combination with all the options of lower arm to evaluate the cost function. The combination resulting in minimum cost would be sent to the modulator.

11.3 Simulation Results

The performance of the proposed strategy is validated by performing simulations on a three-phase MMC with 18 SMs per arm, as shown in Fig. 11.2.

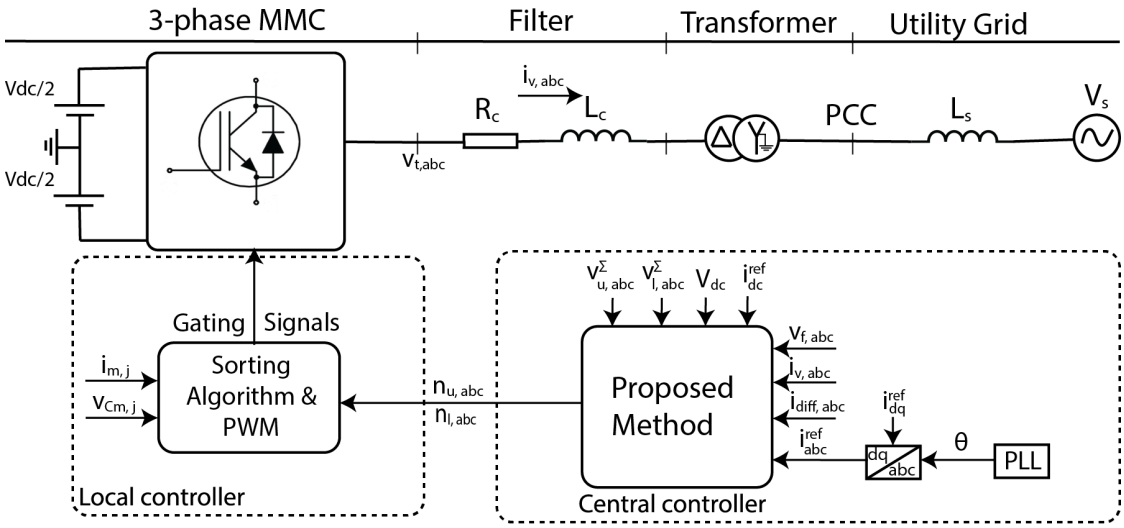

Figure 11.2: Control Block Diagram

The scenario used for simulation is that the converter is operating with an active current reference set to 50 A. The parameters used for simulation are summarized in in Table 11.2.

Table 11.2: Simulation Parameters

Parameter	**Value**
MMC nominal power (base power)	50 kVA
AC system nominal voltage (base voltage)	350 V
Nominal frequency	50 Hz
Arm inductance (L)	1.55 mH
Arm resistance (R)	0.01Ω
Submodule capacitance (C)	20000μF
Transformer voltage rating (T)	400 V / 400 V
Transformer power rating	50 kVA
Transformer inductance	0.04 pu
Transformer resistance	0.006 pu
DC side reference voltage	700 V
Number of SMs per arm (N)	18
Sampling time (Ts)	70μs

The THD results for the full I-FCS-MPC method from [3] and full I-FCS-MPC with the proposed method are shown in Fig. 11.3 and Fig. 11.4 respectively. Similarly, the THD results for the modified reduced I-FCS-MPC method from [13] and modified reduced I-FCS-MPC with the proposed method are shown in Fig. 11.5 and Fig. 11.6 respectively.

These results show that there is 56% reduction of THD with the proposed method as compared to [3] and 55% reduction of THD as compared to [13]. The increased reduction of THD with the use of the proposed method with full I-FCS-MPC [3] as compared to [13] shows that the observation that the solution from modified I-FCS-MPC method (which do not consider all the voltage levels) is at maximum ± 0.5 away from the discrete solution is not always valid. However, it is still a good approximation as there is not a significant difference in the THDs of both methods as evident from Fig. 11.4 and Fig. 11.6.

The impact of including options such as ± 0.0625 on THD for modified

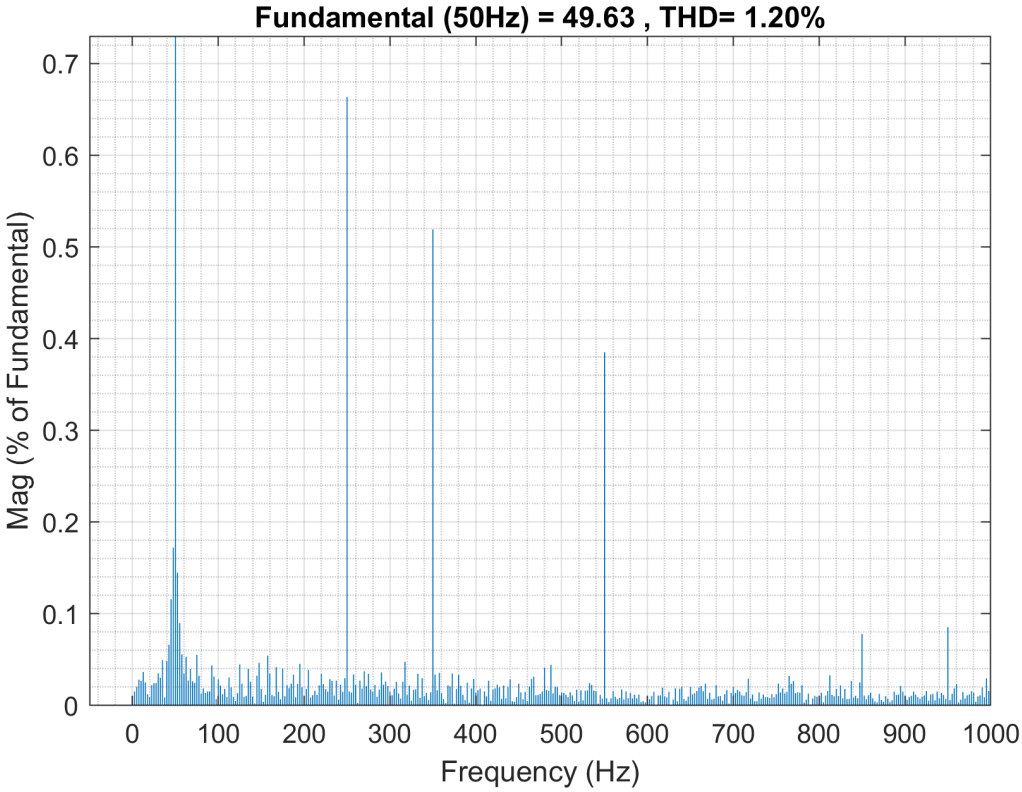

Figure 11.3: THD Full Indirect FCS-MPC

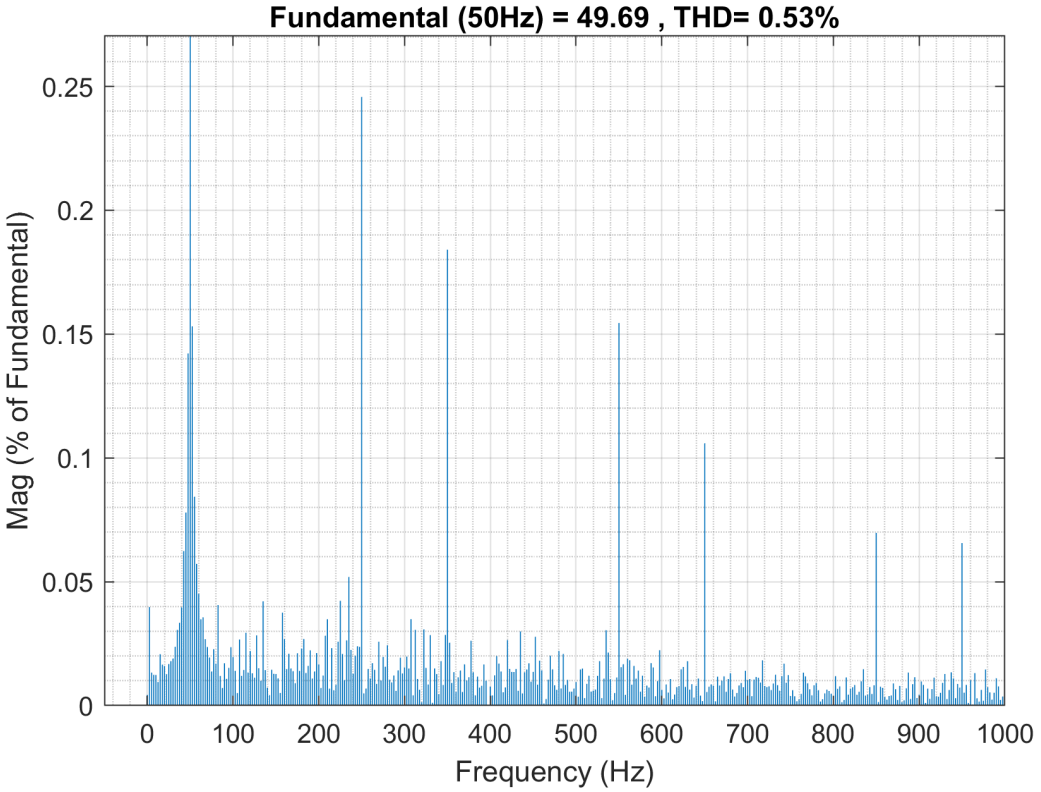

Figure 11.4: THD Full Indirect FCS-MPC with Proposed Method

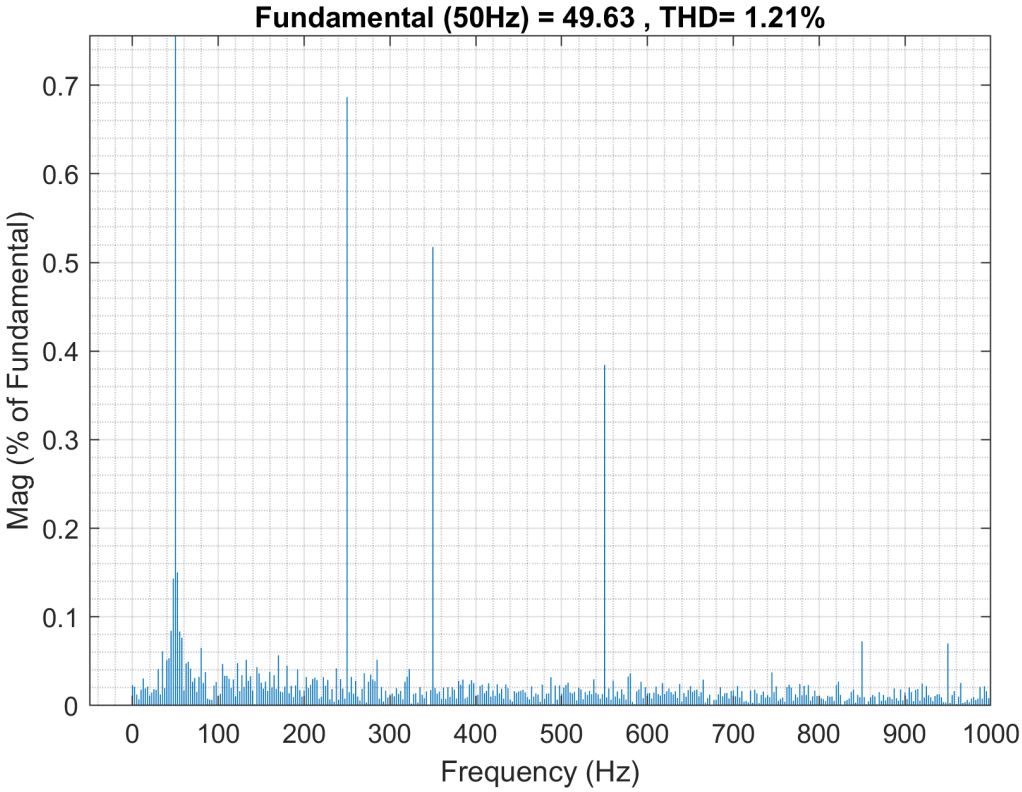

Figure 11.5: THD Modified Reduced Indirect FCS-MPC

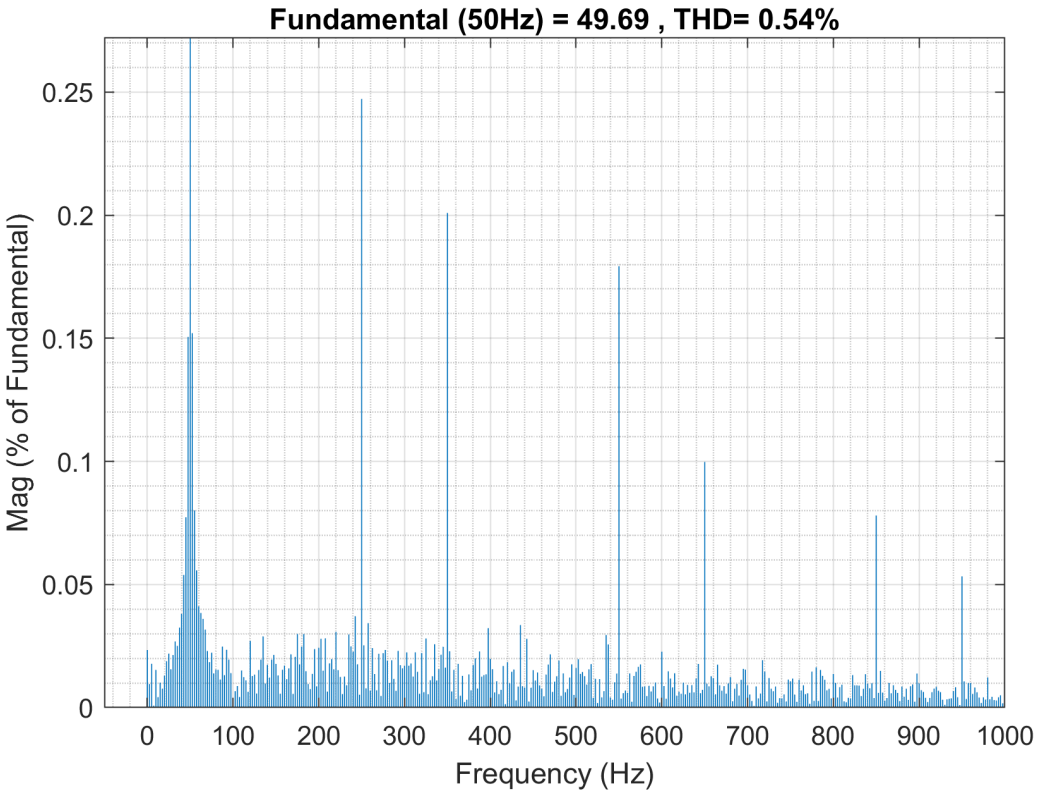

Figure 11.6: THD Modified Reduced Indirect FCS-MPC with Proposed Method

I-FCS-MPC is shown in Fig. 11.7. It can be observed that there is little to gain by adding these options as the THD improvement is not significant as compared to without ±0.0625 options.

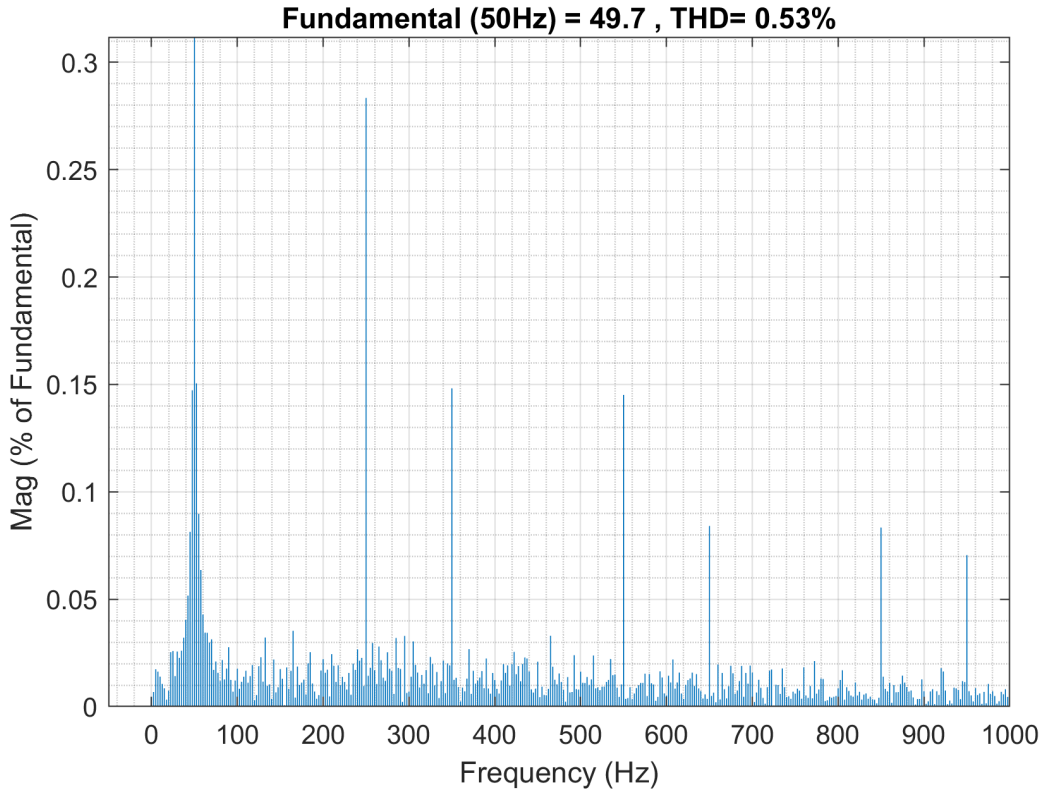

Figure 11.7: THD Modified Reduced Indirect FCS-MPC with Proposed Method using additional options ±0.0625

The results of the proposed method with modified reduced I-FCS-MPC for all the state variables under active power reversal at t=0.5s are shown in Fig. 11.8 which shows that all of them are tracking their reference

accurately.

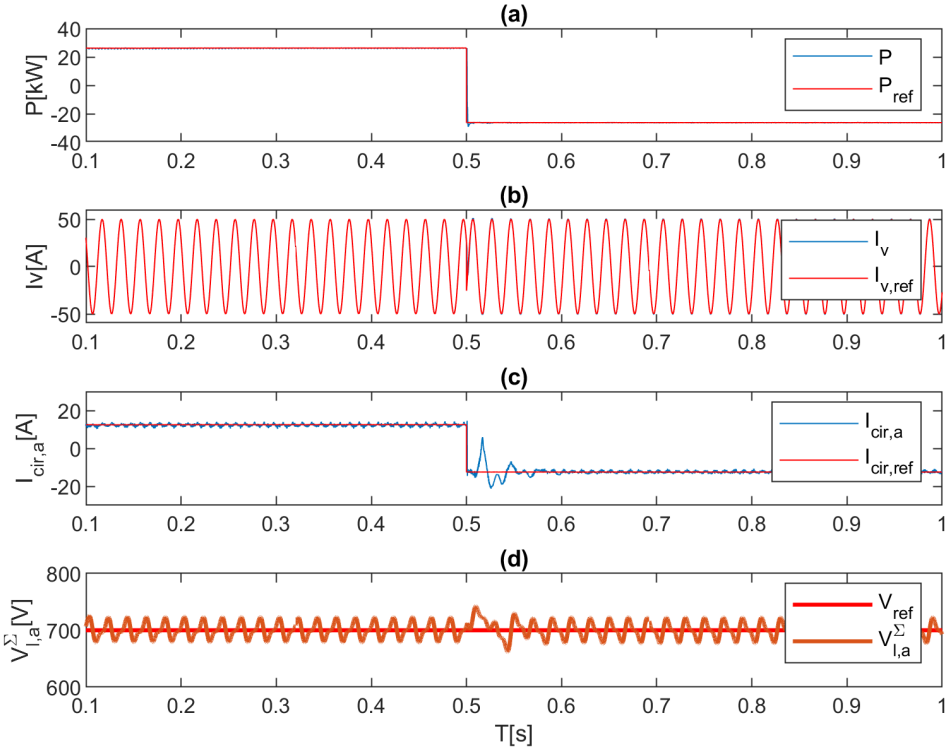

Figure 11.8: Proposed Method with Modified Reduced Indirect FCS-MPC: (a) real power, (b) phase-a current (c) phase-a circulating current, (d) summation of the capacitor voltages in the lower arm of phase a

The impact of the proposed method on the switching frequency is illustrated in Fig. 11.9 where a comparison of the switching frequency of each SM in the upper arm of phase a is shown for the proposed method and modified reduced I-FCS-MPC [13]. The results show that the reduction of the

THD is obtained at the cost of an increase in the switching frequency. This increase is due to the non-integer levels and the use of a PWM modulator.

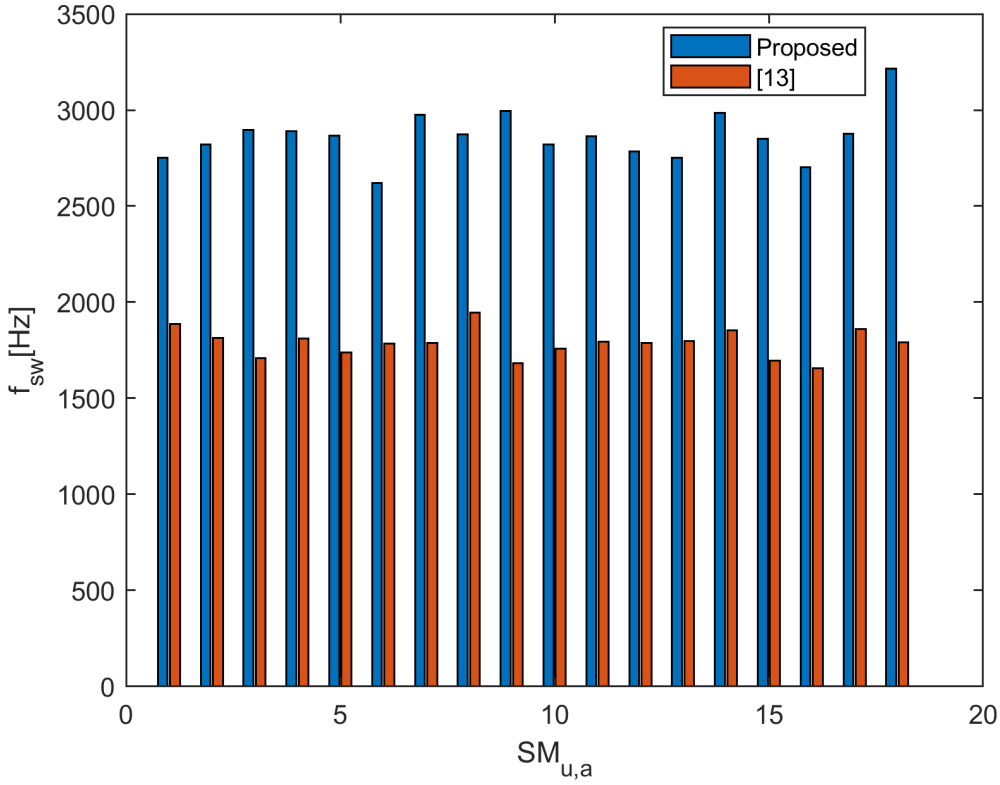

Figure 11.9: Average Switching Frequency over 20 cycles of all the SMs in the upper arm of phase a using proposed method and [13]

11.4 Discussion on the Application of the Proposed Method

The proposed method gives a general framework to improve the steady-state response of the FCS-MPC based methods where optimization is performed over voltage levels. Therefore, it can also be applied to power converters with low number of voltage levels *i.e.*, two or three. However, with very few voltage levels a higher non-integer resolution may be required as in this case it would become more important to get closer to the continuous solution. Then, for power converters with a high number of voltage levels there might be little to gain as the THD would already be very low. Therefore, the main application of the proposed method could be for power converters with a medium number of voltage levels.

The impact on the THD results for modified reduced I-FCS-MPC [13] and proposed methods when the number of SMs is reduced to 12 is shown in Fig. 11.10 and Fig. 11.11, respectively. These results are for the same simulation parameters as in Table I except the number of SMs per arm is now 12. As expected, the THD is higher as compared to the case when there was 18 SM/arm as the total number of voltage levels are reduced from 19 to 13. However, in terms of improvement, these results show that the proposed method offers more advantage when the number of voltage levels is low as in this case the THD is reduced by 65% by the proposed method as compared to [13].

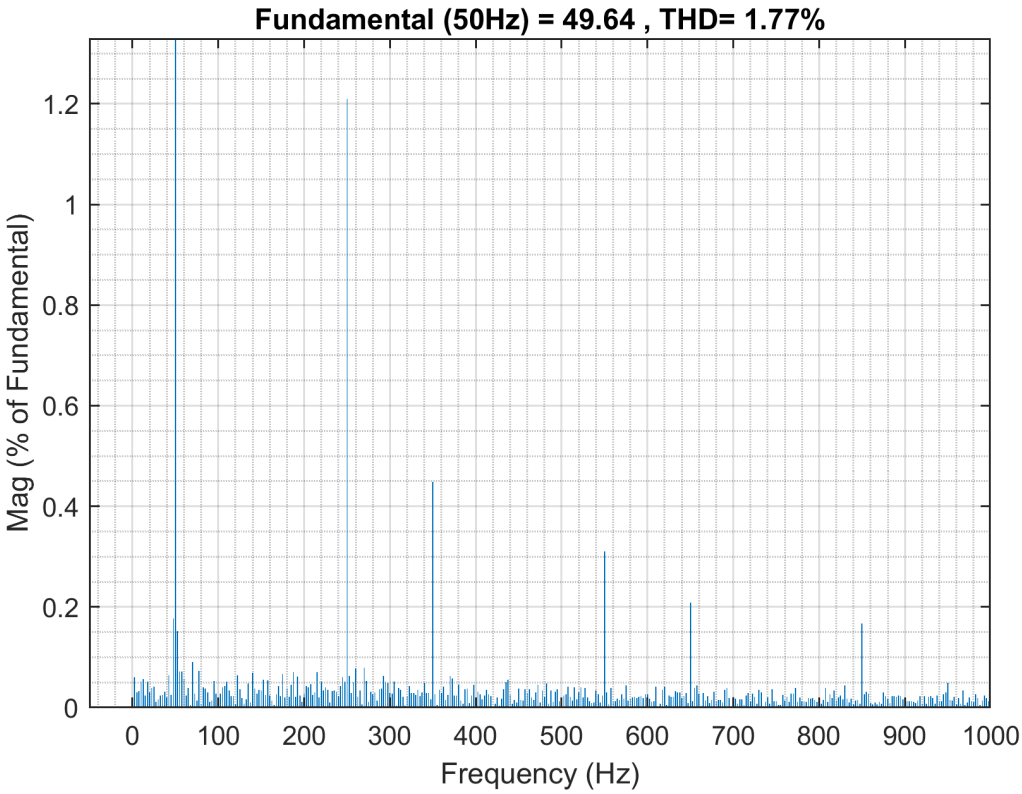

Figure 11.10: THD Modified Reduced Indirect FCS-MPC with 12 SMs per arm

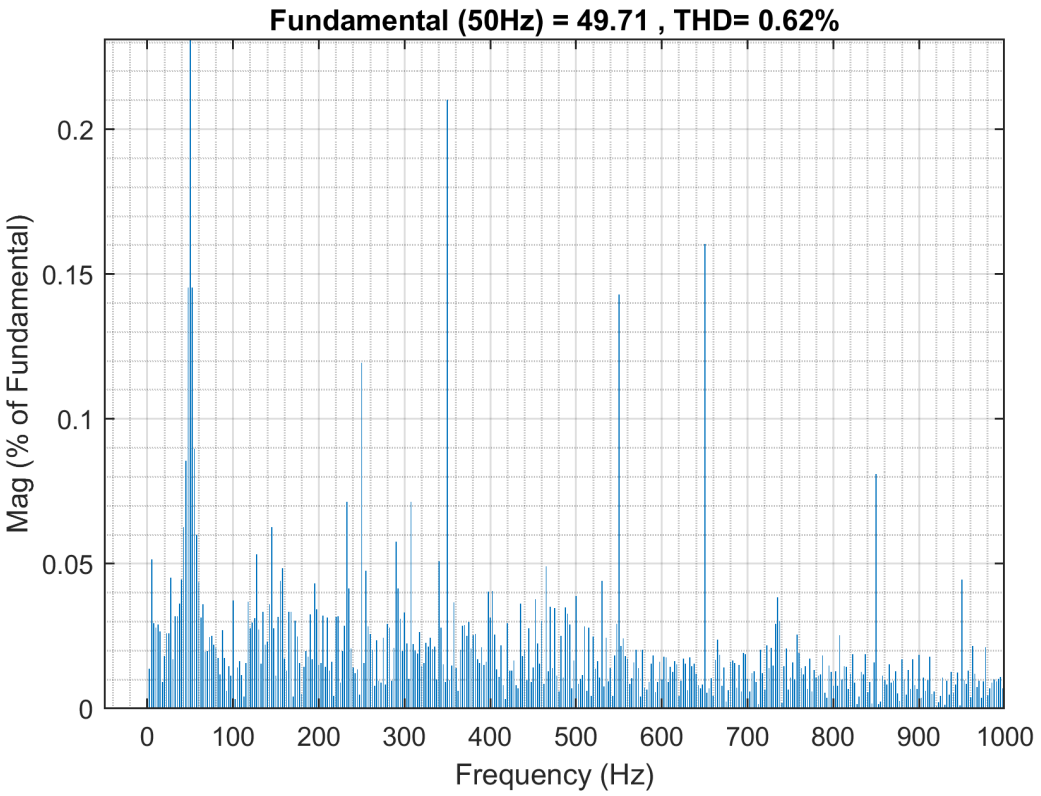

Figure 11.11: THD Modified Reduced Indirect FCS-MPC with Proposed Method with 12 SMs per arm

11.5 Conclusion

In this chapter, a very simple method for improving the steady-state response of the I-FCS-MPC technique is presented. The proposed method improves the THD response significantly as compared to I-FCS-MPC with just a slight increase in the computational burden. This increase in computational burden is independent of the prediction horizon and the number of voltage levels. Moreover, the presented method does not require the explicit calculation of duty cycles. However, it increases the switching frequency. The proposed method can find applications in medium voltage converters where the number of voltage levels is not very high.

Bibliography

[1] A. Dekka, B. Wu, V. Yaramasu, R. L. Fuentes and N. R. Zargari, "Model Predictive Control of High-Power Modular Multilevel Converters—An Overview," in *IEEE Journal of Emerging and Selected Topics in Power Electronics,* vol. 7, no. 1, pp. 168-183, March 2019,

[2] S. Vazquez, J. Rodriguez, M. Rivera, L. G. Franquelo and M. Norambuena, "Model Predictive Control for Power Converters and Drives: Advances and Trends," in *IEEE Transactions on Industrial Electronics,* vol. 64, no. 2, pp. 935-947, Feb. 2017

[3] M. Vatani, B. Bahrani, M. Saeedifard and M. Hovd, "Indirect Finite Control Set Model Predictive Control of Modular Multilevel Converters," in *IEEE Transactions on Smart Grid,* vol. 6, no. 3, pp. 1520-1529, May 2015

[4] F. Kieferndorf, P. Karamanakos, P. Bader, N. Oikonomou, and T. Geyer, "Model predictive control of the internal voltages of a five-level active neutral point clamped converter," in *Proc. IEEE Energy Convers. Congr. Expo.,* Sep. 2012, pp. 1676–1683.

[5] M. Norambuena, S. Dieckerhoff, S. Kouro and J. Rodriguez, "Finite control set model predictive control of a stacked multicell converter with reduced computational cost," *IECON 2015 - 41st Annual Conference of the IEEE Industrial Electronics Society,* Yokohama, Japan, 2015, pp. 001819-001824

[6] G. Darivianakis, T. Geyer and W. van der Merwe, "Model predictive current control of modular multilevel converters," *2014 IEEE Energy Conversion Congress and Exposition (ECCE),* 2014, pp. 5016-5023

[7] S. Fuchs, M. Jeong and J. Biela, "Long Horizon, Quadratic Programming Based Model Predictive Control (MPC) for Grid Connected Modular Multilevel Converters (MMC)," *IECON 2019 - 45th Annual Conference of the IEEE Industrial Electronics Society,* 2019, pp. 1805-1812

[8] S. Fuchs and J. Biela, "Impact of the Prediction Error on the Performance of Model Predictive Controllers with Long Prediction Horizons for Modular Multilevel Converters - Linear vs. Nonlinear System Models," *2018 20th European Conference on Power Electronics and Applications (EPE'18 ECCE Europe),* 2018, pp. P.1-P.9.

[9] J. Wang, Y. Tang, P. Lin, X. Liu and J. Pou, "Deadbeat Predictive Current Control for Modular Multilevel Converters With Enhanced Steady-State Performance and Stability," in *IEEE Transactions on Power Electronics,* vol. 35, no. 7, pp. 6878-6894, July 2020

[10] H. Mahmoudi, M. Aleenejad and R. Ahmadi, "Modulated Model Predictive Control of Modular Multilevel Converters in VSC-HVDC Systems," in *IEEE Transactions on Power Delivery,* vol. 33, no. 5, pp. 2115-2124, Oct. 2018

[11] D. Zhou, S. Yang, and Y. Tang, "Model predictive current control of modular multilevel converters with phase-shifted pulse-width modulation," in *IEEE. Trans. Ind. Electron.,* vol. 66, no. 6, pp. 4368–4378, Jun. 2019

[12] J. Wang, X. Liu, Q. Xiao, D. Zhou, H. Qiu and Y. Tang, "Modulated Model Predictive Control for Modular Multilevel Converters With Easy Implementation and Enhanced Steady-State Performance," in *IEEE Transactions on Power Electronics*, vol. 35, no. 9, pp. 9107-9118, Sept. 2020

[13] S. Hamayoon, M. Hovd, J. A. Suul and M. Vatani, "Modified Reduced Indirect Finite Control Set Model Predictive Control of Modular Multilevel Converters," in *IEEE COMPEL 2020,* Aalborg, Denmark, pp. 1-6

[14] Z. Gong, X. Wu, P. Dai and R. Zhu, "Modulated Model Predictive Control for MMC-Based Active Front-End Rectifiers Under Unbalanced Grid Conditions," in *IEEE Transactions on Industrial Electronics,* vol. 66, no. 3, pp. 2398-2409, March 2019

Chapter 12

Fault Detection, Localization and Clearance for MMC based on Indirect Finite Control Set Model Predictive Control

In this chapter, indirect finite control set model predictive control (I-FCS-MPC) is used for detecting, localizing, and tolerating open-circuit failures in the transistors without the use of arm voltage sensors. The fault is detected by the main controller whereas the localization is performed in the local controller which is used for the sorting algorithm. The main controller utilizes the discrete mathematical model to estimate the arm voltages using state measurements from present and previous sampling instants. The arm voltage command given by the main controller in the previous sampling instant is then compared with the estimated arm voltage to detect the fault. The fault signal is sent to the local controller where a counter is increased for the potential faulty SMs. The fault is then localized to the specific SM whose count first goes above a threshold value. Finally, this SM is bypassed using

a bypass switch and a redundant SM is inserted in its place. The proposed fault detection and localization method does not require any additional sensors. Simulation results demonstrate that the fault can be detected, localized, and cleared within one fourth of the fundamental period.

12.1 Introduction

Modular multilevel converters (MMCs) have many excellent features such as modular structure, reduced filter requirements, reduced voltage stress on switches, redundancy, and high-quality output voltage [1–5]. These features have made them as one of the most promising technology for high voltage applications such as high voltage direct current transmission systems (HVDC).

One of the main concerns for MMC is reliable operation as it consists of a large number of power semiconductor switches which are the most fragile components in power electronics systems [6]. According to an estimate 38% of the faults in power systems are due to the failure of these power semiconductor devices [7]. It is desirable that MMC operation is not interrupted especially for HVDC applications, even if some of the SMs fail [9]. Therefore, an efficient fault tolerant control strategy that detects and tolerates the SM faults quickly is required to ensure reliable operation of the MMC. Various methods of fault detection and tolerance for MMCs have been studied in literature [8–25]. Some of these methods use redundant SMs for instance [8, 9] and some do not utilize redundant SMs [12, 25] for fault tolerant operation. In strategies that do not utilize redundant SMs, the loss of a faulty SM will generally cause an increase in the voltage of all other SMs to compensate for the faulty SM. These strategies increase the stress on SM components and would not work if this increased voltage is higher than the rated value for SM capacitor voltage. The methods that use redundant SMs simply bypass the faulty SM and insert the redundant SM in its place.

Most of the existing methods on fault tolerant operation of the MMC are proposed for conventional cascade based control of MMCs. In recent years,

model predictive control (MPC) has emerged as a promising control technique for MMCs as it can easily handle multi-input multi-output (MIMO) nature, non-linearity of MMCs, time delays, and constraints. However, the study of fault-tolerant operation for MMC based on the MPC approach is limited [26] and only a few [6, 22, 24, 25] have considered MPC for fault-tolerant operation. Among these, the MPC techniques for fault detection and tolerance proposed in [6, 22] are based on the switching states. Therefore, its computational complexity would become very high when the number of SMs in each arm of MMC are high such as for HVDC applications, thus making their real time application impractical. The method proposed in [24] tolerates a single SM fault by adding an extra switch in the MMC structure. However, this modification changes the location of arm inductance and thus the mathematical model of MMC. In [25], it is assumed that the fault is detected and only fault tolerant operation is considered without redundant SMs. As it does not consider redundant SMs, the operating range would be limited.

In recent years, many works based on MPC have been proposed for MMC [26]. The main research efforts have been to reduce the computational complexity for making the real-time application of MPC for MMC possible. Therefore, the MPC strategy that is preferred for MMC is indirect FCS-MPC where optimization over voltage levels instead of switching states is performed. In this chapter, the fault detection, localization, and tolerance scheme based on indirect FCS-MPC [27] for MMC using redundant SMs is proposed.

The fault detection is performed by the main controller where MPC generates the optimal insertion index (number of SMs to be inserted). The fault detection is based on the comparison of the estimated arm voltage with the arm voltage commanded by the MPC in the previous sampling instant. The estimated arm voltage using the mathematical model of MMC is calculated from the state measurements in the present and previous sampling instant. The main controller is sending the fault signal to the local controller where sorting is being performed. Once, the fault signal is true, then the counter for the potential faulty SMs is increased. The SM whose count first goes above a threshold value is the faulty one and it is then

bypassed using the bypass switch and replaced by some redundant SM. It is further noted that the open-circuit fault in an SM can be due to any of the two switches. Therefore, a separate counter for each type of fault is used. The main contributions can be summarized as:

- A fault detection and tolerance method for open-circuit fault in SM based on indirect FCS-MPC is proposed
- The proposed method does not require any additional sensors.
- The proposed method can be used to detect faults in multiple SMs
- The proposed algorithm can distinguish between faults caused by the two switches of the SM.

12.2 MMC Behavior Under Open Circuit Faults

The SM configuration is shown in Fig. 12.1. There are two switches, therefore there can be two types of faults *i.e.*, fault due to S_1 and fault due to S_2. The characteristics of SM with and without fault are summarized in Table 12.1.

It can be observed from Table 12.1 that the S_1 fault impact occurs only when the arm current is negative and S_2 fault impact occurs when the arm current is positive. Both types of faults will result in increased voltage of that SM with respect to normal SMs *i.e.*, during S_1 fault the capacitor cannot discharge, and under S_2 fault capacitor overcharges.

12.3 Proposed Fault Detection and Fault Tolerance Method

12.3.1 Fault Detection

From Table 12.1 the following two main observations are used for fault detection:

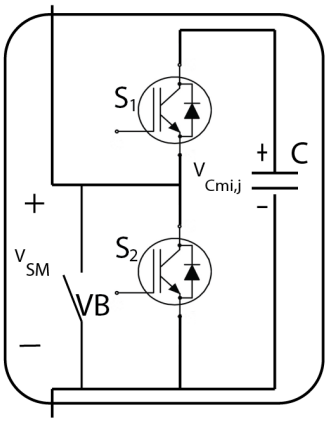

Figure 12.1: SM Configuration

Table 12.1: SM capacitor Characteristics under normal and faulty conditions

Operation	$\mathbf{i_{u,l,j}}$	**SM State**	**Capacitor**	**Output Voltage**
Normal	>0	Inserted	Charged	v_{SM}
	<0	Inserted	Discharged	v_{SM}
	>0 or <0	Bypassed	Unchanged	0
S_1 fault	>0	Inserted	Charged	v_{SM}
	<0	Inserted	Unchanged	0
	>0 or <0	Bypassed	Unchanged	0
S_2 fault	>0	Inserted	Charged	v_{SM}
	<0	Inserted	Discharged	v_{SM}
	>0	Bypassed	Charged	v_{SM}
	<0	Bypassed	Unchanged	0

- Obs1: if the fault is due to S_1 then the actual arm voltage would be less than the commanded arm voltage from the MPC whenever the faulty SM is in inserted state and arm current is negative.
- Obs2: if the fault is due to S_2 then the actual arm voltage would be more than the commanded arm voltage from the MPC whenever the faulty SM is in bypassed state and arm current is positive.

It is noted here that the main controller does not need either the information of arm current direction nor whether an SM was inserted or bypassed to detect the fault.

The proposed method utilizes the mathematical model of the MMC for fault detection. Discretizing (2.13a) and (2.13b) and solving for arm voltages with measurements at present and previous sampling instants, the following expressions are obtained for estimated arm voltage at the previous sampling instant:

$$v_{u,j,est}(k-1) = \frac{H_1 - H_2}{2} \tag{12.1a}$$

$$v_{l,j,est}(k-1) = \frac{H_1 + H_2}{2} \tag{12.1b}$$

where

$$H_1 = (i_{v,j}(k) - i_{v,j}(k-1))\frac{L + 2L_c}{Ts} + Ri_{v,j}(k-1) - 2V_{f,j}(k-1) \tag{12.2}$$

$$H_2 = (i_{cir,j}(k) - i_{cir,j}(k-1))\frac{2L}{Ts} + 2Ri_{cir,j}(k-1) - V_{dc} \tag{12.3}$$

The estimated arm voltages in (12.1) are compared with the commanded arm voltage by the main controller (MPC) in the previous sampling instant. The commanded arm voltages are given as:

$$v_{u,j,cmd}(k-1) = \frac{n_{u,j}(k-1)v^{\Sigma}_{u,j}(k-1)}{N + M - F_u} \tag{12.4a}$$

$$v_{l,j,cmd}(k-1) = \frac{n_{l,j}(k-1)v^{\Sigma}_{l,j}(k-1)}{N + M - F_l} \tag{12.4b}$$

where M is the number of redundant SMs and $F_{u/l}$ are the number of faulty SMs in the upper and lower arm.

Based on the observations Obs1 and Obs2, whenever (12.1) is less than (12.4) by at least $V_{dc}/N \pm ripple$ then the fault is detected and it is due to S_1 and whenever (12.1) is more than (12.4) by at least $V_{dc}/N \pm ripple$ then the fault is detected and it is due to S_2. It is noted here that the difference between (12.1) and (12.4) should be at least $|V_{dc}/N \pm ripple|$ for the fault to be valid.

12.3.2 Fault Localization and Clearance

Although the fault has been detected by the previous method, the information about which SM is faulty is still unknown and therefore the fault cannot be cleared yet. The fault localization is performed in the local controller where sorting is performed. The fault signal from the main controller with the information about the fault type *i.e.*, due to S_1 or S_2 is sent to the local controller. The local controller maintains two counters for each SM. If the fault was due to S_1 then the counter 1 of each inserted SM in the previous sampling instant is increased. If the fault was due to S_2 then the counter 2 of each bypassed SM in the previous sampling instant is increased. Then the SM whose count first goes above a threshold value is identified as the faulty SM and $F_{u/l}$ is increased. The faulty SM is then bypassed using the bypass switch and is replaced by one of the redundant SMs. Thereafter the counter of each SM is set to zero again so that any other faulty SM can be identified as well. The information about the faulty SM is preserved by keeping an array of bypass switch states.

It is noted here that the MMC is operated in hot reserve mode where the redundant SMs are also equally treated by the control algorithm i.e., kept at V_{dc}/N. The overall flowchart for the proposed method is shown in Fig. 12.2 where F_{s1} and F_{s2} are fault flags for S_1 and S_2 faults, respectively.

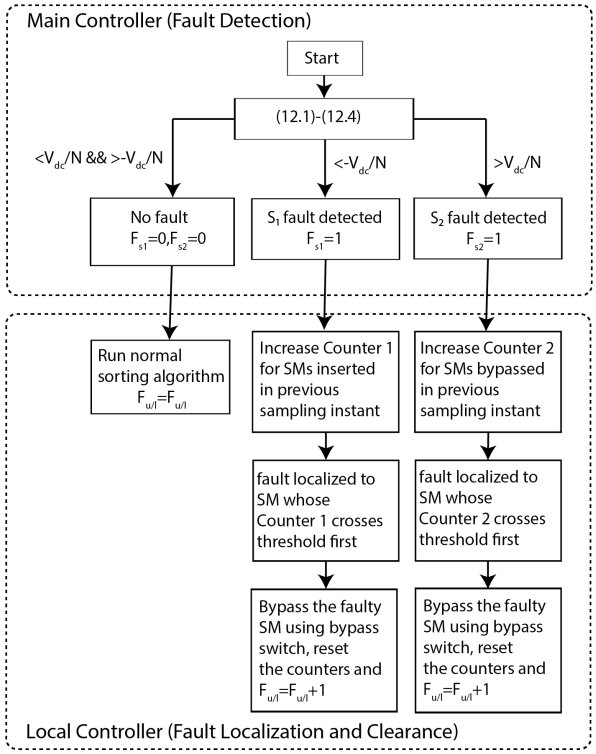

Figure 12.2: Flowchart for the proposed method

12.3.3 Selection of Threshold Value

In this work, the threshold for the counter is fixed to $N/2 + 3$ where N is the total number of SMs without redundant SMs. Therefore, the SM whose count reaches this threshold first is the faulty one. The threshold value chosen will ensure that no healthy SM is mistaken for a faulty SM. As in the worst case for S_1 fault, the initial fault could happen when the insertion index is equal to N then the insertion index needs to be less than N for at least $N/2$ times under fault conditions so that all the healthy SMs have been put out of operation at least once by the conventional sorting

algorithm [5]. As there can be cases when the insertion index remains N for one or two sampling instants under fault conditions so an additional 3 is added to $N/2$. Similarly, for the worst case of S_2 fault, the initial fault could happen when the insertion index is 0 and then the insertion index needs to be more than 0 for at least $N/2$ times under fault conditions so that all the healthy SMs have been put in operation at least once by the sorting algorithm. The additional 3 is added for the same reason that the insertion index can remain 0 for one or two sampling instants under fault conditions.

It is worth pointing out that although the threshold value is dependent on the total number of submodules, the fault can be still detected and cleared within one fundamental period. This is due to the advancement in processor technology which has made possible the realization of much lower sampling times for instance $50\mu s$ which means for an ac wave of 50 Hz a fundamental period will be completed in 400 sampling instants. Typically for high voltage applications the number of SMs ranges from 200 to 400 SMs/arm [2] thus resulting in an $N/2$ of 200 for worst case scenario which is half of the sampling instants required for completing one fundamental period of a 50 Hz wave.

12.4 Comparison with Other Strategies

The comparison of the proposed method with other strategies considering open circuit switch faults is shown in Table 12.2. Only MPC-based strategies are considered to make a fair comparison. The proposed method has one or more advantages over all the existing MPC-based methods. Moreover, the existing MPC based methods do not consider redundant SMs and as a result, the SM capacitors need to be oversized as they have to handle more voltage in fault-tolerant operation. Furthermore, if this higher voltage in tolerant mode becomes more than the rated voltage then the SM capacitors would be damaged and may even explode.

Table 12.2: Comparison with other MPC based Strategies

Method	Features							
	FD	FL	FT	Overall Computational Burden	Speed	Additional Sensors/Components	Redundant SMs	Distinguish b/w S_1 and S_2 fault
Proposed	Y	Y	Y	Low	within fundamental period	N	Y	Y
[6],[22]	Y	Y	Y	Very High	within fundamental period	N	N	Y
[24]	Y	Y	Y	Low	at least 5 fundamental periods	Y	N	N
[25]	N	N	Y	Low	NA	N	N	N

* FD=Fault Detection, FL=Fault Localization, FT=Fault Tolerance, Y=Yes, N=No, NA=Not Applicable

12.5 Simulation Results

The performance of the proposed strategy is validated by performing simulations on a three-phase MMC with 18 SMs per arm, as shown in Fig. 12.3. Among these 16 SMs are used in normal operation and the remaining two SMs serve the purpose of redundant SMs. The scenario used for

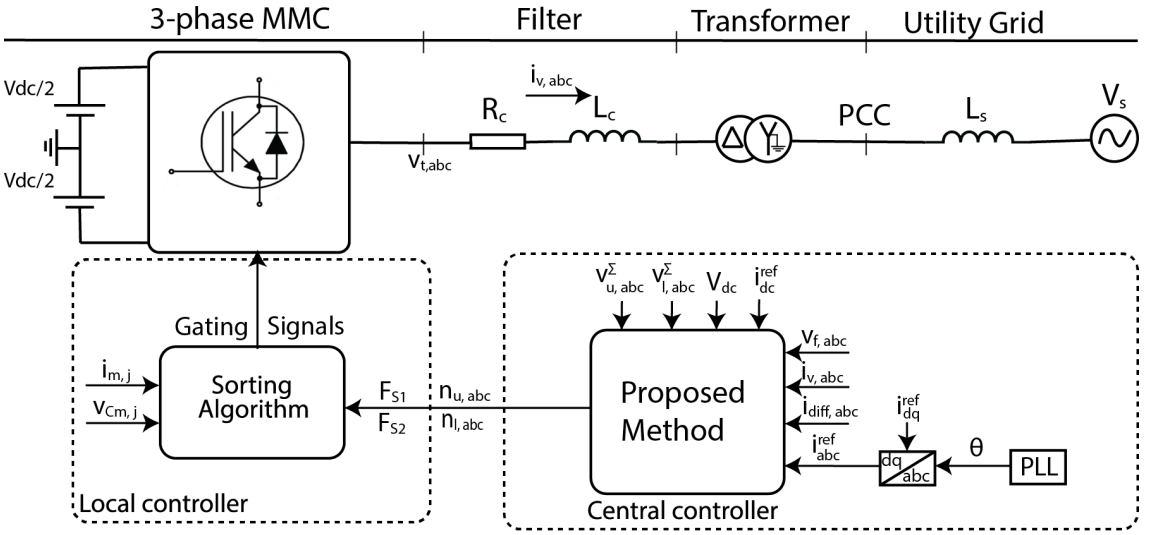

Figure 12.3: Control Block Diagram

simulation is that initially, the converter is operating in normal mode with an active current reference set to 40 A. The parameters used for simulation are summarized in Table 12.3.

Table 12.3: Simulation Parameters

Parameter	**Value**
MMC nominal power (base power)	50 kVA
AC system nominal voltage (base voltage)	150 V
Nominal frequency	50 Hz
Arm inductance (L)	1.55 mH
Arm resistance (R)	0.01Ω
Submodule capacitance (C)	20000μF
Transformer voltage rating (T)	400 V / 400 V
Transformer power rating	50 kVA
Transformer inductance	0.04 pu
Transformer resistance	0.006 pu
DC side reference voltage	400 V
Number of SMs per arm (N)	16
Number of redundant SMs per arm (M)	2
Sampling time (Ts)	70μs

In the following discussion, the open-circuit switch faults were generated by emulating the behavior of open-circuit faults as given in Table 12.1. At t=0.23s the S_1 fault is applied to the first SM in the upper arm of phase a. Figs. 12.4 and 12.5 shows the overall response of all the state variables for both cases *i.e.*, if the fault is left uncleared and if the fault is cleared by the proposed method. The results show that none of the state variables is being tracked accurately if the fault is not cleared *i.e.*, the ac-current and circulating current have distortions, and the resulting summation voltages would create energy imbalance between the upper and lower arm.

Results for the scenario when S_2 fault is applied at t=0.23s, are shown in Figs. 12.6 and 12.7. In this case, the distortions in circulating current are more severe as the faulty SM capacitor would always be inserted when the arm current is positive. This results in voltage increase at a faster rate for S_2 fault as compared to S_1 fault because in S_1 fault the SM voltage

is unchanged on faulty condition whereas under S_2 fault the SM capacitor gets charged and voltage increases (see Table 12.1).

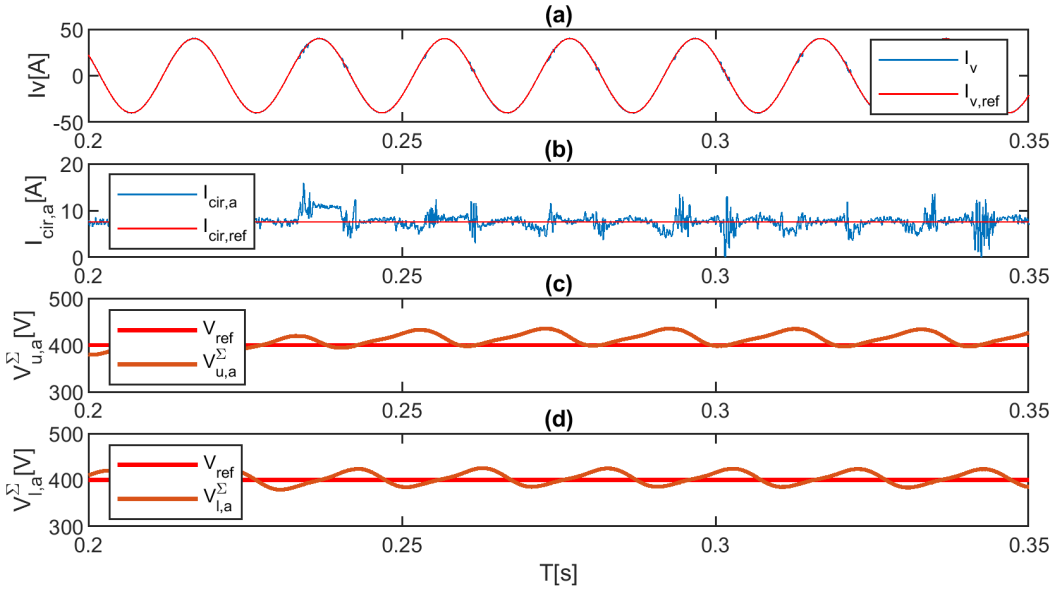

Figure 12.4: S_1 Fault Uncleared (a) AC-current (b) circulating current (c,d) Summation voltages upper and lower arm phase a

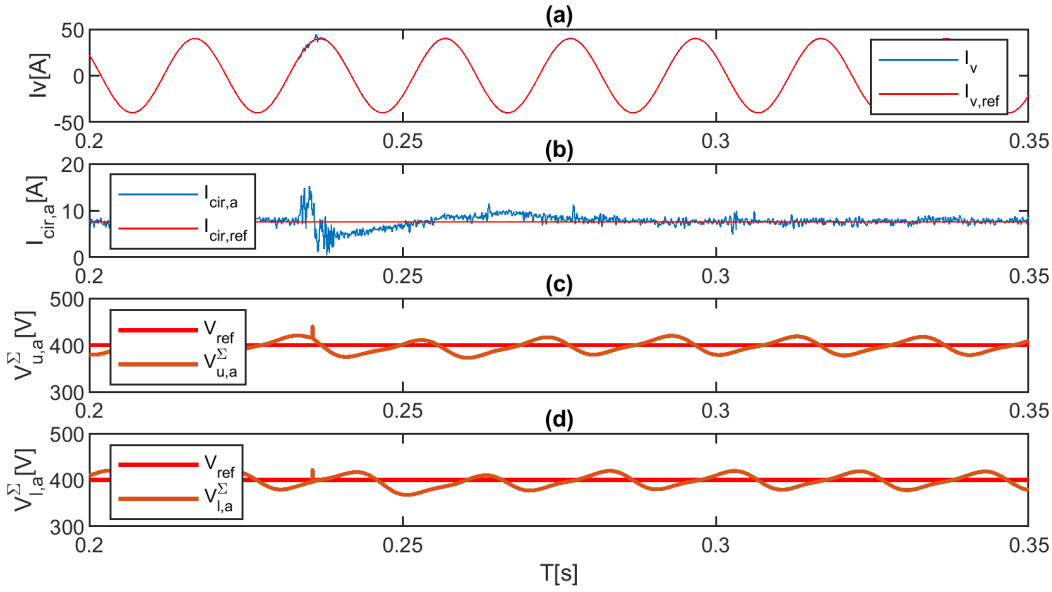

Figure 12.5: S_1 Fault Cleared (a) AC-current (b) circulating current (c,d) Summation voltages upper and lower arm phase a

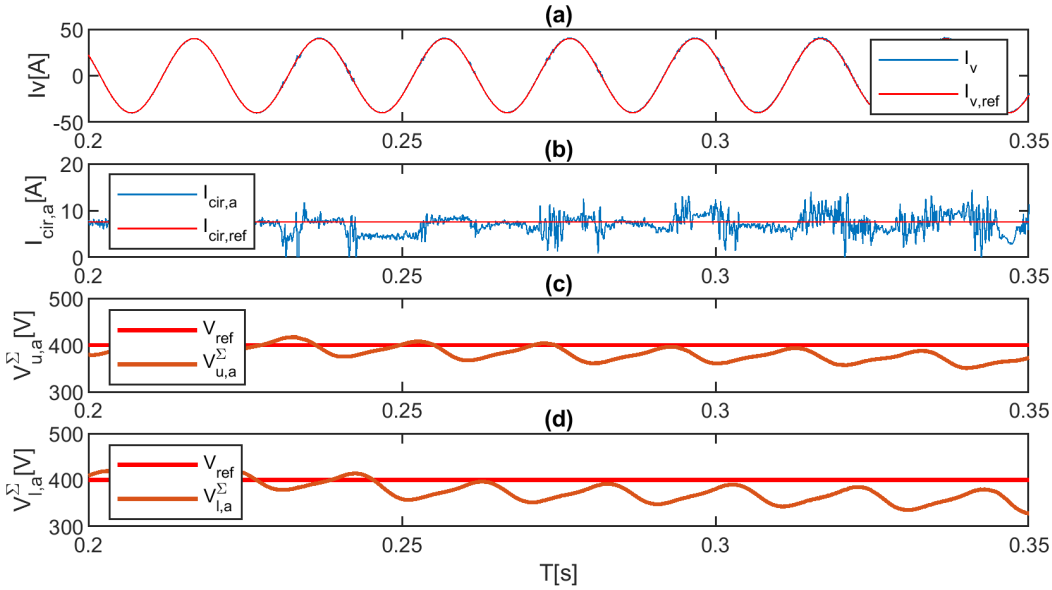

Figure 12.6: S_2 Fault Uncleared (a) AC-current (b) circulating current (c,d) Summation voltages upper and lower arm phase a

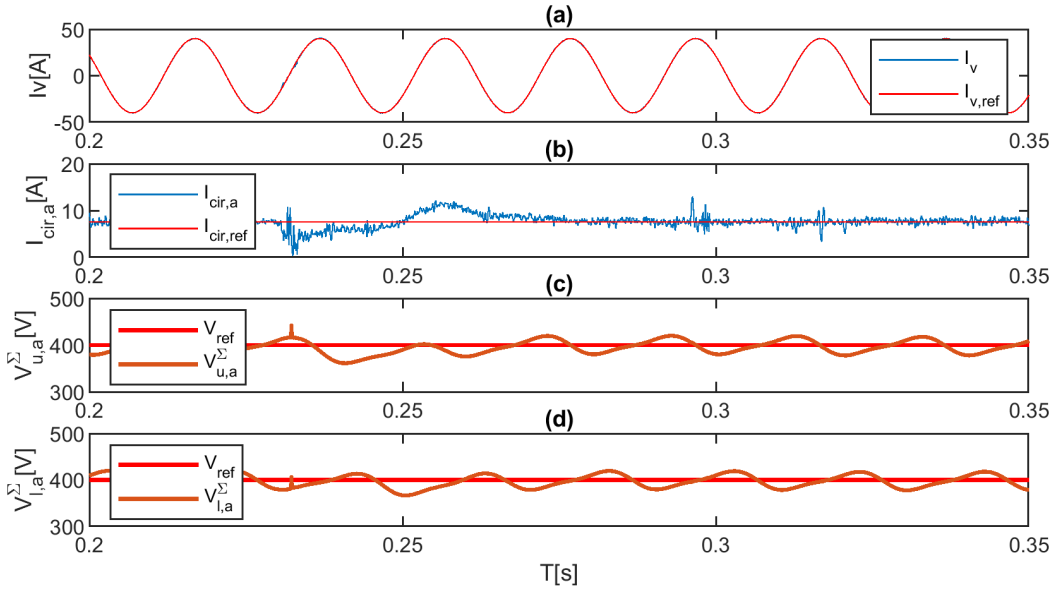

Figure 12.7: S_2 Fault Cleared (a) AC-current (b) circulating current (c,d) Summation voltages upper and lower arm phase a

Figures 12.8 and 12.9 shows individual SM capacitor voltages in the upper arm of phase a under both types of faults with and without the proposed method. The faulty SM voltage keeps on increasing for both faults if the faults are not cleared as already discussed. Therefore, if faults are left uncleared then the faulty SM voltage would eventually become higher than the rated voltage of the capacitor and damage the capacitor or might even explode the capacitor if the voltage becomes too large. With the proposed method, as soon as the fault is localized to the faulty SM then it is bypassed using the bypass switch B as shown in Fig. 12.1 and a redundant SM takes its place.

In Fig. 12.10 the fault detection (denoted by FD) and localization (denoted by FL) signals for both faults are shown for the positive direction of power flow. It can be observed that fault detection and localization for

S_2 fault is quicker than S_1 fault. This is due to the direction of power flow which was positive for this simulation scenario. As a consequence, the arm current is more positive during one fundamental period. Therefore, under this scenario, S_2 fault occurs more often as its impact occurs when the arm current is positive (see Table 12.1). So, the count associated with S_2 fault reaches the threshold faster and gets cleared early as compared to S_1 fault. In the case of negative power flow, the arm current would be more negative in one fundamental period. As the S_1 fault impact occurs when the arm current is negative (see Table 12.1), it would occur more often as compared to S_2 fault in this scenario. Therefore, S_1 fault would be detected and cleared early as compared to S_2 fault for this power direction.

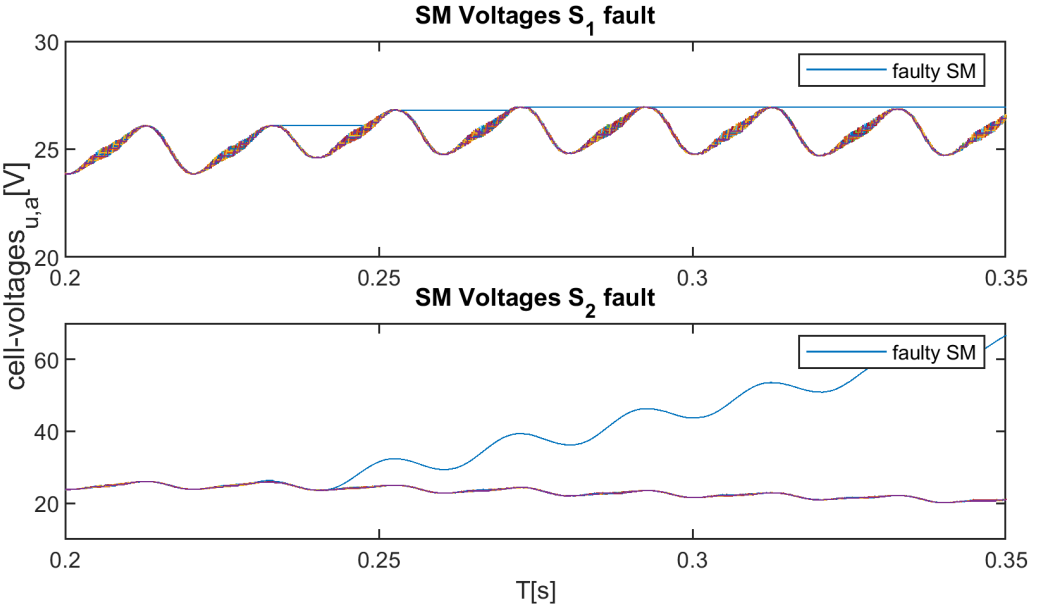

Figure 12.8: Individual SM Capacitor Voltages under both types of faults without proposed method

It can also be observed that fault detection is very fast *i.e.*, the fault is

detected in less than 5ms even for S_1 and is localized to the faulty SM in around 5ms. As soon as the fault is localized, the faulty SM is removed by the bypass switch and is replaced by a redundant SM. Therefore, the fault has been cleared and no fault is detected afterward. It is noted here that the fault detection signal switches between 0 and 1 because the faulty SM is not always inserted/bypassed by the sorting algorithm.

The fault detection and localization signals in the reverse power direction are shown in Fig. 12.11 under both types of faults. As explained earlier, in this power direction S_1 fault is detected and cleared earlier as compared to S_2 fault.

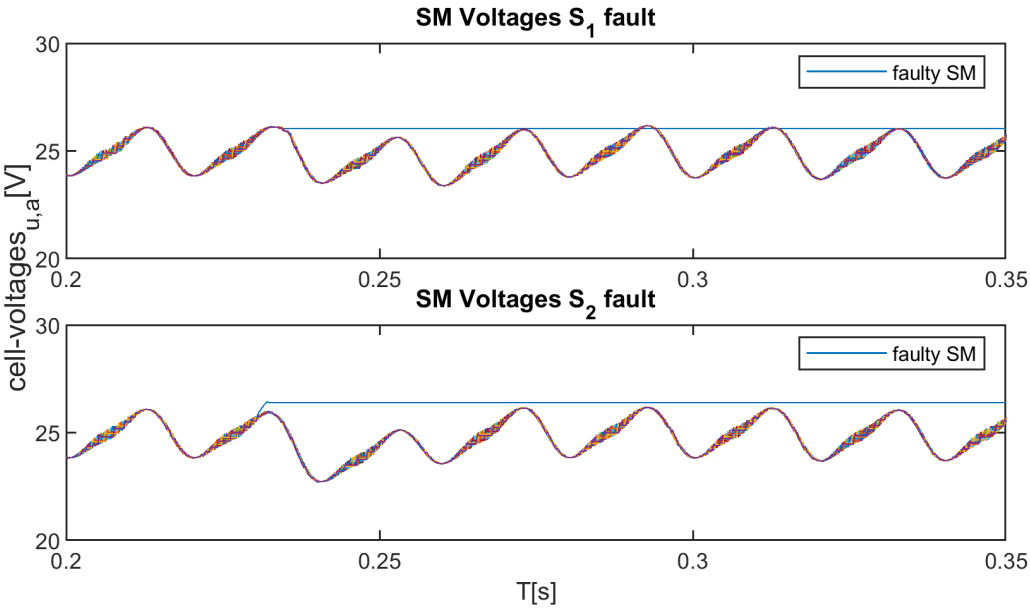

Figure 12.9: Individual SM Capacitor Voltages under both types of faults with proposed method

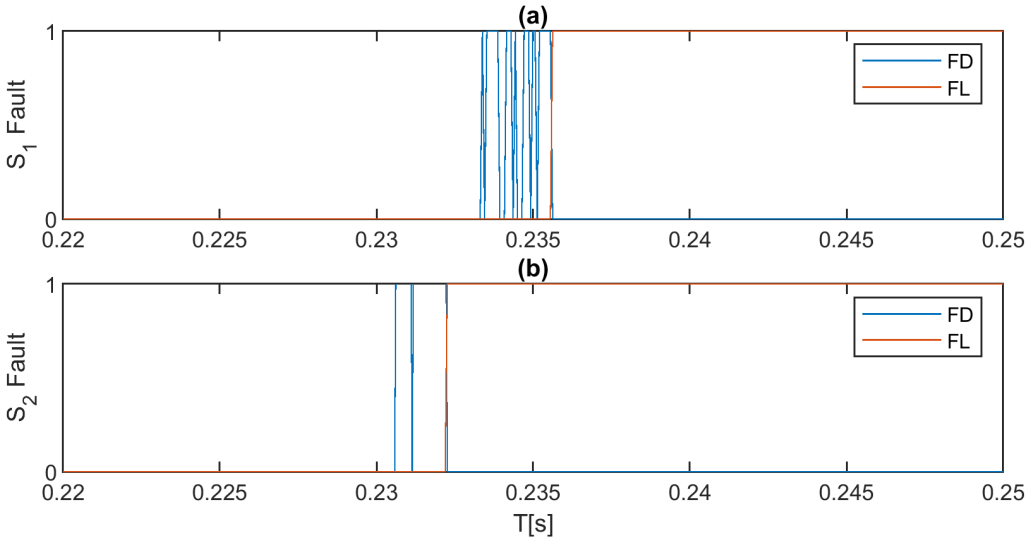

Figure 12.10: Fault Detection and Localization Signals (positive power flow) (a) S_1 fault (b) S_2 fault

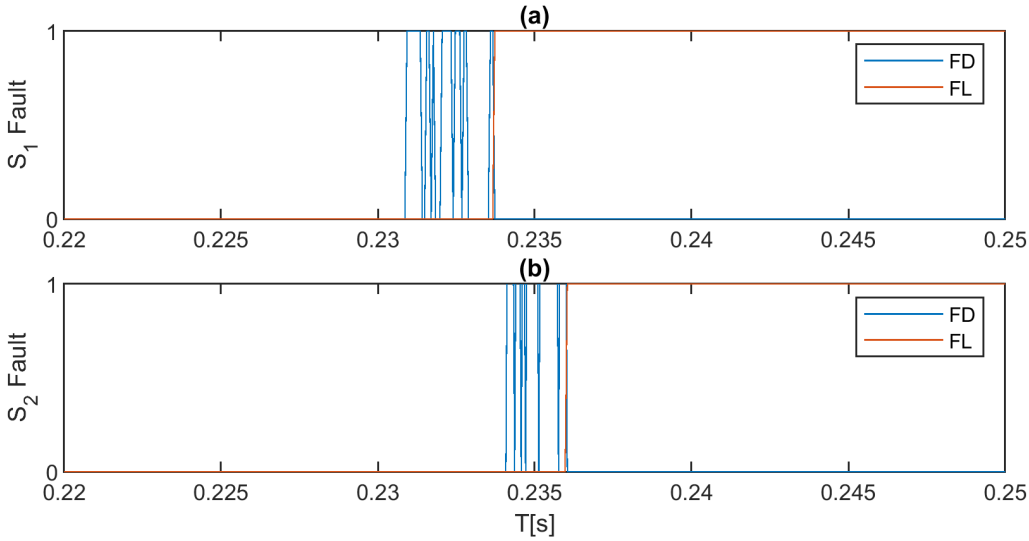

Figure 12.11: Fault Detection and Localization Signals (negative power flow) (a) S_1 fault (b) S_2 fault

12.6 Conclusion

In this chapter, a method for fault detection, localization, and clearance based on indirect finite control set model predictive control is presented for MMCs. It is shown that the proposed method detects, localizes, and clears the fault within just around 5ms i.e., 1/4th of the fundamental period. The proposed method also provides information regarding the fault type i.e., due to S1 or S2. Moreover, no additional sensors are required to execute the developed method.

Bibliography

[1] K. Sharifabadi, L. Harnefors, H.-P. Nee, S. Norrga, and R. Teodorescu, *Design, Control and Application of Modular Multilevel Converters for HVDC Transmission Systems.* United States: Wiley-IEEE press, 2016.

[2] D. Sixing, A. Dekka, B. Wu and N. Zargari, *Modular Multilevel Converters: Analysis Control and Applications,* Hoboken, NJ, USA:Wiley, Feb. 2018.

[3] A. Lesnicar and R. Marquardt, "An innovative modular multilevel converter topology suitable for a wide power range," in *Proc. IEEE PowerTec Conf.*, Bologna, Italy, Jun. 2003, vol. 3, pp. 272–277.

[4] A. Nami, J. Liang, F. Dijkhuizen and G. D. Demetriades, "Modular Multilevel Converters for HVDC Applications: Review on Converter Cells and Functionalities," in *IEEE Transactions on Power Electronics,* vol. 30, no. 1, pp. 18-36, Jan. 2015

[5] M. Saeedifard and R. Iravani, "Dynamic Performance of a Modular Multilevel Back-to-Back HVDC System," *IEEE Transactions on Power Delivery,* vol. 25, no. 4, pp. 2903-2912, Oct. 2010

[6] D. Zhou, S. Yang and Y. Tang, "A Voltage-Based Open-Circuit Fault Detection and Isolation Approach for Modular Multilevel Converters With Model-Predictive Control," in *IEEE Transactions on Power Electronics,* vol. 33, no. 11, pp. 9866-9874, Nov. 2018

[7] B. Lu and S. Sharma, "A Literature Review of IGBT Fault Diagnostic and Protection Methods for Power Inverters," *2008 IEEE Industry Applications Society Annual Meeting,* 2008, pp. 1-8

[8] K. Li, L. Yuan, Z. Zhao, S. Lu and Y. Zhang, "Fault-Tolerant Control of MMC With Hot Reserved Submodules Based on Carrier Phase Shift Modulation," in *IEEE Transactions on Power Electronics*, vol. 32, no. 9, pp. 6778-6791, Sept. 2017

[9] B. Li, S. Shi, B. Wang, G. Wang, W. Wang and D. Xu, "Fault Diagnosis and Tolerant Control of Single IGBT Open-Circuit Failure in Modular Multilevel Converters," in *IEEE Transactions on Power Electronics,* vol. 31, no. 4, pp. 3165-3176, April 2016

[10] G. T. Son et al., "Design and Control of a Modular Multilevel HVDC Converter With Redundant Power Modules for Noninterruptible Energy Transfer," in *IEEE Transactions on Power Delivery,* vol. 27, no. 3, pp. 1611-1619, July 2012

[11] G. Liu, Z. Xu, Y. Xue and G. Tang, "Optimized Control Strategy Based on Dynamic Redundancy for the Modular Multilevel Converter," in *IEEE Transactions on Power Electronics,* vol. 30, no. 1, pp. 339-348, Jan. 2015

[12] P. Hu, D. Jiang, Y. Zhou, Y. Liang, J. Guo and Z. Lin, "Energy-balancing Control Strategy for Modular Multilevel Converters Under Submodule Fault Conditions," in *IEEE Transactions on Power Electronics,* vol. 29, no. 9, pp. 5021-5030, Sept. 2014

[13] G. Konstantinou, J. Pou, S. Ceballos and V. G. Agelidis, "Active Redundant Submodule Configuration in Modular Multilevel Converters," in *in IEEE Transactions on Power Delivery,* vol. 28, no. 4, pp. 2333-2341, Oct. 2013

[14] S. Yang, Y. Tang and P. Wang, "Seamless Fault-Tolerant Operation of a Modular Multilevel Converter With Switch Open-Circuit Fault Di-

agnosis in a Distributed Control Architecture," in *IEEE Transactions on Power Electronics,* vol. 33, no. 8, pp. 7058-7070, Aug. 2018

[15] R. Picas, J. Zaragoza, J. Pou and S. Ceballos, "Reliable Modular Multilevel Converter Fault Detection With Redundant Voltage Sensor," in *IEEE Transactions on Power Electronics,* vol. 32, no. 1, pp. 39-51, Jan. 2017

[16] Q. Yang, J. Qin and M. Saeedifard, "Analysis, Detection, and Location of Open-Switch Submodule Failures in a Modular Multilevel Converter," in *IEEE Transactions on Power Delivery,* vol. 31, no. 1, pp. 155-164, Feb. 2016

[17] Q. Xiao et al., "A Novel Operation Scheme for Modular Multilevel Converter With Enhanced Ride-Through Capability of Submodule Faults," in *IEEE Journal of Emerging and Selected Topics in Power Electronics,* vol. 9, no. 2, pp. 1258-1268, April 2021

[18] S. Farzamkia, H. Iman-Eini, M. Noushak and A. Hadizadeh, "Improved Fault-Tolerant Method for Modular Multilevel Converters by Combined DC and Neutral-Shift Strategy," in *IEEE Transactions on Industrial Electronics,* vol. 66, no. 3, pp. 2454-2462, March 2019

[19] F. Deng, M. Jin, C. Liu, M. Liserre and W. Chen, "Switch Open-Circuit Fault Localization Strategy for MMCs Using Sliding-Time Window Based Features Extraction Algorithm," in *IEEE Transactions on Industrial Electronics,* vol. 68, no. 10, pp. 10193-10206, Oct. 2021

[20] X. Chen, J. Liu, Z. Deng, S. Song, S. Du and D. Wang, "A Diagnosis Strategy for Multiple IGBT Open-Circuit Faults of Modular Multilevel Converters," in *IEEE Transactions on Power Electronics,* vol. 36, no. 1, pp. 191-203, Jan. 2021

[21] J. Zhang, X. Hu, S. Xu, Y. Zhang and Z. Chen, "Fault Diagnosis and Monitoring of Modular Multilevel Converter With Fast Response of Voltage Sensors," in *IEEE Transactions on Industrial Electronics,* vol. 67, no. 6, pp. 5071-5080, June 2020

[22] D. Zhou, P. Tu, H. Qiu and Y. Tang, "Finite-Control-Set Model Predictive Control of Modular Multilevel Converters With Cascaded Open-Circuit Fault Ride-Through," in *IEEE Journal of Emerging and Selected Topics in Power Electronics,* vol. 8, no. 3, pp. 2943-2953, Sept. 2020

[23] D. Zhou, H. Qiu, S. Yang and Y. Tang, "Submodule Voltage Similarity-Based Open-Circuit Fault Diagnosis for Modular Multilevel Converters," in *IEEE Transactions on Power Electronics,* vol. 34, no. 8, pp. 8008-8016, Aug. 2019

[24] Y. Sun, Z. Li and Z. Zhang, "Open-Circuit Fault Diagnosis and Fault-Tolerant Control with Sequential Indirect Model Predictive Control for Modular Multilevel Converters," *2019 4th IEEE Workshop on the Electronic Grid (eGRID),* 2019, pp. 1-6

[25] K. Xu, S. Xie, X. Wang, B. Zhang and S. Bian, "Model Predictive-based Fault-tolerant Control for Modular Multilevel Converters Without Redundant Submodules," *2018 IEEE International Power Electronics and Application Conference and Exposition (PEAC),* 2018, pp. 1-5

[26] A. Dekka, B. Wu, V. Yaramasu, R. L. Fuentes and N. R. Zargari, "Model Predictive Control of High-Power Modular Multilevel Converters—An Overview," in *IEEE Journal of Emerging and Selected Topics in Power Electronics,* vol. 7, no. 1, pp. 168-183, March 2019,

[27] S. Hamayoon, M. Hovd, J. A. Suul and M. Vatani, "Modified Reduced Indirect Finite Control Set Model Predictive Control of Modular Multilevel Converters," *IEEE COMPEL 2020*, Aalborg, Denmark, pp. 1-6,

Chapter 13

Conclusion & Potential Future Directions

In this thesis, five methods have been proposed to address the issue of computational complexity and dynamic performance of the modular multilevel converter. The main goal of these methods was to offer high dynamic performance while keeping the computational complexity low so that the real-time implementation remains possible. In addition to these methods, a novel circulating current reference is also proposed to regulate the summation voltages without the need of an outer loop. Moreover, an open circuit switch fault detection, localization and tolerance method based on MPC for MMC is proposed. Further, a method to balance the switching frequencies of SMs of MMC with only sorting algorithm *i.e.*, without the need of an explicit modulator, and a general framework to improve the steady-state response of finite control set model predictive control with an explicit modulator is also suggested. The main conclusions are as under and it also highlights how this thesis moved forward:

- In the modified reduced indirect FCS-MPC (MRI-FCS-MPC) method the large step is fixed to a specific number. Therefore, this number needs to be tuned for MMCs with different number of SMs. Moreover,

for MMCs with a very high number of SMs changes of $0, +/-1, +/-5$ will not be enough.

- The high steps based MPC (HS-MPC) discussed in chapter 9 makes the calculation of large step dynamic as opposed to MRI-FCS-MPC. However, again for MMCs with a very high number of SMs changes of $0, +/-1, +/-large-step$ will not be enough. This will be mainly due to the requirement to increase the small neighborhood *i.e.*, changes of $0, +/-1$ will not be enough then for operating at or near the steady state.

- Another drawback of the previous two methods is that the calculation of insertion index is dependent on the insertion index of the previous sampling instant. As a result, if the neighborhood of insertion indices to be investigated is kept small then the dynamic response becomes slower and if this neighborhood is enlarged then the computational burden increases.

- In order to address above, the bisection and backstepping based MPC methods were proposed. These methods make the selection of insertion index independent from the insertion index in the previous sampling instant. As a result, only a small neighborhood needs to be considered around the rounded off result (insertion index) obtained from backstepping and bisection algorithms. Both of these methods would also work well with MMCs with high number of SMs. However, their computational complexities would slightly increase because of the assumption used in bisection and backstepping stage.

- All of the previous methods, computational complexity is still dependent on the number of SMs. Moreover, due to their discrete nature they have reduced steady state performance where the number of SMs are in low to medium range. Therefore, the active set method was proposed to make the computational complexity independent of the number of SMs. In addition, this method results in continuous output (modulation index). Therefore, a PWM modulator is used which

then results in reduced THD. The advantages of this method are that it's computational complexity is independent of the number of SMs and it offers better steady state response. A disadvantage is that it requires the use of explicit PWM modulator due to it's continuous nature. Moreover, it is only for a prediction horizon of one as it is based on analytical expressions.

- Nonlinear model predictive control (NMPC) makes the computational complexity independent of the number of SMs and can also be extended for longer prediction horizons easily. Therefore, it can be concluded that NMPC approaches are the best for MMC. Two approaches were presented to deal with the continuous nature of NMPC. The experimental validation of NMPC will be done as future work.

- To equally distribute the losses among the SMs, a modified sorting algorithm was proposed. The advantage of this method is that it achieves the fixed switching frequency without the need of an explicit PWM modulator.

- A general framework to improve the steady state response of indirect FCS-MPC approaches was also proposed. The advantage of this method is that it improves the steady state response without the need to calculate duty cycles as opposed to existing methods in literature.

- The indirect FCS-MPC method for open circuit switch fault detection, localization and tolerance was proposed as the existing literature on this topic was rare. The proposed method showed that fault detection, localization and tolerance using MPC is very fast.

- The modifications required for real-time implementation highlighted a problem associated with ac-side voltage prediction. This was rectified by proposing a very simple method of grid voltage estimation or a virtual ac-side voltage approach. This shows that traditional MPC based methods which only consider a time delay compensation of one sampling instant may run into problems as the ac-side voltage

prediction does not appear (as it's impact is very low) when just considering a time delay of one sampling instant.

13.1 Future Research Directions

Some of the possible future research directions are provided below:

- In practice the MMC is mostly connected in three-phase three wire system. Therefore, zero sequence voltage cannot cause zero sequence current. However, usually the model for MMC is derived for a three-phase four wire system. As a result, zero sequence current would appear. Hence, zero sequence voltage compensation is required. When this zero-sequence voltage compensation is considered then the phases cannot be treated independently i.e., instead of independent cost functions for each phase, a single cost function for the whole system is required. Methods based on single cost function for three-phase model of MMC exist in literature. However, their computational complexity is very high. New methods need to be investigated in this direction as three phase model based MPC methods are more accurate.

- The stability proof of FCS-MPC was tried in this work by approximating FCS-MPC with a polynomial and then proving stability of these polynomial controllers using sum of squares programming and MMC model. However, the attempt was not successful. The reason is most probably the formulation of the model for SOS problem. This could be another research direction. Moreover, there is no generic stability proof for FCS-MPC in the existing literature. A generic stability proof would be a valuable contribution in this regard.

- Although methods were proposed in this thesis that reduced the computational complexity while giving high performance, these methods (except NMPC) still cannot be extended beyond a prediction horizon of 5 or 6. Therefore, methods based on sphere decoding [1–4] which can easily be extended to a prediction horizon of 50 or 100 for

power converters with linear models should be expanded to non-linear models.

- When this thesis was being conducted many methods based on artificial intelligence/machine learning have been proposed [5–13]. These methods have a very big advantage as they make the problem independent from model parameters mismatch. However, these methods still have a higher computational complexity and need more research. The methods that mimic FCS-MPC have a high computational complexity at the design stage whereas the methods that add an online system identification stage have a high computational complexity during the operations stage.

- The backstepping method proposed in this thesis did not provide an analysis on how the coefficients in the controller should be selected. An optimal way to select these can be a potential research direction as it will lead to improved performance of the backstepping method.

- The MPC based methods for power converters have already been adopted by industry in some capacity and it is expected that their share would gradually increase. In this regard, an interesting research direction could be to check interoperability between different power converters operating with different algorithms. For instance, one MMC may be operated by conventional PI based control and another MMC could be operating with MPC based method.

- While conducting experiments for this thesis, it was noted that the transition from PI based to MPC control was okay. However, from MPC to PI transition the system tripped. This could be investigated and it would be interesting if some method is proposed to deal with this issue. As one could then try to operate with a hybrid method i.e. application of MPC during transients and application of PI during steady state operation.

- The poor performance of PI based control when the power is changed from negative to positive as shown in Chapter 9 in this thesis could

also be investigated and an improved PI control design can be developed that offers good performance in both directions. For example, gain scheduling can be tried.

- One of the issues with MPC based methods in practical applications would be at startup. Because of large time delays in practical systems, the MPC would initially have poor performance but once the converter starts its operation then MPC would work fine for all the later reference changes. A proper startup method for MPC based methods could be developed as a future work.

Bibliography

[1] J. Raath, T. Mouton and T. Geyer, "Alternative Sphere Decoding Algorithm for Long-horizon Model Predictive Control of Multi-level Inverters," in *2020 IEEE 21st Workshop on Control and Modeling for Power Electronics (COMPEL),* 2020, pp. 1-8

[2] P. Karamanakos, T. Geyer, T. Mouton and R. Kennel, "Computationally efficient sphere decoding for long-horizon direct model predictive control," in *2016 IEEE Energy Conversion Congress and Exposition (ECCE),* 2016, pp. 1-8

[3] P. Karamanakos, T. Geyer and R. P. Aguilera, "Long-Horizon Direct Model Predictive Control: Modified Sphere Decoding for Transient Operation," in *IEEE Transactions on Industry Applications,* vol. 54, no. 6, pp. 6060-6070, Nov.-Dec. 2018

[4] P. Karamanakos, T. Geyer and R. Kennel, "Reformulation of the long-horizon direct model predictive control problem to reduce the computational effort," in *2014 IEEE Energy Conversion Congress and Exposition (ECCE),* 2014, pp. 3512-3519

[5] S. Wang, T. Dragicevic, Y. Gao and R. Teodorescu, "Neural Network Based Model Predictive Controllers for Modular Multilevel Converters," in *IEEE Transactions on Energy Conversion,* vol. 36, no. 2, pp. 1562-1571, June 2021

[6] S. Wang, T. Dragicevic, G. F. Gontijo, S. K. Chaudhary and R. Teodorescu, "Machine Learning Emulation of Model Predictive Control for Modular Multilevel Converters," in *IEEE Transactions on Industrial Electronics,* vol. 68, no. 11, pp. 11628-11634, Nov. 2021

[7] W. Wu et al., "Model-Free Sequential Predictive Control for MMC with Variable Candidate Set," in *IEEE Journal of Emerging and Selected Topics in Power Electronics*

[8] X. Liu et al., "Event-Triggered Neural-Predictor-Based FCS-MPC for MMC," in *IEEE Transactions on Industrial Electronics,* vol. 69, no. 6, pp. 6433-6440, June 2022

[9] X. Liu et al., "Neural Predictor-Based Low Switching Frequency FCS-MPC for MMC With Online Weighting Factors Tuning," in *IEEE Transactions on Power Electronics,* vol. 37, no. 4, pp. 4065-4079, April 2022

[10] X. Liu et al., "Neural Predictor-Based Dynamic Surface Predictive Control for Power Converters," in *IEEE Transactions on Industrial Electronics*

[11] X. Liu et al., "Event-Triggered ESO-Based Robust MPC for Power Converters," in *IEEE Transactions on Industrial Electronics*

[12] X. Liu et al., "Data-Driven Neural Predictors-Based Robust MPC for Power Converters," in *IEEE Transactions on Power Electronics,* vol. 37, no. 10, pp. 11650-11661, Oct. 2022

[13] X. Liu, L. Qiu, Y. Fang, K. Wang, Y. Li and J. Rodríguez, "A Fuzzy Approximation for FCS-MPC in Power Converters," in *IEEE Transactions on Power Electronics,* vol. 37, no. 8, pp. 9153-9163, Aug. 2022

ISBN 978-82-326-7158-8 (printed ver.)
ISBN 978-82-326-7157-1 (electronic ver.)
ISSN 1503-8181 (printed ver.)
ISSN 2703-8084 (online ver.)

NTNU
Norwegian University of
Science and Technology